

Third-order corrections to the slow-roll expansion: calculation and constraints with Planck, ACT, SPT, and BICEP/Keck

Mario Ballardini,^{a,b,c} Alessandro Davoli, Salvatore Samuele Sirletti^{a,b,d}

^aDipartimento di Fisica e Scienze della Terra, Università degli Studi di Ferrara, via Giuseppe Saragat 1, 44122 Ferrara, Italy

^bINFN, Sezione di Ferrara, via Giuseppe Saragat 1, 44122 Ferrara, Italy

^cINAF/OAS Bologna, via Piero Gobetti 101, 40129 Bologna, Italy

^dDipartimento di Fisica, Università di Trento, Via Sommarive 14, 38123 Povo, Trento, Italy

E-mail: mario.ballardini@unife.it, alessandro.davoli91@gmail.com, salvatoresamuele.sirletti@unife.it

Abstract. We investigate the primordial power spectra (PPS) of scalar and tensor perturbations, derived through the slow-roll approximation. By solving the Mukhanov-Sasaki equation and the tensor perturbation equation with Green’s function techniques, we extend the PPS calculations to third-order corrections, providing a comprehensive expansion in terms of slow-roll parameters with an independent approach to the solution of the integrals compared to the one previously presented in the literature. We investigate the accuracy of the analytic predictions starting from first-order corrections up to third-order ones with the numerical solutions of the perturbation equations for a selection of single-field slow-roll inflationary models. We derive the constraints on the Hubble flow functions ϵ_i from *Planck*, ACT, SPT, and BICEP/Keck data. We find an upper bound $\epsilon_1 \lesssim 0.002$ at 95% CL dominated by BICEP/Keck data and robust to all the different combination of datasets. We derive the constraint $\epsilon_2 \simeq 0.031 \pm 0.004$ at 68% confidence level (CL) from the combination of *Planck* data and late-time probes such as baryon acoustic oscillations, redshift space distortions, and supernovae data at first order in the slow-roll expansion. The uncertainty on ϵ_2 gets larger including second- and third-order corrections, allowing for a non-vanishing running and running of the running respectively, leading to $\epsilon_2 \simeq 0.034 \pm 0.007$ at 68% CL. We find $\epsilon_3 \simeq 0.1 \pm 0.4$ at 95% CL both at second and at third order in the slow-roll expansion of the spectra. ϵ_4 remains always unconstrained. The combination of *Planck* and SPT data, compatible among each others, leads to slightly tighter constraints on ϵ_2 and ϵ_3 . On the contrary, the combination of *Planck* data with ACT measurements, which point to higher values of the scalar spectral index compared to *Planck* findings, leads to shifts in the means and maximum likelihood values for ϵ_2 and ϵ_3 . We discuss the results obtained for different dataset combinations and different multipole cuts.

Contents

1	Introduction	1
2	Third-Order Calculation	3
2.1	Primordial Scalar Perturbations	5
2.2	Primordial Tensor Perturbations	6
2.3	The Primordial Power Spectra Including Third-Order Corrections	7
2.3.1	The Primordial Power Spectrum of Scalar Perturbations	10
2.3.2	The Primordial Power Spectrum of Tensor Perturbations	13
3	Accuracy of Slow-Roll Analytic Power Spectra Against the Exact Numerical Solution	15
3.1	Background Dynamics	15
3.2	Perturbation Equations	16
3.3	Initial Conditions	16
3.4	Inflationary Models	16
3.5	Accuracy of Slow-Roll Analytic Spectra	19
4	Data Analysis and Cosmological Constraints	24
4.1	Results	26
4.2	Combined Results	29
4.3	Future CMB Constraints	31
5	Conclusions	34
A	Useful Integrals	38
B	Super-Hubble Limits for the Integrals	44
C	Parameterisation of the Power Spectra	46
D	Impact of the Prior Range	49

1 Introduction

Cosmic inflation [1–6], a period of accelerated expansion in the early universe, provides a compelling framework for understanding the initial conditions that led to the large-scale structure we observe today. During this epoch, quantum fluctuations in the *inflaton field*, a scalar field driving inflation, are stretched to macroscopic scales, seeding the primordial density perturbations and gravitational waves that later evolve into the cosmic microwave background (CMB) anisotropies and the inhomogeneous distribution of galaxies.

The dynamics of the scalar perturbations are encapsulated in the Mukhanov-Sasaki equation [7, 8], a second-order differential equation governing the evolution of perturbations in the inflating universe. An analogous equation can be defined for the tensor perturbations. Under the slow-roll approximation, where the inflaton field evolves slowly compared to the Hubble expansion rate, it is possible to derive approximate solutions through a perturbative expansion in terms of slow-roll parameters.

The primordial power spectra (PPS) are typically characterised by the scalar spectral index n_s and the tensor-to-scalar ratio r , which are critical parameters for comparing theoretical predictions with observational data from CMB experiments [9–11]. Indeed, the standard phenomenological parameterisation of the dimensionless PPS of scalar and tensor perturbations corresponds to

$$\mathcal{P}_\zeta(k) = A_s \left(\frac{k}{k_*} \right)^{n_s-1}, \quad \mathcal{P}_t(k) = r A_s \left(\frac{k}{k_*} \right)^{n_t}, \quad (1.1)$$

where A_s is the scalar amplitude, n_s (n_t) is the scalar (tensor) spectral index, $r \equiv A_t/A_s$ is the tensor-to-scalar ratio, and $k_* = 0.05 \text{ Mpc}^{-1}$ a reference pivot scale. Eqs. (1.1) can be improved by exploiting the analytic dependence of the slow-roll power spectra of primordial perturbations on the values of the Hubble parameter and the hierarchy of its time derivatives, known as the Hubble flow functions (HFFs)

$$\epsilon_{i+1}(N) = \frac{d \ln |\epsilon_i|}{dN}, \quad \epsilon_1(N) = -\frac{d \ln H}{dN}, \quad (1.2)$$

where $dN \equiv d \ln a$ is the number of e -folds.

Gong and Stewart have utilised the Green’s function technique in Ref. [12] to solve the Mukhanov-Sasaki equation perturbatively; see Refs. [7, 13–18] for earlier work based on the slow-roll perturbative expansion. This approach has provided valuable insights into the power spectra of scalar and tensor perturbations by incorporating higher-order corrections in the slow-roll expansion at second order or next-to-next-to-leading order (NNLO) in Refs. [12, 19, 20] and at third order or next-to-next-to-next-to-leading order (N3LO) in Refs. [21, 22]. In addition to the calculation based on the Green’s function method, derivations based on other approximation schemes are available in the literature, such as the uniform approximation [23], the Wentzel-Kramers-Brillouin (WKB) approximation [24, 25], or the method of comparison equations [26].

Such analytic methods allow one to accurately connect the expansion parameters ϵ_i to the physical parameters of specific single-field slow-roll inflationary models and to deal with a versatile framework to be applied for parameter inference [27–29]. The accuracy of these analytic predictions is crucial, especially in the light of future cosmological surveys that will offer unprecedented precision in measuring the CMB anisotropies and the large-scale structure (LSS) of the Universe.

Cosmological observations from future experiments dedicated to the measurements of CMB polarisation, such as Simons Observatory [30] and CMB-S4 [31, 32], from ground and from space, such as LiteBIRD [33, 34], will be able to reduce the uncertainties on the PPS of scalar and tensor fluctuations. The situation will be further improved by the complementarity of future galaxy survey experiments, such as

from *Euclid* [35–38], that will open for the opportunity of measuring ultra-large scales, thanks to its large observed volume, as well as small scales of matter distribution in the full nonlinear regime. The combination of these will drastically improve our understanding of the early-Universe physics and of cosmic inflation reducing significantly the uncertainties on ϵ_1 , mostly from measurements of the B-mode of the CMB, and reducing the allowed $\epsilon_2 - \epsilon_3$ parameter space, mostly from small-scale measurements (and thanks to the increased the lever arm between the large and small angular scales).

In this paper, we calculate the PPS of scalar and tensor perturbations up to third-order corrections in the slow-roll expansion. While these results have been already presented by Auclair and Ringeval [21], we obtain them with a different approach to the integrals. Moreover, we compare our final findings to the results obtained in Ref. [21], and we systematically compare our results to the numerical solutions of the Mukhanov-Sasaki and tensor perturbation equations to validate the effectiveness and importance of the PPS solutions at third order.

Given the expected sensitivity of current CMB surveys, such as *Planck* [39], ACT [40], SPT [41], and BICEP/Keck [42], we derive constraints on the HFF parameters considering different truncation of the PPS expansion at first order, second order, and third order, investigating the implications on the spectral indices, their runnings, and the running of the runnings. We also present forecasts for a futuristic cosmic-variance level CMB space mission.

We structure the paper as follows. After this introduction, we review the theoretical framework of the Mukhanov-Sasaki and tensor perturbation equations and their solution via Green’s functions in the context of slow-roll inflation and present the derivation of the third-order equations of the PPS in section 2. In section 3, we compare the analytic results with numerical solutions and discuss the implications for a selection of two single-field inflationary models. Section 4 is dedicated to constraints on the slow-roll parameters. We conclude in section 5.

2 Third-Order Calculation

Starting from the action for a single scalar field ϕ minimally coupled to gravity

$$\mathcal{S} = \int d^4x \sqrt{-g} \left[\frac{M_{\text{Pl}}^2}{2} R - \frac{1}{2} \partial_\mu \phi \partial^\mu \phi - V(\phi) \right] \quad (2.1)$$

the Friedmann and Klein-Gordon equations for the cosmological background are, respectively

$$H^2 = \frac{1}{3M_{\text{Pl}}^2} \left(\frac{\dot{\phi}^2}{2} + V \right), \quad \ddot{\phi} + 3H\dot{\phi} + V_\phi = 0, \quad (2.2)$$

where $V_\phi \equiv dV/d\phi$ and the background metric is chosen to be the flat Friedmann-Lemaître-Robertson-Walker one given by

$$ds^2 = -dt^2 + a^2(t) dx^2, \quad (2.3)$$

where t is the proper time, $a(t)$ is the scale factor, and x^i are the three-dimensional comoving spatial coordinates. The equation of motion for the gauge-invariant quantity v at leading order in perturbations, also known as Mukhanov-Sasaki equation for the scalar perturbations, is

$$v_k^{(s,t)''}(\tau) + [k^2 - U^{(s,t)}(\tau)] v_k^{(s,t)}(\tau) = 0, \quad (2.4)$$

where v_k is the mode function in Fourier space, and $'$ means derivative with respect to the conformal time τ , defined as $dt \equiv a(\tau)d\tau$. For the scalar perturbations, the mode function corresponds to the Mukhanov variable $v_k^{(s)}(\tau) \equiv a(\tau)\sqrt{2\epsilon_1(\tau)}\zeta_k(\tau)$ [43] and the potential corresponds to $U^{(s)}(\tau) \equiv z''/z$ where $z(\tau) \equiv a(\tau)\sqrt{2\epsilon_1(\tau)}$. For the tensor perturbations, the mode function corresponds to $v_k^{(t)}(\tau) \equiv a(\tau)h_k(\tau)$ and the potential to $U^{(t)}(\tau) \equiv a''/a$. Following the procedure introduced in Ref. [12], eq. (2.4) can be rewritten as

$$\frac{d^2 y^{(s,t)}}{dx^2} + \left[1 - \frac{U^{(s,t)}(\tau)}{k^2} \right] y^{(s,t)} = 0, \quad (2.5)$$

where $y^{(s,t)} \equiv \sqrt{2k} v_k^{(s,t)}$ and $x \equiv -k\tau$; both $y(x)$ satisfy the asymptotic flat-space vacuum condition, i.e. Bunch-Davies initial conditions

$$\lim_{x \rightarrow \infty} y(x) = e^{ix}. \quad (2.6)$$

Let us then introduce the function $g^{(s,t)}(\ln x) \equiv \tau^2 U^{(s,t)}(x) - 2$. In terms of these functions, we can rewrite eq. (2.5) as

$$\frac{d^2 y^{(s,t)}}{dx^2} + \left(1 - \frac{2}{x^2} \right) y^{(s,t)} = \frac{g^{(s,t)}(\ln x)}{x^2} y^{(s,t)}. \quad (2.7)$$

The solution to eq. (2.7) for both scalar and tensor perturbations, using Green's function method, developed in Ref. [12], can be written in an integral form as

$$y(x) = y_0(x) + \frac{i}{2} \int_x^\infty \frac{du}{u^2} g(\ln u) y(u) [y_0^*(u)y_0(x) - y_0^*(x)y_0(u)], \quad (2.8)$$

where $y_0(x)$ is the solution to the corresponding homogeneous equation, i.e.

$$y_0(x) = \left(1 + \frac{i}{x} \right) e^{ix}. \quad (2.9)$$

The idea is to perform a series expansion for g for both scalar and tensor perturbations as

$$g(\ln x) \equiv \sum_{n=0}^{\infty} \frac{g_{n+1}}{n!} (\ln x)^n, \quad (2.10)$$

where quantity x can then be expressed in terms of the slow-roll parameters up to third order as

$$x = -k \int \frac{dt}{a} \simeq \frac{k}{aH} [1 + \epsilon_1 + \epsilon_1^2 + \epsilon_1^3 + \epsilon_1\epsilon_2 + 3\epsilon_1^2\epsilon_2 + \epsilon_1\epsilon_2^2 + \epsilon_1\epsilon_2\epsilon_3 + \mathcal{O}(\epsilon^4)]. \quad (2.11)$$

Finally, in order to find a perturbatively solution to eq. (2.8), we can expand y as

$$y(x) \equiv \sum_{n=0}^{\infty} y_n(x), \quad (2.12)$$

where $y_0(x)$ is the homogeneous solution eq. (2.9) and $y_n(x)$ is of order n in the slow-roll expansion.

2.1 Primordial Scalar Perturbations

Following Ref. [12], it is convenient to introduce the function

$$f^{(s)}(\ln x) \equiv zx, \quad (2.13)$$

where

$$g^{(s)}(\ln x) = \frac{1}{f^{(s)}} \left[\frac{d^2 f^{(s)}}{(d \ln x)^2} - 3 \frac{d f^{(s)}}{d \ln x} \right]. \quad (2.14)$$

We can express the g_n coefficients in eq. (2.10), for both scalar and tensor perturbations, up to third order as

$$g_1 \simeq -3 \frac{f_1}{f_0} + \frac{f_2}{f_0} \quad (2.15a)$$

$$g_2 \simeq 3 \frac{f_1^2}{f_0^2} - 3 \frac{f_2}{f_0} - \frac{f_1 f_2}{f_0^2} + \frac{f_3}{f_0} \quad (2.15b)$$

$$g_3 \simeq -3 \frac{f_1^3}{f_0^3} + \frac{9}{2} \frac{f_1 f_2}{f_0^2} - \frac{3}{2} \frac{f_3}{f_0}, \quad (2.15c)$$

where, in general, the ratio f_n/f_0 is of order n in the slow-roll parameters. We perform a series expansion also for f as

$$f(\ln x) \equiv \sum_{n=0}^{\infty} \frac{f_n}{n!} (\ln x)^n, \quad (2.16)$$

where the coefficients f_n can be computed from

$$f_n = \left. \frac{d^n f}{(d \ln x)^n} \right|_{x=1}. \quad (2.17)$$

We Taylor expand around $x = 1$ using eq. (2.11). This leads to different coefficient compared to the expansion performed in Ref. [12] around horizon crossing $aH = k$ as explained in Ref. [28]. Keeping terms up to third order in the slow-roll parameters, we

have

$$f_0^{(s)} \simeq \frac{a\dot{\phi}}{H} \Big|_{x=1}, \quad (2.18a)$$

$$f_1^{(s)} \simeq \frac{a\dot{\phi}}{H} \left[1 - \frac{aH}{k} \left(1 + \frac{\epsilon_2}{2} \right) \right]_{x=1}, \quad (2.18b)$$

$$f_2^{(s)} \simeq \frac{a\dot{\phi}}{H} \left[1 - 3\frac{aH}{k} \left(1 + \frac{\epsilon_2}{2} \right) + \left(\frac{aH}{k} \right)^2 \left(2 - \epsilon_1 + \frac{3\epsilon_2}{2} - \frac{\epsilon_1\epsilon_2}{2} + \frac{\epsilon_2\epsilon_3}{2} + \frac{\epsilon_2^2}{4} \right) \right]_{x=1}, \quad (2.18c)$$

$$\begin{aligned} f_3^{(s)} \simeq & \frac{a\dot{\phi}}{H} \left[1 - 7\frac{aH}{k} \left(1 + \frac{\epsilon_2}{2} \right) + \left(\frac{aH}{k} \right)^2 \left(12 - 6\epsilon_1 + 9\epsilon_2 - 3\epsilon_1\epsilon_2 + \frac{3\epsilon_2^2}{2} + 3\epsilon_2\epsilon_3 \right) \right. \\ & - \left(\frac{aH}{k} \right)^3 \left(6 - 7\epsilon_1 + \frac{11\epsilon_2}{2} + 2\epsilon_1^2 + \frac{3\epsilon_2^2}{2} + 3\epsilon_2\epsilon_3 - 6\epsilon_1\epsilon_2 \right. \\ & \left. \left. + \epsilon_1^2\epsilon_2 - \frac{5\epsilon_1\epsilon_2^2}{4} - \frac{3\epsilon_1\epsilon_2\epsilon_3}{2} + \frac{3\epsilon_2^2\epsilon_3}{4} + \frac{\epsilon_2^3}{8} + \frac{\epsilon_2\epsilon_3^2}{2} + \frac{\epsilon_2\epsilon_3\epsilon_4}{2} \right) \right]_{x=1} \end{aligned} \quad (2.18d)$$

and then using eq. (2.15), we find for the primordial scalar perturbations

$$g_1^{(s)} \simeq 3\epsilon_1 + \frac{3}{2}\epsilon_2 + 4\epsilon_1^2 + \frac{13}{2}\epsilon_1\epsilon_2 + \frac{1}{4}\epsilon_2^2 + 5\epsilon_1^3 + \frac{35}{2}\epsilon_1^2\epsilon_2 + \frac{15}{2}\epsilon_1\epsilon_2^2 + \frac{1}{2}\epsilon_2\epsilon_3 + 5\epsilon_1\epsilon_2\epsilon_3, \quad (2.19a)$$

$$g_2^{(s)} \simeq -3\epsilon_1\epsilon_2 - 11\epsilon_1^2\epsilon_2 - \frac{13}{2}\epsilon_1\epsilon_2^2 - \frac{3}{2}\epsilon_2\epsilon_3 - 8\epsilon_1\epsilon_2\epsilon_3 - \frac{1}{2}\epsilon_2^2\epsilon_3 - \frac{1}{2}\epsilon_2\epsilon_3^2 - \frac{1}{2}\epsilon_2\epsilon_3\epsilon_4, \quad (2.19b)$$

$$g_3^{(s)} \simeq \frac{3}{2}\epsilon_1\epsilon_2^2 + \frac{3}{2}\epsilon_1\epsilon_2\epsilon_3 + \frac{3}{4}\epsilon_2\epsilon_3^2 + \frac{3}{4}\epsilon_2\epsilon_3\epsilon_4. \quad (2.19c)$$

2.2 Primordial Tensor Perturbations

We can repeat the same procedure applied to the scalar perturbations on the quantity

$$f^{(t)}(\ln x) \equiv ax, \quad (2.20)$$

where

$$g^{(t)}(\ln x) = \frac{1}{f^{(t)}} \left[\frac{d^2 f^{(t)}}{(d \ln x)^2} - 3 \frac{d f^{(t)}}{d \ln x} \right]. \quad (2.21)$$

For tensor perturbations, f and g coefficients up to third order correspond to

$$f_0^{(t)} \simeq a|_{x=1}, \quad (2.22a)$$

$$f_1^{(t)} \simeq a \left(1 - \frac{aH}{k} \right)_{x=1}, \quad (2.22b)$$

$$f_2^{(t)} \simeq a \left[1 - 3 \frac{aH}{k} + \left(\frac{aH}{k} \right)^2 (2 - \epsilon_1) \right]_{x=1}, \quad (2.22c)$$

$$f_3^{(t)} \simeq a \left[1 - 7 \frac{aH}{k} + \left(\frac{aH}{k} \right)^2 (12 - 6\epsilon_1) - \left(\frac{aH}{k} \right)^3 (6 - 7\epsilon_1 + 2\epsilon_1^2 - \epsilon_1\epsilon_2) \right]_{x=1} \quad (2.22d)$$

and

$$g_1^{(t)} \simeq 3\epsilon_1 + 4\epsilon_1^2 + 4\epsilon_1\epsilon_2 + 5\epsilon_1^3 + 14\epsilon_1^2\epsilon_2 + 4\epsilon_1\epsilon_2^2 + 4\epsilon_1\epsilon_2\epsilon_3, \quad (2.23a)$$

$$g_2^{(t)} \simeq -3\epsilon_1\epsilon_2 - 11\epsilon_1^2\epsilon_2 - 4\epsilon_1\epsilon_2^2 - 4\epsilon_1\epsilon_2\epsilon_3, \quad (2.23b)$$

$$g_3^{(t)} \simeq \frac{3}{2}\epsilon_1\epsilon_2^2 + \frac{3}{2}\epsilon_1\epsilon_2\epsilon_3. \quad (2.23c)$$

2.3 The Primordial Power Spectra Including Third-Order Corrections

Now that we have the g_n for both scalar and tensor perturbations up to third-order in slow-roll parameters, in order to solve eq. (2.7) we need to calculate the recursive solutions of eq. (2.8) up to third-order corrections, which corresponds to

$$y(x) \simeq y_0(x) + y_1(x) + y_2(x) + y_3(x). \quad (2.24)$$

In this case there are unique solutions for y_0 , y_1 , y_2 , and y_3 since the dependence on the slow-roll parameters, thus the differences between scalar and tensor perturbations, are only encoded in the g_n functions.

Since the right hand side of eq. (2.7) is at least of order one in the slow-roll expansion, the lowest order solution to that equation is simply the homogeneous solution $y_0(x)$, eq. (2.9).

The first-order correction to eq. (2.9) is obtained by substituting $g = g_1$ and $y = y_0$ into the right hand side of eq. (2.8), we can easily find

$$\begin{aligned} y_1(x) &= \frac{ig_1}{2} \int_x^\infty \frac{du}{u^2} y_0(u) [y_0^*(u)y_0(x) - y_0^*(x)y_0(u)] \\ &= \frac{ig_1}{3} \left[\frac{2}{x} e^{ix} + i y_0^*(x) \int_x^\infty \frac{du}{u} e^{2iu} \right]. \end{aligned} \quad (2.25)$$

The second-order correction is made of two pieces, namely

$$y_2(x) = y_{21}(x) + y_{22}(x), \quad (2.26)$$

where we substitute $g = g_1 + g_2 \ln x$ and $y = y_0 + y_1$ into eq. (2.8) finding

$$\begin{aligned} y_{21}(x) &= \frac{ig_1}{2} \int_x^\infty \frac{du}{u^2} y_1(u) [y_0^*(u)y_0(x) - y_0^*(x)y_0(u)] \\ &= -\frac{ig_1^2}{9} \left[\frac{2}{3x} e^{ix} - \left(\frac{5}{3x} - \frac{i}{3} \right) e^{-ix} \int_x^\infty \frac{du}{u} e^{2iu} + i y_0(x) \int_x^\infty \frac{du}{u} e^{-2iu} \int_u^\infty \frac{dt}{t} e^{2it} \right] \end{aligned} \quad (2.27a)$$

$$\begin{aligned} y_{22}(x) &= \frac{ig_2}{2} \int_x^\infty \frac{du}{u^2} y_0(u) \ln u [y_0^*(u)y_0(x) - y_0^*(x)y_0(u)] \\ &= \frac{ig_2}{3} \left[\frac{8}{3x} e^{ix} + \frac{2}{x} \ln x e^{ix} + \frac{7i}{3} y_0^*(x) \int_x^\infty \frac{du}{u} e^{2iu} + i y_0^*(x) \int_x^\infty \frac{du}{u} e^{2iu} \ln u \right]. \end{aligned} \quad (2.27b)$$

The third-order correction is made of three pieces, namely

$$y_3(x) = y_{31}(x) + y_{32}(x) + y_{33}(x), \quad (2.28)$$

here, we substitute $g = g_1 + g_2 \ln x + g_3 \ln^2 x$ and $y = y_0 + y_1 + y_2$ into eq. (2.8) finding

$$y_{31}(x) \equiv \frac{ig_1}{2} \int_x^\infty \frac{du}{u^2} y_2(u) [y_0^*(u)y_0(x) - y_0^*(x)y_0(u)] \quad (2.29a)$$

$$y_{32}(x) \equiv \frac{ig_2}{2} \int_x^\infty \frac{du}{u^2} y_1(u) \ln u [y_0^*(u)y_0(x) - y_0^*(x)y_0(u)] \quad (2.29b)$$

$$y_{33}(x) \equiv \frac{ig_3}{4} \int_x^\infty \frac{du}{u^2} y_0(u) \ln^2 u [y_0^*(u)y_0(x) - y_0^*(x)y_0(u)]. \quad (2.29c)$$

Because of the large number of terms, it is worth considering these three contributions separately. Splitting the first contribution to the third-order correction, taking into account eqs. (2.27a) and (2.27b), we have

$$\begin{aligned} y_{31}(x) &= \frac{g_1^3}{18} \int_x^\infty \frac{du}{u^2} \left[\frac{2e^{iu}}{3u} - \left(\frac{5}{3u} - \frac{i}{3} \right) e^{-iu} \int_u^\infty \frac{dt}{t} e^{2it} + i y_0(u) \int_u^\infty \frac{dt}{t} e^{-2it} \int_t^\infty \frac{ds}{s} e^{2is} \right] \\ &\quad [y_0^*(u)y_0(x) - y_0^*(x)y_0(u)] \\ &\quad - \frac{g_1 g_2}{6} \int_x^\infty \frac{du}{u^2} \left[\frac{8e^{iu}}{3u} + \frac{2e^{iu} \ln u}{u} + \frac{7i}{3} y_0^*(u) \int_u^\infty \frac{dt}{t} e^{2it} + i y_0^*(u) \int_u^\infty \frac{dt}{t} e^{2it} \ln t \right] \\ &\quad [y_0^*(u)y_0(x) - y_0^*(x)y_0(u)] \\ &\equiv y_{311} + y_{312}. \end{aligned} \quad (2.30a)$$

These two terms correspond to

$$\begin{aligned} y_{311} &= \frac{g_1^3}{27} \left[\frac{4ie^{ix}}{9x} - \left(\frac{2}{9} + \frac{10i}{9x} \right) e^{-ix} \int_x^\infty \frac{du}{u} e^{2iu} + \frac{2}{3} \left(-1 + \frac{2i}{x} \right) e^{ix} \int_x^\infty \frac{du}{u} e^{-2iu} \int_u^\infty \frac{dt}{t} e^{2it} \right. \\ &\quad \left. - \left(1 - \frac{i}{x} \right) e^{-ix} \int_x^\infty \frac{du}{u} e^{2iu} \int_u^\infty \frac{dt}{t} e^{-2it} \int_t^\infty \frac{ds}{s} e^{2is} \right] \end{aligned} \quad (2.31a)$$

and

$$\begin{aligned}
y_{312} = & \frac{i g_1 g_2}{9} \left[- \left(\frac{28}{9x} + \frac{2 \ln x}{3x} \right) e^{ix} - \left(\frac{26i}{9} - \frac{16}{9x} \right) e^{-ix} \int_x^\infty \frac{du}{u} e^{2iu} \right. \\
& + \left(\frac{5}{3x} - \frac{i}{3} \right) e^{-ix} \int_x^\infty \frac{du}{u} e^{2iu} \ln u + \frac{7}{3} \left(\frac{1}{x} - i \right) e^{ix} \int_x^\infty \frac{du}{u} e^{-2iu} \int_u^\infty \frac{dt}{t} e^{2it} \\
& \left. + \left(\frac{1}{x} - i \right) e^{ix} \int_x^\infty \frac{du}{u} e^{-2iu} \int_u^\infty \frac{dt}{t} e^{2it} \ln t \right]. \quad (2.31b)
\end{aligned}$$

Here, it is convenient to rewrite the last integral as

$$\int_x^\infty \frac{du}{u} e^{-2iu} \int_u^\infty \frac{dt}{t} e^{2it} \ln t = \int_x^\infty \frac{du}{u} e^{-2iu} \int_x^\infty \frac{dt}{t} e^{2it} \ln t - \int_x^\infty \frac{du}{u} e^{2iu} \ln u \int_u^\infty \frac{dt}{t} e^{-2it}. \quad (2.32)$$

For the second contribution to the third-order correction, taking into account eq. (2.25), we have

$$y_{32}(x) = -\frac{g_1 g_2}{6} \int_x^\infty \frac{du}{u^2} \left[\frac{2e^{iu}}{u} + i y_0^*(u) \int_u^\infty \frac{dt}{t} e^{2it} \right] \ln u [y_0^*(u) y_0(x) - y_0^*(x) y_0(u)]. \quad (2.33)$$

The result is

$$\begin{aligned}
y_{32}(x) = & \frac{i g_1 g_2}{9} \left[- \left(\frac{28}{9x} + \frac{2 \ln x}{3x} \right) e^{ix} - \left(\frac{26i}{9} + \frac{2}{9x} - \frac{2 \ln x}{x} \right) e^{-ix} \int_x^\infty \frac{du}{u} e^{2iu} \right. \\
& - \frac{1}{3} \left(\frac{1}{x} + i \right) e^{-ix} \int_x^\infty \frac{du}{u} e^{2iu} \ln u + \frac{7}{3} \left(\frac{1}{x} - i \right) e^{ix} \int_x^\infty \frac{du}{u} e^{-2iu} \int_u^\infty \frac{dt}{t} e^{2it} \\
& \left. + \left(\frac{1}{x} - i \right) e^{ix} \int_x^\infty \frac{du}{u} e^{-2iu} \ln u \int_u^\infty \frac{dt}{t} e^{2it} \right]. \quad (2.34)
\end{aligned}$$

The third contribution to the third-order correction, taking into account eq. (2.9), reads

$$y_{33}(x) = \frac{i g_3}{4} \int_x^\infty \frac{du}{u^2} \left(1 + \frac{i}{u} \right) e^{iu} \ln^2 u [y_0^*(u) y_0(x) - y_0^*(x) y_0(u)]. \quad (2.35)$$

The result is

$$\begin{aligned}
y_{33}(x) = & \frac{i g_3}{6} \left[\left(\frac{52}{9x} + \frac{16 \ln x}{3x} + \frac{2 \ln^2 x}{x} \right) e^{ix} + \frac{50}{9} \left(\frac{1}{x} + i \right) e^{-ix} \int_x^\infty \frac{du}{u} e^{2iu} \right. \\
& \left. + \frac{14}{3} \left(\frac{1}{x} + i \right) e^{-ix} \int_x^\infty \frac{du}{u} e^{2iu} \ln u + \left(\frac{1}{x} + i \right) e^{-ix} \int_x^\infty \frac{du}{u} e^{2iu} \ln^2 u \right]. \quad (2.36)
\end{aligned}$$

We have collected in appendix A the integral manipulations, iterating integration by parts, used to obtain the results reported here.

We are interested in the asymptotic form of $y(x)$ in the super-Hubble limit, that is $x \rightarrow 0$; in this limit the asymptotic forms for $y_0(x)$, $y_1(x)$, $y_{21}(x)$, $y_{22}(x)$, $y_{31}(x)$, $y_{32}(x)$, and $y_{33}(x)$ are

$$y_0(x) \rightarrow ix^{-1} \quad (2.37a)$$

$$y_1(x) \rightarrow \frac{ig_1}{3} \left[\left(\alpha + \frac{i\pi}{2} \right) x^{-1} - \frac{\ln x}{x} \right] \quad (2.37b)$$

$$y_{21}(x) \rightarrow \frac{ig_1^2}{18} \left[\left(i\pi\alpha - \frac{i\pi}{3} + \frac{\pi^2}{4} + \alpha^2 - \frac{2}{3}\alpha - 4 \right) x^{-1} - 2 \left(\alpha - \frac{1}{3} + \frac{i\pi}{2} \right) \frac{\ln x}{x} + \frac{\ln^2 x}{x} \right] \quad (2.37c)$$

$$y_{22}(x) \rightarrow \frac{ig_2}{6} \left[\left(\frac{i\pi}{3} - \frac{\pi^2}{12} + \frac{2\alpha}{3} + i\pi\alpha + \alpha^2 \right) x^{-1} - \frac{2 \ln x}{3x} - \frac{\ln^2 x}{x} \right] \quad (2.37d)$$

$$\begin{aligned} y_{31}(x) \rightarrow & \frac{ig_1^3}{27} \left[\left(\frac{\alpha^3}{6} - \frac{\alpha^2}{3} + \frac{i\pi\alpha^2}{4} + \frac{\pi^2\alpha}{8} - \frac{16\alpha}{9} - \frac{i\pi\alpha}{3} - \frac{7\zeta(3)}{3} + 4 - \frac{\pi^2}{12} + \frac{5i\pi^3}{48} - \frac{8i\pi}{9} \right) x^{-1} \right. \\ & + \left(-\frac{\alpha^2}{2} - \frac{i\pi\alpha}{2} + \frac{2\alpha}{3} + \frac{i\pi}{3} - \frac{\pi^2}{8} + \frac{16}{9} \right) \frac{\ln x}{x} \\ & + \left. \left(\frac{\alpha}{2} - \frac{1}{3} + \frac{i\pi}{4} \right) \frac{\ln^2 x}{x} - \frac{\ln^3 x}{6x} \right] \\ & + \frac{ig_1g_2}{6} \left[\left(\frac{\alpha^3}{3} - \frac{2\alpha^2}{3} + \frac{i\pi\alpha^2}{6} + \frac{5\pi^2\alpha}{36} + \frac{4i\alpha}{3} - \frac{4\alpha}{27} + \frac{2i\pi\alpha}{3} + \frac{4i}{3} - \frac{16}{9} \right. \right. \\ & - \frac{7\pi^2}{54} + \frac{i\pi^3}{72} - \frac{38i\pi}{27} + \frac{2\pi}{3} \left. \right) x^{-1} - \left(\frac{\alpha^2}{3} + \frac{2\alpha}{9} + \frac{i\pi\alpha}{3} - \frac{\pi^2}{36} - \frac{4}{27} + \frac{i\pi}{9} \right) \frac{\ln x}{x} \\ & + \left. \frac{2 \ln^2 x}{9x} + \frac{\ln^3 x}{9x} \right] \quad (2.37e) \end{aligned}$$

$$\begin{aligned} y_{32}(x) \rightarrow & \frac{ig_1g_2}{6} \left[\left(\frac{2\alpha^2}{3} + \frac{4i\alpha}{3} - \frac{76\alpha}{27} + \frac{2i\pi\alpha}{3} + \frac{4i}{3} + \frac{8}{9} - \frac{38i\pi}{27} - \frac{2\pi}{3} + \frac{11\pi^2}{54} \right) x^{-1} \right. \\ & - \left. \left(\frac{2\alpha}{9} + \frac{i\pi}{9} - \frac{4}{27} \right) \frac{\ln x}{x} - \left(\frac{\alpha}{3} + \frac{i\pi}{6} - \frac{2}{9} \right) \frac{\ln^2 x}{x} + \frac{2 \ln^3 x}{9x} \right] \quad (2.37f) \end{aligned}$$

$$\begin{aligned} y_{33}(x) \rightarrow & \frac{ig_3}{6} \left[\left(\frac{\alpha^3}{3} + \frac{\alpha^2}{3} + \frac{i\pi\alpha^2}{2} + \frac{2\alpha}{9} + \frac{i\pi\alpha}{3} - \frac{\pi^2\alpha}{12} - \frac{2\zeta(3)}{3} \right. \right. \\ & + \left. \left. \frac{i\pi}{9} + \frac{4}{3} + \frac{i\pi^3}{24} - \frac{\pi^2}{36} \right) x^{-1} - \frac{2 \ln x}{9x} - \frac{\ln^2 x}{3x} - \frac{\ln^3 x}{3x} \right] \quad (2.37g) \end{aligned}$$

where $\alpha \equiv 2 - \ln 2 - \gamma$ and $\gamma \simeq 0.5772$ is the Euler-Mascheroni constant. We have described in appendix B the procedure adopted to derive the super-Hubble solutions of the integrals needed to derive the asymptotic solution above.

2.3.1 The Primordial Power Spectrum of Scalar Perturbations

The dimensionless PPS of the comoving curvature perturbation ζ_k is defined as

$$\mathcal{P}_\zeta(k) = \frac{k^3}{2\pi^2} \lim_{x \rightarrow 0} |\zeta_k|^2 = \frac{k^3}{2\pi^2} \lim_{x \rightarrow 0} \left| \frac{v_k^{(s)}}{z} \right|^2 = \frac{k^2}{4\pi^2} \lim_{x \rightarrow 0} \left| \frac{y^{(s)}}{z} \right|^2. \quad (2.38)$$

We are interested in the evaluation of the PPS at horizon crossing. While we have already expanded the g_n around $x = 1$, we have to perform the same expansion for the squared modulus of $1/(xz)$ entering eq. (2.38) when writing explicitly $y^{(s)}$, that corresponds to

$$\begin{aligned} \left| \frac{1}{xz} \right|^2 &\simeq \left(\frac{H^2}{k\dot{\phi}} \right)^2 \left[1 - 2\epsilon_1 - 2\epsilon_1\epsilon_2 + \epsilon_1^2 - 2\epsilon_1\epsilon_2^2 - 2\epsilon_1\epsilon_2\epsilon_3 \right. \\ &\quad + (2\epsilon_1 + \epsilon_2 + \epsilon_1\epsilon_2 - 2\epsilon_1^2 - 2\epsilon_1^2\epsilon_2 + \epsilon_1\epsilon_2^2 + 2\epsilon_1\epsilon_2\epsilon_3) \ln x \\ &\quad + \left(2\epsilon_1^2 + \epsilon_1\epsilon_2 + \frac{\epsilon_2^2}{2} - \frac{\epsilon_2\epsilon_3}{2} + 3\epsilon_1^2\epsilon_2 + \frac{\epsilon_1\epsilon_2^2}{2} - \epsilon_1\epsilon_2\epsilon_3 \right) \ln^2 x \\ &\quad \left. + \left(\frac{4\epsilon_1^3}{3} + \frac{\epsilon_1\epsilon_2^2}{3} + \frac{\epsilon_2^3}{6} - \frac{2\epsilon_1\epsilon_2\epsilon_3}{3} - \frac{\epsilon_2^2\epsilon_3}{2} + \frac{\epsilon_2\epsilon_3^2}{6} + \frac{\epsilon_2\epsilon_3\epsilon_4}{6} \right) \ln^3 x \right]. \end{aligned} \quad (2.39)$$

Finally, we expand the HFF and the Hubble parameter around a conformal time τ_* as

$$\begin{aligned} \epsilon_i(\tau) &\simeq \epsilon_{i*} \left[1 - \epsilon_{i+1*}(1 + \epsilon_{1*} + \epsilon_{1*}^2 + \epsilon_{1*}\epsilon_{2*}) \ln \left(\frac{\tau}{\tau_*} \right) \right. \\ &\quad + \frac{\epsilon_{i+1*}}{2} (\epsilon_{i+1*} + \epsilon_{i+2*} + \epsilon_{1*}\epsilon_{2*} + 2\epsilon_{1*}\epsilon_{i+1*} + 2\epsilon_{1*}\epsilon_{i+2*}) \ln^2 \left(\frac{\tau}{\tau_*} \right) \\ &\quad \left. - \frac{\epsilon_{i+1*}}{6} (\epsilon_{i+1*}^2 + \epsilon_{i+2*}^2 + 3\epsilon_{i+1*}\epsilon_{i+2*} + \epsilon_{i+2*}\epsilon_{i+3*}) \ln^3 \left(\frac{\tau}{\tau_*} \right) \right], \end{aligned} \quad (2.40)$$

$$\begin{aligned} H(\tau) &\simeq H_* \left[1 + (\epsilon_{1*} + \epsilon_{1*}^2 + \epsilon_{1*}^3 + \epsilon_{1*}^2\epsilon_{2*}) \ln \left(\frac{\tau}{\tau_*} \right) \right. \\ &\quad + \left(\frac{\epsilon_{1*}^2}{2} + \epsilon_{1*}^3 - \frac{1}{2}\epsilon_{1*}\epsilon_{2*} - \frac{3}{2}\epsilon_{1*}^2\epsilon_{2*} \right) \ln^2 \left(\frac{\tau}{\tau_*} \right) \\ &\quad \left. + \left(\frac{\epsilon_{1*}^3}{6} - \frac{1}{2}\epsilon_{1*}^2\epsilon_{2*} + \frac{1}{6}\epsilon_{1*}\epsilon_{2*}^2 + \frac{1}{6}\epsilon_{1*}\epsilon_{2*}\epsilon_{3*} \right) \ln^3 \left(\frac{\tau}{\tau_*} \right) \right]. \end{aligned} \quad (2.41)$$

Actually, in order to compute the scalar PPS, we need the squared expansion of the Hubble parameter, which reads

$$\begin{aligned} H^2(\tau) &\simeq H_*^2 \left[1 + (2\epsilon_{1*} + 2\epsilon_{1*}^2 + 2\epsilon_{1*}^3 + 2\epsilon_{1*}^2\epsilon_{2*}) \ln \left(\frac{\tau}{\tau_*} \right) \right. \\ &\quad + (2\epsilon_{1*}^2 + 4\epsilon_{1*}^3 - \epsilon_{1*}\epsilon_{2*} - 3\epsilon_{1*}^2\epsilon_{2*}) \ln^2 \left(\frac{\tau}{\tau_*} \right) \\ &\quad \left. + \left(\frac{4\epsilon_{1*}^3}{3} - 2\epsilon_{1*}^2\epsilon_{2*} + \frac{1}{3}\epsilon_{1*}\epsilon_{2*}^2 + \frac{1}{3}\epsilon_{1*}\epsilon_{2*}\epsilon_{3*} \right) \ln^3 \left(\frac{\tau}{\tau_*} \right) \right]. \end{aligned} \quad (2.42)$$

By combining eq. (2.38) with eqs. (2.19), (2.24), (2.39), (2.40) and (2.42), the

dimensionless PPS for scalar fluctuation expanded around the pivot scale k_* reads

$$\begin{aligned}
\mathcal{P}_\zeta(k) = & \frac{H_*^2}{8\pi^2\epsilon_{1*}} \left\{ \left[1 - 2(1-\alpha)\epsilon_{1*} + \left(-3 - 2\alpha + 2\alpha^2 + \frac{\pi^2}{2} \right) \epsilon_{1*}^2 + \alpha\epsilon_{2*} \right. \right. \\
& + \left(-6 + \alpha + \alpha^2 + \frac{7\pi^2}{12} \right) \epsilon_{1*}\epsilon_{2*} + \frac{1}{8} (-8 + 4\alpha^2 + \pi^2) \epsilon_{2*}^2 \\
& + \frac{1}{24} (-12\alpha^2 + \pi^2) \epsilon_{2*}\epsilon_{3*} - \frac{1}{24} (-16 + 24\alpha - 4\alpha^3 - 3\alpha\pi^2 + 2\zeta(3)) (8\epsilon_{1*}^3 + \epsilon_{2*}^3) \\
& + \frac{1}{12} (-72\alpha + 36\alpha^2 + 13\pi^2 + 8\alpha\pi^2 - 12\zeta(3)) \epsilon_{1*}^2\epsilon_{2*} \\
& - \frac{1}{24} (16 + 24\alpha - 12\alpha^2 - 8\alpha^3 - 15\pi^2 - 6\alpha\pi^2 + 28\zeta(3)) \epsilon_{1*}\epsilon_{2*}^2 \\
& + \frac{1}{24} (16 + 4\alpha^3 - \alpha\pi^2 - 8\zeta(3)) (\epsilon_{2*}\epsilon_{3*}^2 + \epsilon_{2*}\epsilon_{3*}\epsilon_{4*}) \\
& + \frac{1}{24} (48\alpha - 12\alpha^3 - 5\alpha\pi^2) \epsilon_{2*}^2\epsilon_{3*} \\
& \left. + \frac{1}{12} (-8 + 72\alpha - 12\alpha^2 - 8\alpha^3 + \pi^2 - 6\alpha\pi^2 - 8\zeta(3)) \epsilon_{1*}\epsilon_{2*}\epsilon_{3*} \right] \\
& + \left[-2\epsilon_{1*} + 2(-2\alpha + 1)\epsilon_{1*}^2 - \epsilon_{2*} + (-2\alpha - 1)\epsilon_{1*}\epsilon_{2*} - \alpha\epsilon_{2*}^2 + \alpha\epsilon_{2*}\epsilon_{3*} \right. \\
& - \frac{1}{8} (-8 + 4\alpha^2 + \pi^2) (8\epsilon_{1*}^3 + \epsilon_{2*}^3) - \frac{2}{3} (-9 + 9\alpha + \pi^2) \epsilon_{1*}^2\epsilon_{2*} \\
& - \frac{1}{4} (-4 + 4\alpha + 4\alpha^2 + \pi^2) \epsilon_{1*}\epsilon_{2*}^2 + \frac{1}{2} (-12 + 4\alpha + 4\alpha^2 + \pi^2) \epsilon_{1*}\epsilon_{2*}\epsilon_{3*} \\
& + \frac{1}{24} (-12\alpha^2 + \pi^2) (\epsilon_{2*}\epsilon_{3*}^2 + \epsilon_{2*}\epsilon_{3*}\epsilon_{4*}) + \frac{1}{24} (-48 + 36\alpha^2 + 5\pi^2) \epsilon_{2*}^2\epsilon_{3*} \left. \right] \ln\left(\frac{k}{k_*}\right) \\
& + \frac{1}{2} \left[4\epsilon_{1*}^2 + 2\epsilon_{1*}\epsilon_{2*} + 6\epsilon_{1*}^2\epsilon_{2*} + \epsilon_{2*}^2 - \epsilon_{2*}\epsilon_{3*} + (1 + 2\alpha)(\epsilon_{1*}\epsilon_{2*}^2 - 2\epsilon_{1*}\epsilon_{2*}\epsilon_{3*}) \right. \\
& \left. + \alpha(8\epsilon_{1*}^3 + \epsilon_{2*}^3 - 3\epsilon_{2*}^2\epsilon_{3*} + \epsilon_{2*}\epsilon_{3*}^2 + \epsilon_{2*}\epsilon_{3*}\epsilon_{4*}) \right] \ln^2\left(\frac{k}{k_*}\right) \\
& + \frac{1}{6} \left(-8\epsilon_{1*}^3 - 2\epsilon_{1*}\epsilon_{2*}^2 - \epsilon_{2*}^3 + 4\epsilon_{1*}\epsilon_{2*}\epsilon_{3*} + 3\epsilon_{2*}^2\epsilon_{3*} - \epsilon_{2*}\epsilon_{3*}^2 - \epsilon_{2*}\epsilon_{3*}\epsilon_{4*} \right) \ln^3\left(\frac{k}{k_*}\right) \left. \right\} \\
\end{aligned} \tag{2.43}$$

where all the terms divergent in eq. (2.37) proportional to $\ln x$ cancel exactly. Here, we have written the scalar PPS with respect to a fixed pivot scale k_* , using $k_*\tau_* = -1$ leading to

$$\frac{\tau}{\tau_*} = -\frac{k}{k_*}. \tag{2.44}$$

From eq. (2.43), we can derive the third-order slow-roll expansion for the scalar spectral index n_s and its runnings α_s and β_s . We can define the scalar spectral index

as

$$\begin{aligned}
n_s(k) &\equiv 1 + \frac{d \ln \mathcal{P}_\zeta}{d \ln k} & (2.45) \\
&= \left[1 - 2\epsilon_{1*} - \epsilon_{2*} - 2\epsilon_{1*}^2 - (3 - 2\alpha)\epsilon_{1*}\epsilon_{2*} + \alpha\epsilon_{2*}\epsilon_{3*} - 2\epsilon_{1*}^3 \right. \\
&\quad + (-15 + 6\alpha + \pi^2)\epsilon_{1*}^2\epsilon_{2*} + \frac{1}{12}(-84 + 36\alpha - 12\alpha^2 + 7\pi^2)\epsilon_{1*}\epsilon_{2*}^2 \\
&\quad + \frac{1}{12}(-72 + 48\alpha - 12\alpha^2 + 7\pi^2)\epsilon_{1*}\epsilon_{2*}\epsilon_{3*} + \frac{1}{4}(-8 + \pi^2)\epsilon_{2*}^2\epsilon_{3*} \\
&\quad \left. + \left(-\frac{\alpha^2}{2} + \frac{\pi^2}{24}\right)\epsilon_{2*}\epsilon_{3*}^2 + \left(-\frac{\alpha^2}{2} + \frac{\pi^2}{24}\right)\epsilon_{2*}\epsilon_{3*}\epsilon_{4*} \right] \\
&\quad + (-2\epsilon_{1*}\epsilon_{2*} - 6\epsilon_{1*}^2\epsilon_{2*} - 3\epsilon_{1*}\epsilon_{2*}^2 + 2\alpha\epsilon_{1*}\epsilon_{2*}^2 - \epsilon_{2*}\epsilon_{3*} - 4\epsilon_{1*}\epsilon_{2*}\epsilon_{3*} \\
&\quad + 2\alpha\epsilon_{1*}\epsilon_{2*}\epsilon_{3*} + \alpha\epsilon_{2*}\epsilon_{3*}^2 + \alpha\epsilon_{2*}\epsilon_{3*}\epsilon_{4*}) \ln\left(\frac{k}{k_*}\right) \\
&\quad + \left(-\epsilon_{1*}\epsilon_{2*}^2 - \epsilon_{1*}\epsilon_{2*}\epsilon_{3*} - \frac{1}{2}\epsilon_{2*}\epsilon_{3*}^2 - \frac{1}{2}\epsilon_{2*}\epsilon_{3*}\epsilon_{4*}\right) \ln^2\left(\frac{k}{k_*}\right). & (2.46)
\end{aligned}$$

The running of the scalar spectral index [44] reads

$$\alpha_s(k) \equiv \frac{dn_s}{d \ln k} \quad (2.47)$$

$$\begin{aligned}
&= [-2\epsilon_{1*}\epsilon_{2*} - \epsilon_{2*}\epsilon_{3*} - 6\epsilon_{1*}^2\epsilon_{2*} + (-3 + 2\alpha)\epsilon_{1*}\epsilon_{2*}^2 - 2(2 - \alpha)\epsilon_{1*}\epsilon_{2*}\epsilon_{3*} + \alpha\epsilon_{2*}\epsilon_{3*}^2 \\
&\quad + \alpha\epsilon_{2*}\epsilon_{3*}\epsilon_{4*}] + (-2\epsilon_{1*}\epsilon_{2*}^2 - 2\epsilon_{1*}\epsilon_{2*}\epsilon_{3*} - \epsilon_{2*}\epsilon_{3*}^2 - \epsilon_{2*}\epsilon_{3*}\epsilon_{4*}) \ln\left(\frac{k}{k_*}\right). \quad (2.48)
\end{aligned}$$

The running of the running of the scalar spectral index is given by

$$\beta_s(k) \equiv \frac{d\alpha_s}{d \ln k} \quad (2.49)$$

$$= -2\epsilon_{1*}\epsilon_{2*}^2 - 2\epsilon_{1*}\epsilon_{2*}\epsilon_{3*} - \epsilon_{2*}\epsilon_{3*}^2 - \epsilon_{2*}\epsilon_{3*}\epsilon_{4*}. \quad (2.50)$$

2.3.2 The Primordial Power Spectrum of Tensor Perturbations

The dimensionless PPS for the two polarisation of gravitational waves generated during inflation, defined as

$$\mathcal{P}_t(k) \equiv 2\mathcal{P}_h(k) = \frac{2k^3}{\pi^2} \lim_{x \rightarrow 0} |h_k|^2 = \frac{2k^3}{\pi^2} \lim_{x \rightarrow 0} \left| \frac{v_k^{(t)}}{a} \right|^2 = \frac{k^2}{\pi^2} \lim_{x \rightarrow 0} \left| \frac{y^{(t)}}{a} \right|^2, \quad (2.51)$$

can be easily calculated following the same procedure described before and substituting eq. (2.23) to the asymptotic solutions in eq. (2.37), where for primordial tensor

fluctuations we need

$$\begin{aligned}
\left| \frac{1}{xa} \right|^2 &\simeq \left(\frac{H}{k} \right)^2 \left[1 - 2\epsilon_1 - 2\epsilon_1\epsilon_2 + \epsilon_1^2 - 2\epsilon_1\epsilon_2^2 - 2\epsilon_1\epsilon_2\epsilon_3 \right. \\
&\quad + (2\epsilon_1 + 2\epsilon_1\epsilon_2 - 2\epsilon_1^2 - 2\epsilon_1^2\epsilon_2 + 2\epsilon_1\epsilon_2^2 + 2\epsilon_1\epsilon_2\epsilon_3) \ln x \\
&\quad + (2\epsilon_1^2 - \epsilon_1\epsilon_2 + 3\epsilon_1^2\epsilon_2 - \epsilon_1\epsilon_2^2 - \epsilon_1\epsilon_2\epsilon_3) \ln^2 x \\
&\quad \left. + \frac{1}{3} (4\epsilon_1^3 - 6\epsilon_1^2\epsilon_2 + \epsilon_1\epsilon_2^2 + \epsilon_1\epsilon_2\epsilon_3) \ln^3 x \right]. \tag{2.52}
\end{aligned}$$

Results for the dimensionless PPS, tensor spectral index, running of the tensor spectral index, and running of the running of the tensor spectral index, expanded around a pivot scale k_* , are reported below. We find respectively

$$\begin{aligned}
\mathcal{P}_t(k) &= \frac{2H_*^2}{\pi^2} \left\{ \left[1 + (-2 + 2\alpha)\epsilon_{1*} + \frac{1}{2}(-6 - 4\alpha + 4\alpha^2 + \pi^2)\epsilon_{1*}^2 \right. \right. \\
&\quad + \left(-2 + 2\alpha - \alpha^2 + \frac{\pi^2}{12} \right) \epsilon_{1*}\epsilon_{2*} - \frac{1}{3}(-16 + 24\alpha - 4\alpha^3 - 3\alpha\pi^2 + 2\zeta(3))\epsilon_{1*}^3 \\
&\quad + \frac{1}{12}(-96 + 72\alpha + 36\alpha^2 - 24\alpha^3 + 13\pi^2 - 10\alpha\pi^2)\epsilon_{1*}^2\epsilon_{2*} \\
&\quad \left. - \frac{1}{12}(8 - 24\alpha + 12\alpha^2 - 4\alpha^3 - \pi^2 + \alpha\pi^2 + 8\zeta(3))(\epsilon_{1*}\epsilon_{2*}^2 + \epsilon_{1*}\epsilon_{2*}\epsilon_{3*}) \right] \\
&\quad + \left[-2\epsilon_{1*} + 2\epsilon_{1*}^2 - 4\alpha\epsilon_{1*}^2 + (-2 + 2\alpha)\epsilon_{1*}\epsilon_{2*} - (-8 + 4\alpha^2 + \pi^2)\epsilon_{1*}^3 \right. \\
&\quad + \frac{1}{6}(-36 - 36\alpha + 36\alpha^2 + 5\pi^2)\epsilon_{1*}^2\epsilon_{2*} \\
&\quad \left. + \frac{1}{12}(-24 + 24\alpha - 12\alpha^2 + \pi^2)(\epsilon_{1*}\epsilon_{2*}^2 + \epsilon_{1*}\epsilon_{2*}\epsilon_{3*}) \right] \ln \left(\frac{k}{k_*} \right) \\
&\quad + [2\epsilon_{1*}^2 + 4\alpha\epsilon_{1*}^3 - \epsilon_{1*}\epsilon_{2*} + (3 - 6\alpha)\epsilon_{1*}^2\epsilon_{2*} - (-\alpha + 1)(\epsilon_{1*}\epsilon_{2*}^2 + \epsilon_{1*}\epsilon_{2*}\epsilon_{3*})] \ln^2 \left(\frac{k}{k_*} \right) \\
&\quad \left. + \frac{1}{3} (-4\epsilon_{1*}^3 + 6\epsilon_{1*}^2\epsilon_{2*} - \epsilon_{1*}\epsilon_{2*}^2 - \epsilon_{1*}\epsilon_{2*}\epsilon_{3*}) \ln^3 \left(\frac{k}{k_*} \right) \right\}, \tag{2.53}
\end{aligned}$$

$$\begin{aligned}
n_t(k) &= -2\epsilon_{1*} - 2\epsilon_{1*}^2 - 2(1 - \alpha)\epsilon_{1*}\epsilon_{2*} - 2\epsilon_{1*}^3 + (-14 + 6\alpha + \pi^2)\epsilon_{1*}^2\epsilon_{2*} \\
&\quad + \left(-2 + 2\alpha - \alpha^2 + \frac{\pi^2}{12} \right) (\epsilon_{1*}\epsilon_{2*}^2 + \epsilon_{1*}\epsilon_{2*}\epsilon_{3*}) \\
&\quad + (-2\epsilon_{1*}\epsilon_{2*} - 6\epsilon_{1*}^2\epsilon_{2*} - 2\epsilon_{1*}\epsilon_{2*}^2 + 2\alpha\epsilon_{1*}\epsilon_{2*}^2 - 2\epsilon_{1*}\epsilon_{2*}\epsilon_{3*} + 2\alpha\epsilon_{1*}\epsilon_{2*}\epsilon_{3*}) \ln \left(\frac{k}{k_*} \right) \\
&\quad + (-\epsilon_{1*}\epsilon_{2*}^2 - \epsilon_{1*}\epsilon_{2*}\epsilon_{3*}) \ln^2 \left(\frac{k}{k_*} \right), \tag{2.54}
\end{aligned}$$

$$\begin{aligned} \alpha_t(k) = & -2\epsilon_{1*}\epsilon_{2*} - 6\epsilon_{1*}^2\epsilon_{2*} - 2(1-\alpha)\epsilon_{1*}\epsilon_{2*}^2 - 2(1-\alpha)\epsilon_{1*}\epsilon_{2*}\epsilon_{3*} \\ & + 2(-\epsilon_{1*}\epsilon_{2*}^2 - \epsilon_{1*}\epsilon_{2*}\epsilon_{3*}) \ln\left(\frac{k}{k_*}\right), \end{aligned} \quad (2.55)$$

$$\beta_t(k) = -2\epsilon_{1*}\epsilon_{2*}^2 - 2\epsilon_{1*}\epsilon_{2*}\epsilon_{3*}. \quad (2.56)$$

Our results for the dimensionless PPS of scalar and tensor perturbations calculated at third order in the slow-roll expansion, obtained using the integrals and their super-Hubble limits computed and reported in appendix A and in appendix B respectively, agree with the ones previously obtained in Ref. [21] with some negligible differences on the numerical coefficients of the constant part of eqs. (2.43) and (2.53). In appendix C, we report alternative expressions for the PPS.

3 Accuracy of Slow-Roll Analytic Power Spectra Against the Exact Numerical Solution

In this section, we present a comparison between the analytical results obtained above in section 2 at different orders in the slow-roll expansion to the numerical solution for the PPS obtained for two different single-field slow-roll inflationary models.

In order to do so, we solve numerically the coupled system of background and perturbation equations corresponding to the Friedmann equation for a spatially flat universe dominated by a scalar field ϕ , the Klein-Gordon equation governing the background dynamics of a scalar field with standard kinetic term and minimally coupled to gravity, the Mukhanov-Sasaki and the tensor perturbation equations describing the evolution of scalar and tensor primordial perturbations. We describe in the following the adopted strategy to ensure numerical stability.

3.1 Background Dynamics

We time-evolve the background equations in eq. (2.2) in number of e -folds

$$N = \int_{t_i}^t dt H(t) = \ln\left[\frac{a(t)}{a(t_i)}\right]. \quad (3.1)$$

In addition, we rewrite the system of background equations adopting the field redefinition $\psi = \dot{\phi}$. This allows to reduce the background to a system of first-order differential equations. Under these assumptions, the background system becomes

$$\begin{cases} \phi_N \equiv \frac{\psi}{H} = \psi M_{\text{Pl}} \sqrt{\frac{3}{\frac{\psi^2}{2} + V(\phi)}} \\ \psi_N = -3\psi - V_\phi M_{\text{Pl}} \sqrt{\frac{3}{\frac{\psi^2}{2} + V(\phi)}} \end{cases}, \quad (3.2)$$

where the subscript N indicates the derivative with respect to N .

3.2 Perturbation Equations

We also solve the Mukhanov-Sasaki equation and the tensor perturbation equation in number of e -folds. Eqs. eq. (2.4) become

$$v_{kNN}^{(s,t)} = [\epsilon_1(N) - 1]v_{kN}^{(s,t)} + \frac{1}{a^2 H^2} [U^{(s,t)}(N) - k^2] v_k^{(s,t)}, \quad (3.3)$$

where

$$U^{(s)}(N) = \frac{z''}{z} = a^2 H^2 \left(2 - \epsilon_1 + \frac{3\epsilon_2}{2} - \frac{\epsilon_1\epsilon_2}{2} + \frac{\epsilon_2^2}{4} + \frac{\epsilon_2\epsilon_3}{2} \right), \quad (3.4)$$

$$U^{(t)}(N) = \frac{a''}{a} = a^2 H^2 (2 - \epsilon_1). \quad (3.5)$$

We solve separately the perturbation equations for the real and imaginary part of the mode functions as $v_k^{(s,t)} = \text{Re} [v_k^{(s,t)}] + i \text{Im} [v_k^{(s,t)}]$ and we combine them back only at the end.

3.3 Initial Conditions

Concerning the initial conditions, for the background we set the initial value of the scalar field ϕ_i to ensure that there are more than 55 e -folds between the mode $k_* = 0.05 \text{ Mpc}^{-1}$ crosses the Hubble radius and the end of inflation. The initial value of $\dot{\phi}$ is determined using slow-roll initial condition corresponding to $\phi_N|_i \simeq -M_{\text{Pl}}^2 V_\phi / V|_i$.

For the perturbation equations, we impose Bunch-Davies initial conditions a mode at a time when $k = 10^2 aH$. The value 10^2 is just a choice to ensure that all the modes evolved are well within the Hubble horizon at the beginning of their evolution, meaning that we can safely impose the Bunch-Davies vacuum. Modes are then evolved until they became super Hubble for $k = 10^{-3} aH$. The value 10^{-3} ensures that all the modes evolved leave the horizon before their evolution ends. These values define the interval of integration for the number of e -folds. Bunch-Davies initial conditions for the real and the imaginary part of the mode function reads

$$\text{Re} [v_k^{(s,t)}] = \frac{1}{\sqrt{2k}}, \quad \text{Re} [v_{kN}^{(s,t)}] = 0, \quad (3.6)$$

and

$$\text{Im} [v_k^{(s,t)}] = 0, \quad \text{Im} [v_{kN}^{(s,t)}] = -\frac{1}{aH} \sqrt{\frac{k}{2}}. \quad (3.7)$$

Since curvature and tensor perturbations freeze at super-Hubble scales, it is sufficient to calculate the power spectrum for the modes when they are at super-Hubble scales (after horizon crossing) instead of calculating it at the end of inflation.

3.4 Inflationary Models

We study the numerical solution for the scalar and tensor perturbations for the two following single-field slow-roll inflationary potentials

$$V_{\text{T-model}}(\phi) = V_0 \tanh^2 \left(\frac{\phi}{\sqrt{6\alpha}} \right), \quad V_{\text{KKLT}}(\phi) = V_0 \left(1 + \frac{m}{|\phi|} \right)^{-1}. \quad (3.8)$$

The first one corresponds to the T-model of α -attractor inflation [45–50] and the second corresponds to the the inverse linear case of KKL T inflation [51] associated to D6- $\overline{D6}$ potential in type IIA string theory [52, 53].

For the numerical solution, we solve the background equations for a given potential and we insert the solution for the scalar field background into the HFFs entering the perturbation equations

$$\epsilon_1(N) = \frac{\phi_N^2}{2M_{\text{Pl}}^2}, \quad (3.9)$$

$$\epsilon_2(N) = \frac{d \ln |\epsilon_1|}{dN} = \frac{2\phi_{NN}}{\phi_N}, \quad (3.10)$$

$$\epsilon_3(N) = \frac{d \ln |\epsilon_2|}{dN} = \frac{\phi_{NNN}}{\phi_{NN}} - \frac{\phi_{NN}}{\phi_N}. \quad (3.11)$$

For the analytical solution, we calculate the HFFs as functions of the potential slow-roll parameters [16] as explained in details in Refs. [28, 54]. We start from the LO expressions

$$\epsilon_1^{\text{LO}} \simeq \frac{M_{\text{Pl}}^2}{2} \left(\frac{V_\phi}{V} \right)^2, \quad (3.12)$$

$$\epsilon_2^{\text{LO}} \simeq 2M_{\text{Pl}}^2 \left(\frac{V_\phi^2}{V^2} - \frac{V_{\phi\phi}}{V} \right), \quad (3.13)$$

$$\epsilon_3^{\text{LO}} \simeq \frac{2M_{\text{Pl}}^4}{\epsilon_2} \left(\frac{2V_\phi^4}{V^4} - \frac{3V_\phi^2 V_{\phi\phi}}{V^3} + \frac{V_\phi V_{\phi\phi\phi}}{V^2} \right), \quad (3.14)$$

$$\begin{aligned} \epsilon_4^{\text{LO}} \simeq & \frac{2M_{\text{Pl}}^6}{\epsilon_2 \epsilon_3} \left[\frac{8V_\phi^6}{V^6} - \frac{17V_\phi^4 V_{\phi\phi}}{V^5} + \frac{6V_\phi^2 V_{\phi\phi}^2}{V^4} + \frac{5V_\phi^3 V_{\phi\phi\phi}}{V^4} - \frac{V_\phi V_{\phi\phi} V_{\phi\phi\phi}}{V^3} - \frac{V_\phi^2 V_{\phi\phi\phi\phi}}{V^3} + \right. \\ & \left. + \frac{2M_{\text{Pl}}^2}{\epsilon_2} \left(-\frac{4V_\phi^8}{V^8} + \frac{12V_\phi^6 V_{\phi\phi}}{V^7} - \frac{9V_\phi^4 V_{\phi\phi}^2}{V^6} - \frac{4V_\phi^5 V_{\phi\phi\phi}}{V^6} + \frac{6V_\phi^3 V_{\phi\phi} V_{\phi\phi\phi}}{V^5} - \frac{V_\phi^2 V_{\phi\phi\phi\phi}}{V^4} \right) \right]. \end{aligned} \quad (3.15)$$

These equations have been derived by approximating at LO the Hubble parameter as $H^2 \simeq V/(3M_{\text{Pl}})$, which leads to the LO formula of the derivative with respect to N [54]

$$\left. \frac{d}{dN} \right|_{\text{LO}} = -M_{\text{Pl}}^2 \frac{V_\phi}{V} \frac{d}{d\phi}. \quad (3.16)$$

To compare the analytical and numerical solutions, we need to include corrections up to the third order in terms of potential slow-roll parameters. The equations at third order have been already calculated in Ref. [28], we report here the results in terms of the LO HFFs

$$\epsilon_1^{\text{N3LO}} = \left(\epsilon_1 - \frac{1}{3}\epsilon_1\epsilon_2 - \frac{1}{9}\epsilon_1^2\epsilon_2 + \frac{5}{36}\epsilon_1\epsilon_2^2 + \frac{1}{9}\epsilon_1\epsilon_2\epsilon_3 \right) \Big|_{\text{LO}}, \quad (3.17)$$

$$\epsilon_2^{\text{N3LO}} = \left(\epsilon_2 - \frac{1}{6}\epsilon_2^2 - \frac{1}{3}\epsilon_2\epsilon_3 - \frac{1}{6}\epsilon_1\epsilon_2^2 + \frac{1}{18}\epsilon_2^3 - \frac{1}{9}\epsilon_1\epsilon_2\epsilon_3 + \frac{5}{18}\epsilon_2^2\epsilon_3 + \frac{1}{9}\epsilon_2\epsilon_3^2 + \frac{1}{9}\epsilon_2\epsilon_3\epsilon_4 \right) \Big|_{\text{LO}}, \quad (3.18)$$

$$\begin{aligned} \epsilon_3^{\text{N3LO}} = & \left(\epsilon_3 - \frac{1}{3}\epsilon_2\epsilon_3 - \frac{1}{3}\epsilon_3\epsilon_4 - \frac{1}{6}\epsilon_1\epsilon_2^2 - \frac{1}{3}\epsilon_1\epsilon_2\epsilon_3 + \frac{1}{6}\epsilon_2^2\epsilon_3 + \frac{5}{18}\epsilon_2\epsilon_3^2 - \frac{1}{9}\epsilon_1\epsilon_3\epsilon_4 \right. \\ & \left. + \frac{5}{18}\epsilon_2\epsilon_3\epsilon_4 + \frac{1}{9}\epsilon_3^2\epsilon_4 + \frac{1}{9}\epsilon_3\epsilon_4^2 + \frac{1}{9}\epsilon_3\epsilon_4\epsilon_5 \right) \Big|_{\text{LO}}, \end{aligned} \quad (3.19)$$

$$\epsilon_4^{\text{N3LO}} = \left(\epsilon_4 - \frac{1}{3}\epsilon_2\epsilon_3 - \frac{1}{6}\epsilon_2\epsilon_4 - \frac{1}{3}\epsilon_4\epsilon_5 \right) \Big|_{\text{LO}}, \quad (3.20)$$

where all the HFFs on the right hand side have been calculated at LO using eqs. (3.12) to (3.15) and we set in our analysis $\epsilon_5 = 0$.

In order to relate the HFFs in terms of number of e -folds rather than values of the scalar field, we need to solve analytically the expression of the classical inflationary trajectory $\phi(N)$. This is done at LO by solving

$$N(\phi) \simeq -\frac{1}{M_{\text{Pl}}^2} \int_{\phi}^{\phi_{\text{end}}} \frac{V}{V_{\phi}} d\phi, \quad (3.21)$$

and by inverting this relation. ϕ_{end} is the value of the field at the end of inflation, computed by imposing $\epsilon_{1,\text{end}} \equiv \epsilon_1(\phi_{\text{end}}) = 1$, namely when the kinetic term start to dominate over the potential energy. For T-model inflation we found

$$\phi_*^{\text{T}}(N, \alpha) = \sqrt{\frac{3\alpha}{2}} \operatorname{sech}^{-1} \left(\frac{3\alpha}{\alpha\sqrt{\frac{12}{\alpha} + 9} + 4N} \right), \quad (3.22)$$

$$\phi_{\text{end}}^{\text{T}}(\alpha) = \sqrt{\frac{3\alpha}{2}} \sinh^{-1} \left(\frac{2}{\sqrt{3\alpha}} \right), \quad (3.23)$$

and for KKLТ inflation we find

$$\begin{aligned}
\phi_*^{\text{KKLT}}(N, m) = & \frac{1}{2} \left\{ \left[12Nm + (\sqrt{2} - m) m \sqrt{m(2\sqrt{2} + m)} \right. \right. \\
& + \sqrt{2m^2 \left[(2\sqrt{2} - 3m) m + 12N \left(6N + (\sqrt{2} - m) \sqrt{m(2\sqrt{2} + m)} \right) \right]} \right. \\
& \left. \left. - m + m^2 \left[12Nm + (\sqrt{2} - m) m \sqrt{m(2\sqrt{2} + m)} \right] \right. \right. \\
& \left. \left. + \sqrt{2m^2 \left[(2\sqrt{2} - 3m) m + 12N \left(6N + (\sqrt{2} - m) \sqrt{m(2\sqrt{2} + m)} \right) \right]} \right] \right\}^{-1/3},
\end{aligned} \tag{3.24}$$

$$\phi_{\text{end}}^{\text{KKLT}}(m) = \frac{1}{2} \left[\sqrt{m(2\sqrt{2} + m)} - m \right]. \tag{3.25}$$

Once obtained the trajectory $\phi(N)$, it is possible to get the analytical HFFs at LO written with respect to the number of e -folds, namely $\epsilon_i^{\text{LO}}(N)$. Therefore, from these equations we can obtain the ones at N3LO using the eqs. (3.17) to (3.20). Finally, we are able to calculate the scalar and tensor PPS by using eqs. (2.43) and (2.53).

We fix the potential amplitude V_0 in order to normalise the dimensionless scalar PPS to $\mathcal{P}_\zeta(k_*) = 2 \times 10^{-9}$ at $k_* = 0.05 \text{ Mpc}^{-1}$.

The code and the pipeline developed for this section are publicly available.¹

3.5 Accuracy of Slow-Roll Analytic Spectra

In figs. 1 and 2, we present the results for the T-model of α -attractor inflation with $\alpha = 1$, while in figs. 3 and 4 we present the results for KKLТ inflation with $m = 1$. We compare the numerical results with respect to the analytical results calculated at first-, second-, and third-order slow-roll expansion in the range $k \in [10^{-4}, 10^2] \text{ Mpc}^{-1}$. Moreover, we also show the comparison for third-order with $\epsilon_4 = 0$. Such comparison can be found in the literature between the first- and the second-order corrections, see for instance Refs. [20, 55].

In figs. 1 and 3, we present the power spectra comparisons together with the corresponding relative differences of the analytical results with respect to the numerical solutions. In figs. 2 and 4, we present the relative differences of the spectral indices n_s and n_t , their runnings α_s and α_t , and the runnings of the running β_s and β_t . For a certain quantity X , where $X = \{\mathcal{P}_\zeta, \mathcal{P}_t, n_s, n_t, \alpha_s, \alpha_t, \beta_s, \beta_t\}$, the corresponding percentage difference $\%X$ is defined as follows

$$\%X = \left(1 - \frac{X_{\text{analytical}}}{X_{\text{numerical}}} \right) \times 100. \tag{3.26}$$

¹<https://github.com/SirlettiSS/PyPPSinflation.git>

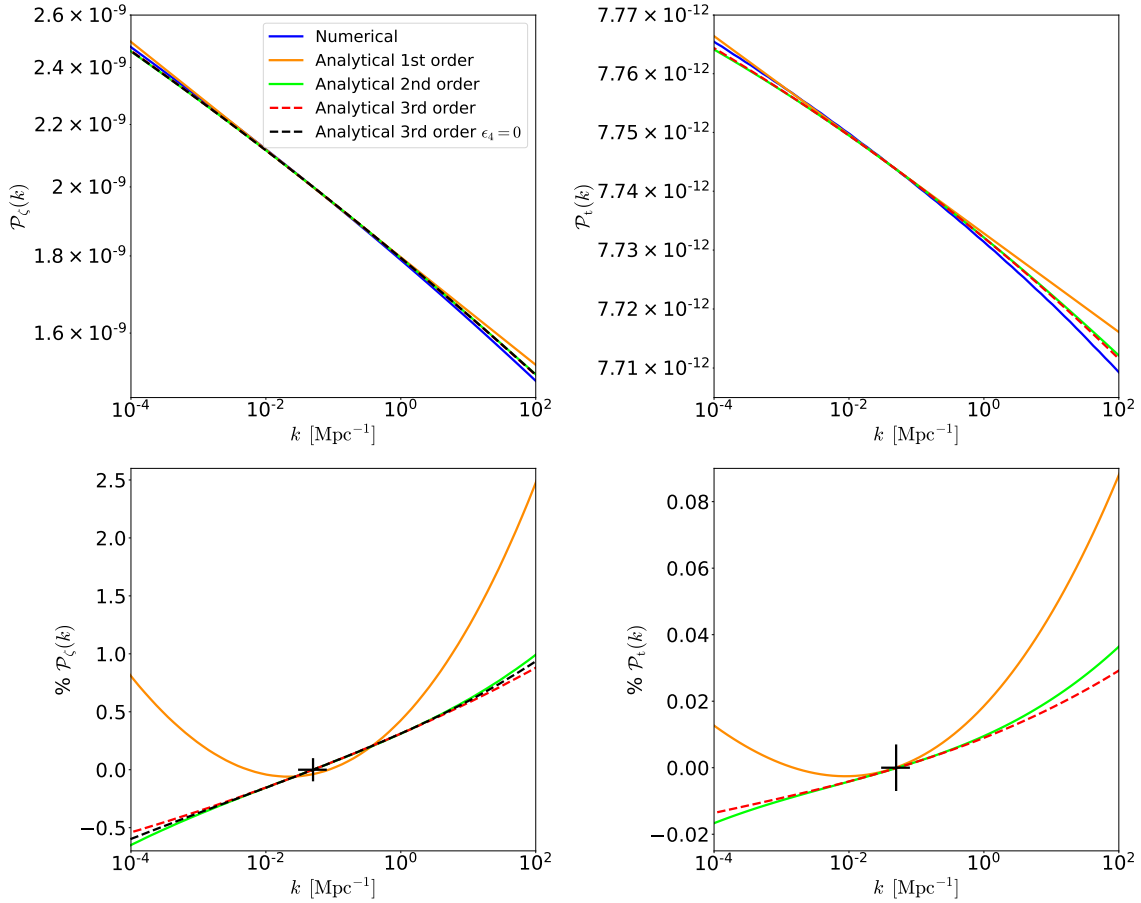


Figure 1. Scalar (left panels) and tensor (right panels) error curves for the T-model α -attractor inflation with $\alpha = 1$. The pivot scale crosses the Hubble horizon 55 e -folds before the end of inflation. We show on the upper panels the dimensionless PPS and on the lower panels the relative differences of the analytic spectra compared to the numerical solution.

As we can observe in figs. 1 and 3, the relative differences on the tensor PPS are one order of magnitude lower than those of the scalar PPS. We also observe that, on the entire k range, the relative errors follow the expected perturbative hierarchy, i.e. the higher the order, the lower the errors. It is also useful to point out that the third-order case with $\epsilon_4 = 0$ acts as a mid-case between the second- and pure third-order. For both models, we observe that around the pivot scale k_* the second- and third-order PPS relative differences are nearly identical and match the numerical results thanks to the normalisation performed. Small differences between the second and third order start to appear around $k \sim 10 \text{ Mpc}^{-1}$ of the order of 0.1% and the curves visibly separate from each other at $k \sim 10^2 \text{ Mpc}^{-1}$ reaching a maximum difference of 0.5% and 0.3%, for T-model and KKLt inflation respectively. For the tensor PPS, small differences between second and third order start to arise at $k \sim 1 \text{ Mpc}^{-1}$, where the relative errors are of the order of 0.01%, and they increase at higher k reaching 0.02% at $k \sim 10^2 \text{ Mpc}^{-1}$.

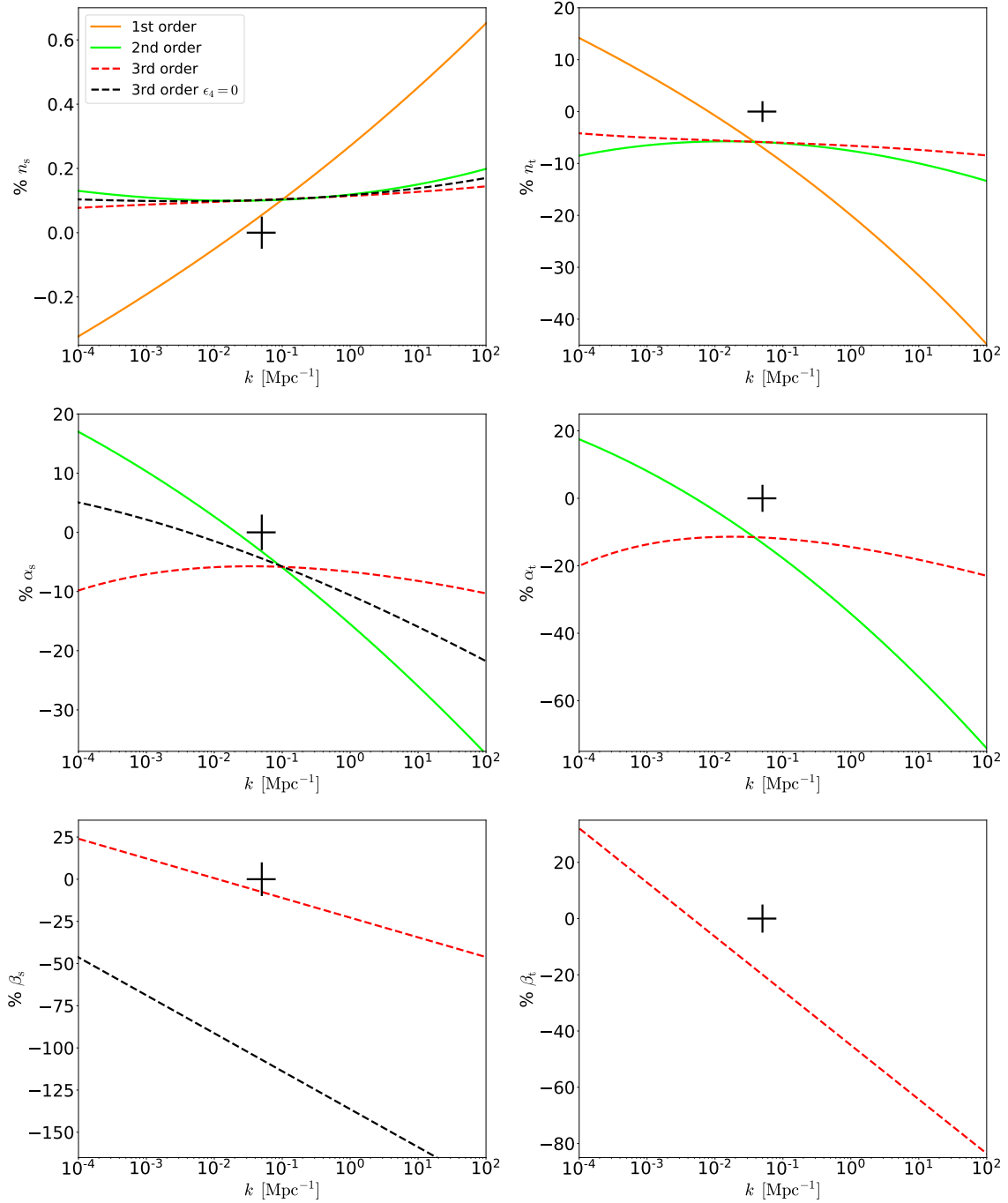


Figure 2. Relative differences with respect to the numerical solution for the spectral index (upper panels), running of the spectral index (central panels), and running of the running of the spectral index (lower panels) for the T-model α -attractor inflation with $\alpha = 1$.

In figs. 2 and 4, we present the relative differences for $n_{s/t}$, $\alpha_{s/t}$, and $\beta_{s/t}$, for T-model and KKL T inflation, respectively. In general, we find larger differences for

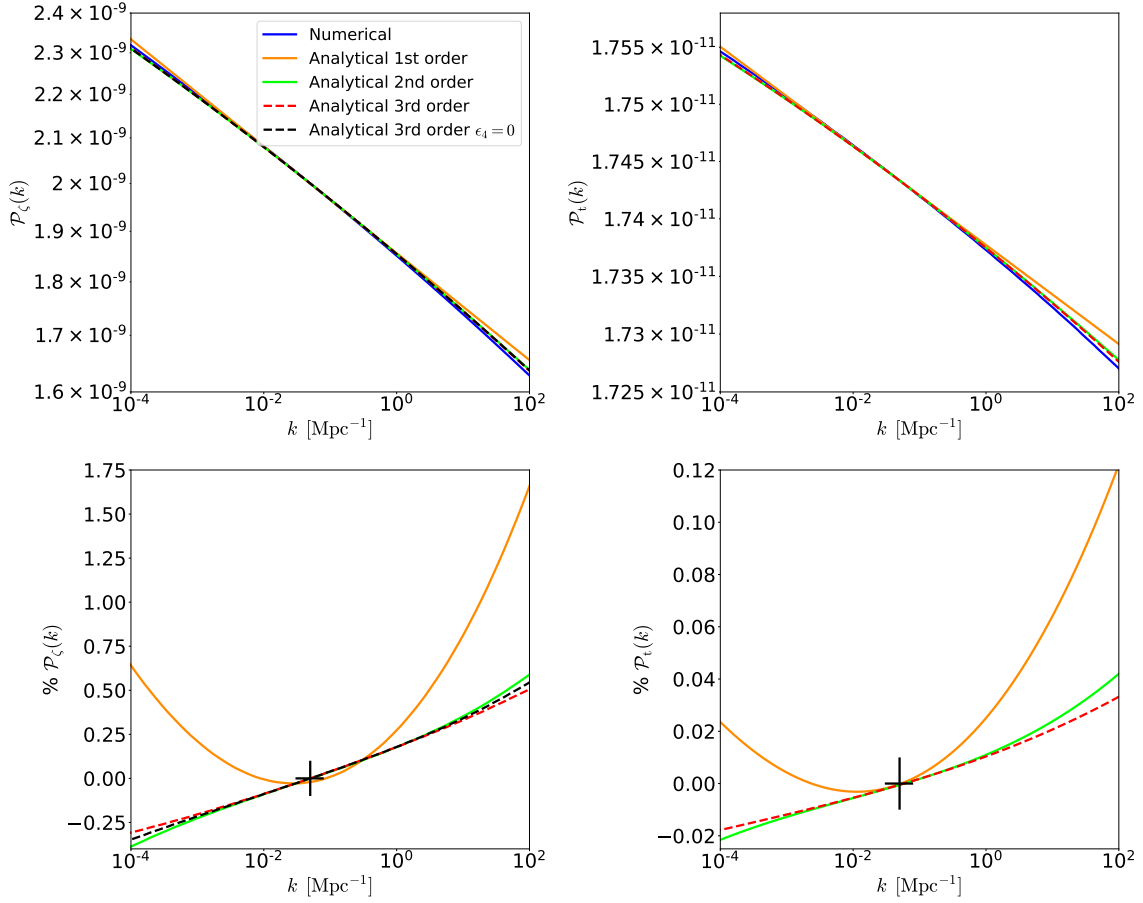


Figure 3. Same as fig. 1 but for KKLT inflation for $m = 1$.

the tensor quantities, however, associated usually to larger observational uncertainties. For the spectral indexes n_s and n_t , we find that around the pivot scale the relative differences are nearly identical, they start to differ from $k \sim 10 \text{ Mpc}^{-1}$. On the other hand, when k is lower than the pivot scale, the differences start to appear from $k \sim 10^{-2} \text{ Mpc}^{-1}$. Including corrections at the second and third order, the relative differences for n_s in both the models are always at most equal or lower than 0.1%, while for n_t they are always at most equal or lower than 10% (in terms of absolute value). For the runnings of the spectral indexes α_s and α_t , we observe increasing differences between the second and the third order moving away from the pivot scale; in both cases these differences are always of the order of $\sim 1\%$ around the pivot scale and they increase reaching the order of $\sim 10\%$.

The third-order relative differences for β_s and β_t are consistently around $\sim 10\%$ for both the models on the range of scales probed by CMB measurements; far from the pivot scale the errors are larger. When we consider the case with third-order corrections and $\epsilon_4 = 0$, β_s exhibits significantly larger differences compared to the numerical result: these errors start to be approximately 50% at $k \sim 10^{-4} \text{ Mpc}^{-1}$ and

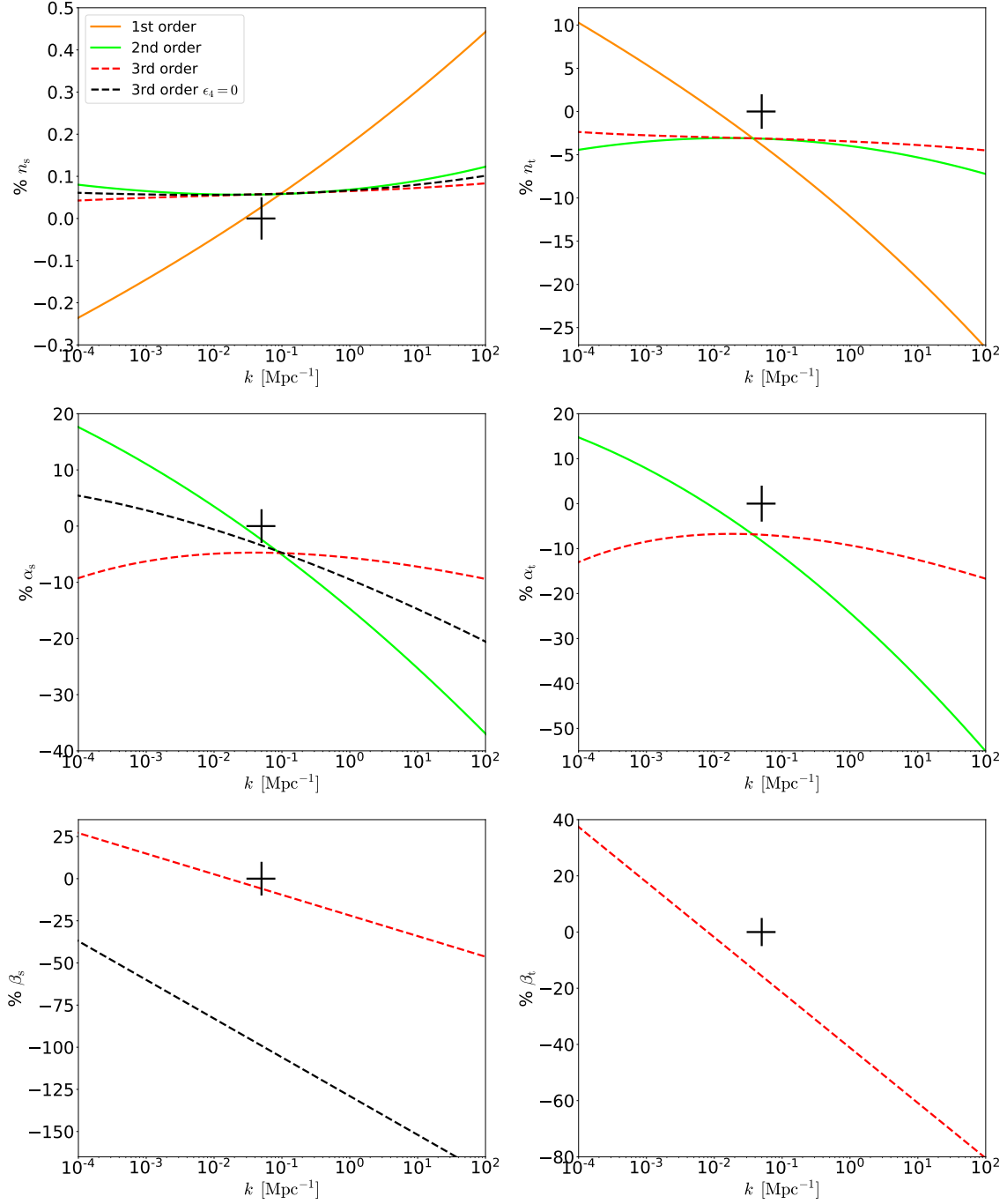


Figure 4. Same as fig. 2 but for KKLt inflation for $m = 1$.

increase up to 150% at $k \sim 10^2 \text{ Mpc}^{-1}$.

Moreover, we also repeated the comparison for larger values of the inflationary parameters, $\alpha = 100$ for T-model inflation and $m = 100$ for KKLt inflation. We observe no significant difference with respect the case presented here for $\alpha = 1$ and

$m = 1$.

We conclude this section showing in fig. 5 the percentage differences on the TT and EE CMB lensed angular power spectra and the absolute differences on the TE spectrum for T-model α -attractor inflation with $\alpha = 1$. The size of the differences is compatible to the one of the scalar PPS shown in fig. 1.

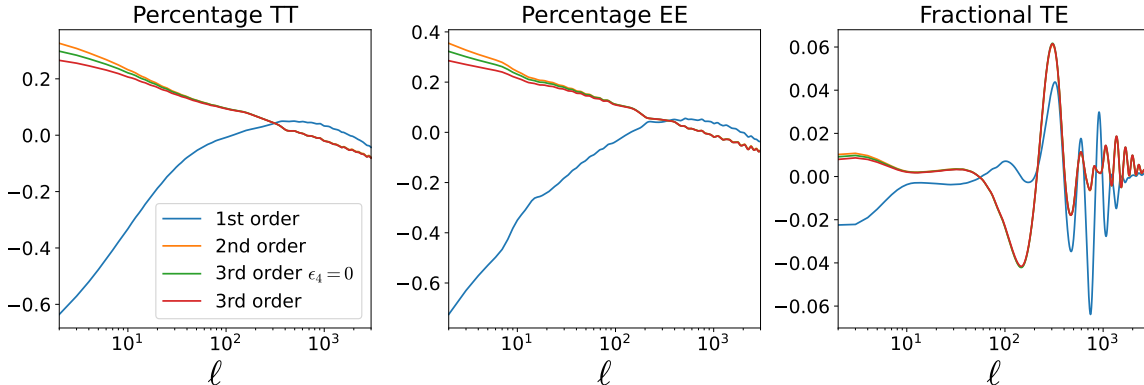


Figure 5. Differences with respect to the numerical solution for the CMB temperature and E-mode polarisation lensed angular power spectra for the T-model α -attractor inflation with $\alpha = 1$.

4 Data Analysis and Cosmological Constraints

In this section, we calculate the uncertainties on the HFFs considering different truncation of the PPS expansion at first, second, and third order. We use `CosmoMC` [56]² connected to our modified version of the code `CAMB` [57, 58].³ Mean values and uncertainties on the parameters reported, as well as the contours plotted, have been obtained using `GetDist` [59].⁴ For the Markov chain Monte Carlo (MCMC) analysis, we vary the standard cosmological parameters for a flat Λ CDM concordance model ω_b , ω_c , H_0 , τ , and $\ln(10^{10} A_s)$,⁵ plus the HFFs ϵ_i . We vary also nuisance and foreground parameters for the likelihood considered. We assume two massless neutrino with $N_{\text{eff}} = 2.046$, and a massive one with fixed minimum mass $m_\nu = 0.06$ eV.

We focus our analysis on comparing different cosmological datasets of primary CMB measurements, i.e. temperature and polarisation anisotropies. We also consider the case adding non-primary CMB datasets. We therefore consider the following datasets:

²<https://github.com/cmbant/CosmoMC>

³<https://github.com/cmbant/CAMB>

⁴<https://github.com/cmbant/getdist>

⁵Note that sampling on the amplitude of the scalar PPS $\ln(10^{10} A_s)$ rather than sampling directly on the amplitude of the scalar field potential V_0 allows to overcome some uncertainties connected to the determination of the end of inflation for which the slow-roll approximation breaks down; see Ref. [60] for analytic advances.

- P18 refers to *Planck* PR3 primary CMB data [61]. Low-multipole data ($\ell < 30$) consists to the `commander` likelihood for temperature and `SimAll` for the E-mode polarisation. On high multipoles ($\ell \geq 30$), we use the `Plik` likelihood including CMB temperature up to $\ell_{\max} = 2508$, E-mode polarisation and temperature-polarisation cross correlation up to $\ell_{\max} = 1996$.⁶
- ACT refers to ACT DR4 TT, EE, TE power spectra [40, 62] covering the multipole range [350, 4000]. When combining ACT with *Planck* data we remove temperature data at a certain threshold to avoid for the unaccounted correlation between the two datasets. We consider two multipole cuts: in the first case we remove *Planck* data in temperature above $\ell > 650$ and in the second case we remove ACT data in temperature below $\ell < 1800$.
- SPT refers to SPT-3G 2018 TT, EE, TE power spectra covering the angular multipole range $750 < \ell < 3000$ [41]. Combining SPT and *Planck* data we do not consider any cut on the multipole range since data *Planck* cover a large amount of sky not observed by SPT.
- BK18 refers B-mode polarisation spectrum for $20 < \ell < 330$ from BICEP2, Keck Array, and BICEP3 observations up to 2018 [42].
- *ext* (external) refers to the combination of late-time probes and non-primary CMB data. We include measurements of baryon acoustic oscillations (BAO) and redshift space distortions (RSD) at low redshift $0.07 < z < 0.2$ from SDSS-I and -II sample as *Main Galaxy Sample* (MGS), BOSS DR12 galaxies over the redshift interval $0.2 < z < 0.6$, eBOSS luminous red galaxies (LRG) and quasars $0.6 < z < 2.2$, and Lyman- α forest samples $1.8 < z < 3.5$ [see 63, for details and references].⁷ We include the Pantheon catalogue of uncalibrated Type Ia Supernovae (SNe) over the redshift range $0.01 < z < 2.3$ [64].⁸ Finally we also include CMB lensing data from *Planck* PR3 considering the conservative multipole range $8 < \ell < 400$ [65].

When considering ACT and SPT data not combined with *Planck* data, we include the *Planck* low- ℓ E-mode polarisation likelihood `SimAll` in order to provide information on the optical depth τ to avoid the use of a Gaussian *Planck*-inspired prior on it. We consider P18+BK18, ACT+BK18, SPT+BK18, P18+ACT+BK18, P18+SPT+BK18, and all these combinations also adding the external datasets.

Prior ranges on the cosmological parameters are collected on table 1. We assume uniform priors on all the HFF parameters ϵ_i . In Refs. [27, 66–68] ϵ_1 has been sampled with a log-uniform prior corresponding effectively to sampling the tensor-to-scalar ratio r with a logarithmic prior; see Refs. [69, 70] for an extended discussion on the use of uniform or logarithmic priors for the tensor-to-scalar ratio. Note also that in

⁶<https://pla.esac.esa.int/pla/#cosmology>

⁷https://svn.sdss.org/public/data/eboss/DR16cosmo/tags/v1_0_1/likelihoods/BAO-plus/

⁸<https://github.com/dscolnic/Pantheon/>

Parameter	Uniform prior
$\Omega_b h^2$	[0.019, 0.025]
$\Omega_c h^2$	[0.095, 0.145]
$100\theta_{\text{MC}}$	[1.03, 1.05]
τ	[0.01, 0.4]
$\ln(10^{10} A_s)$	[2.5, 3.7]
ϵ_1	[0, 0.1]
ϵ_2	[-0.5, 0.5]
ϵ_3	[-0.5, 0.5]
ϵ_4	[-0.5, 0.5]

Table 1. Prior ranges for cosmological parameters used in the Bayesian analysis.

Refs. [27, 66–68] a tighter flat prior was adopted for the second, third, and fourth HFFs, corresponding to $\epsilon_{2,3,4} \in [-0.2, 0.2]$. To ensure the validity of the slow-roll equations derived in section 2 and adopted here, the HFFs should be less than one. We show in appendix D a comparison of the posterior distribution on the sampled and derived inflationary parameters by adopting a larger prior with $\epsilon_{2,3,4} \in [-1, 1]$.⁹

4.1 Results

We first present the constraints on slow-roll parameters obtained through the analytic perturbative expansion in terms of the HFFs ϵ_i for the primordial spectra of cosmological fluctuations during slow-roll inflation. When restricting to first-order expansion, we obtain

$$\epsilon_1 < 0.0022 \quad (95\% \text{ CL, P18 + BK18}), \quad (4.1)$$

$$\epsilon_2 = 0.0332 \pm 0.0046 \quad (68\% \text{ CL, P18 + BK18}), \quad (4.2)$$

$$\epsilon_1 < 0.0023 \quad (95\% \text{ CL, ACT + BK18}), \quad (4.3)$$

$$\epsilon_2 = -0.005 \pm 0.014 \quad (68\% \text{ CL, ACT + BK18}), \quad (4.4)$$

$$\epsilon_1 < 0.0024 \quad (95\% \text{ CL, SPT + BK18}), \quad (4.5)$$

$$\epsilon_2 = 0.032 \pm 0.015 \quad (68\% \text{ CL, SPT + BK18}). \quad (4.6)$$

When second-order contributions in the HFFs are included, we obtain

$$\epsilon_1 < 0.0023 \quad (95\% \text{ CL, P18 + BK18}), \quad (4.7)$$

$$\epsilon_2 = 0.0379 \pm 0.0078 \quad (68\% \text{ CL, P18 + BK18}), \quad (4.8)$$

$$\epsilon_3 = 0.13_{-0.12}^{+0.19} \quad (68\% \text{ CL, P18 + BK18}), \quad (4.9)$$

⁹A detailed comparison of the effect of the size of the priors on the slow-roll parameters was done in Ref. [68] for both second- and third-order results but for a different combination of datasets.

$$\epsilon_1 < 0.0023 \quad (95\% \text{ CL, ACT + BK18}), \quad (4.10)$$

$$\epsilon_2 = -0.007_{-0.014}^{+0.016} \quad (68\% \text{ CL, ACT + BK18}), \quad (4.11)$$

$$\epsilon_3 \text{ unconstrained} \quad (95\% \text{ CL, ACT + BK18}), \quad (4.12)$$

$$\epsilon_1 < 0.0025 \quad (95\% \text{ CL, SPT + BK18}), \quad (4.13)$$

$$\epsilon_2 = 0.035 \pm 0.017 \quad (68\% \text{ CL, SPT + BK18}), \quad (4.14)$$

$$\epsilon_3 \text{ unconstrained} \quad (95\% \text{ CL, SPT + BK18}). \quad (4.15)$$

Including third-order contributions in the HFFs, we find close results to the second-order ones with ϵ_4 unconstrained, see table 2. The addition of external datasets, which are BAO and RSD measurements, SNe, and CMB lensing, leads to slightly tighter uncertainties and consistent mean values for ϵ_2 and ϵ_3 , see table 3.

	P18 + BK18	ACT + BK18	SPT + BK18
	FIRST ORDER		
$\ln(10^{10} A_s)$	3.046 ± 0.015	3.030 ± 0.019	3.038 ± 0.016
ϵ_1 (at 95% CL)	< 0.0022	< 0.0023	< 0.0024
ϵ_2	0.0332 ± 0.0046	-0.005 ± 0.014	0.032 ± 0.015
$n_{s,0.05}$	0.9647 ± 0.0043	1.003 ± 0.014	0.966 ± 0.015
$r_{0.05}$ (at 95% CL)	< 0.035	< 0.037	< 0.039
$n_{t,0.05}$	$-0.0020_{-0.0009}^{+0.0015}$	$-0.0022_{-0.0009}^{+0.0015}$	$-0.0024_{-0.0010}^{+0.0017}$
	SECOND ORDER		
$\ln(10^{10} A_s)$	3.050 ± 0.017	3.029 ± 0.019	3.040 ± 0.017
ϵ_1 (at 95% CL)	< 0.0023	< 0.0023	< 0.0025
ϵ_2	0.0379 ± 0.0078	$-0.007_{-0.014}^{+0.016}$	0.035 ± 0.017
ϵ_3 (at 95% CL)	$0.13_{-0.35}^{+0.30}$	–	–
$n_{s,0.05}$	0.9641 ± 0.0046	$1.003_{-0.013}^{+0.015}$	0.967 ± 0.014
$\alpha_{s,0.05}$	-0.0059 ± 0.0067	$0.0020_{-0.0051}^{+0.0029}$	$-0.006_{-0.010}^{+0.012}$
$r_{0.05}$ (at 95% CL)	< 0.036	< 0.038	< 0.038
$n_{t,0.05}$	$-0.0022_{-0.0010}^{+0.0016}$	$-0.0022_{-0.0010}^{+0.0016}$	$-0.0024_{-0.0010}^{+0.0017}$
$10^5 \alpha_{t,0.05}$	$-8.1_{-3.3}^{+5.9}$	$1.9_{-4.4}^{+2.3}$	$-7.8_{-3.4}^{+6.8}$

Table 2. Constraints on the main (inflationary related) parameters and derived ones (at 68% CL if not otherwise stated) considering P18+BK18, ACT+BK18, and SPT+BK18.

The upper limit on ϵ_1 , as well as the derived constraint on r ($\lesssim 0.04$ at 95% CL), is almost unchanged among the different combination of datasets and different truncation being dominated by BK18 data which are always included. On the other hand, we find different results for ϵ_2 and ϵ_3 moving from *Planck* to ACT data. This difference comes from the almost 3σ tension between *Planck* and ACT data on the inferred value of the scalar spectral index n_s . While the result from *Planck* (combining temperature, E-mode polarisation, and lensing) $n_s = 0.9649 \pm 0.0044$ [71] agrees with the prediction of simplest single-field slow-roll inflationary models, the result from ACT [40] points

	P18 + BK18 + ext	ACT + BK18 + ext	SPT + BK18 + ext
	FIRST ORDER		
$\ln(10^{10} A_s)$	$3.052^{+0.013}_{-0.015}$	3.042 ± 0.014	3.043 ± 0.011
ϵ_1 (at 95% CL)	< 0.0022	< 0.0023	< 0.0025
ϵ_2	0.0306 ± 0.0039	0.003 ± 0.010	0.034 ± 0.012
$n_{s,0.05}$	0.9673 ± 0.0036	0.995 ± 0.010	0.963 ± 0.012
$r_{0.05}$ (at 95% CL)	< 0.036	< 0.036	< 0.039
$n_{t,0.05}$	$-0.0021^{+0.0015}_{-0.0009}$	$-0.0022^{+0.0015}_{-0.0009}$	$-0.0024^{+0.0016}_{-0.0010}$
	SECOND ORDER		
$\ln(10^{10} A_s)$	3.055 ± 0.015	3.041 ± 0.014	3.045 ± 0.012
ϵ_1 (at 95% CL)	< 0.0023	< 0.0023	< 0.0024
ϵ_2	0.0342 ± 0.0071	$0.002^{+0.012}_{-0.010}$	$0.036^{+0.012}_{-0.014}$
ϵ_3 (at 95% CL)	$0.11^{+0.33}_{-0.38}$	–	–
$n_{s,0.05}$	0.9669 ± 0.0038	$0.995^{+0.011}_{-0.010}$	0.965 ± 0.012
$\alpha_{s,0.05}$	-0.0048 ± 0.0065	$0.0011^{+0.0022}_{-0.0031}$	$-0.005^{+0.012}_{-0.010}$
$r_{0.05}$ (at 95% CL)	< 0.037	< 0.037	< 0.038
$n_{t,0.05}$	$-0.0023^{+0.0016}_{-0.0010}$	$-0.0022^{+0.0016}_{-0.0010}$	$-0.0024^{+0.0016}_{-0.0010}$
$10^5 \alpha_{t,0.05}$	$-7.6^{+5.4}_{-3.1}$	$-0.3^{+2.0}_{-2.4}$	$-8.4^{+6.6}_{-3.3}$

Table 3. Same as table 2 in combination with the external datasets, which are BAO and RSD measurements, SNe, and CMB lensing.

to $n_s = 1.008 \pm 0.015$ ($2.8\sigma^{10}$) compatible with a scale invariant Harrison-Zel’dovich (HZ) primordial power spectrum [72–74]. We find that *Planck* ($n_s = 0.9647 \pm 0.0043$ at 68% CL) and ACT ($n_s = 1.003 \pm 0.014$ at 68% CL) results have a 2.6σ on the inferred value of n_s when considering primary CMB only at first order in slow-roll expansion, see table 2. This number does not change when the external data are included, see table 3.

The discrepancy between *Planck* and ACT data at the level of the scalar PPS parameters persists even when allowing a running of the scalar spectral index α_s [73, 74]; in our case when we move to the second-order expansion case. Despite the discrepant results, while *Planck* is consistent with a zero running $\alpha_s = -0.0045 \pm 0.0067$ at 68% CL [71] (and with slow-roll single-field inflation predictions, see Ref. [68]), on the contrary ACT data point to a 2.5σ preference for a positive running $\alpha_s = 0.069 \pm 0.029$ [40]. We find a discrepancy on the inferred value of n_s of 3.8σ with primary CMB alone and 3.2σ in combination with external datasets; larger numbers compared to the ones obtained considering only second-order terms. We find that *Planck* ($\alpha_s = -0.0059 \pm 0.0067$ at 68% CL) and ACT ($\alpha_s = 0.0020^{+0.0029}_{-0.0051}$ at 68% CL) results have a 0.9σ discrepancy on the inferred value of α_s both considering primary CMB only and in combination with external datasets at second order in slow-roll expansion, see tables 2 and 3. SPT data agrees with *Planck* findings but with larger error bars.

¹⁰Quantified as $|n_s^{(P18)} - n_s^{(ACT)}| / \sqrt{\sigma(n_s^{(P18)})^2 + \sigma(n_s^{(ACT)})^2}$; we perform the analogous estimation for the running of the scalar spectral index α_s .

4.2 Combined Results

We present here the results for the two combined cases P18+ACT+BK18, assuming two different multiple cuts, and the combination P18+SPT+BK18. When restricting to first-order expansion, we obtain

$$\epsilon_1 < 0.0024 \quad 95\% \text{ CL, P18 } (\ell_{\text{TT}} < 650) + \text{ACT} + \text{BK18}, \quad (4.16)$$

$$\epsilon_2 = 0.0183 \pm 0.0059 \quad 68\% \text{ CL, P18 } (\ell_{\text{TT}} < 650) + \text{ACT} + \text{BK18}, \quad (4.17)$$

$$\epsilon_1 < 0.0022 \quad 95\% \text{ CL, P18} + \text{ACT } (\ell_{\text{TT}} > 1800) + \text{BK18}, \quad (4.18)$$

$$\epsilon_2 = 0.0312 \pm 0.0044 \quad 68\% \text{ CL, P18} + \text{ACT } (\ell_{\text{TT}} > 1800) + \text{BK18}, \quad (4.19)$$

$$\epsilon_1 < 0.0022 \quad 95\% \text{ CL, P18} + \text{SPT} + \text{BK18}, \quad (4.20)$$

$$\epsilon_2 = 0.0327 \pm 0.0044 \quad 68\% \text{ CL, P18} + \text{SPT} + \text{BK18}. \quad (4.21)$$

When second-order contributions in the HFFs are included, we obtain

$$\epsilon_1 < 0.0023 \quad 95\% \text{ CL, P18 } (\ell_{\text{TT}} < 650) + \text{ACT} + \text{BK18}, \quad (4.22)$$

$$\epsilon_2 = 0.0166^{+0.0045}_{-0.0057} \quad 68\% \text{ CL, P18 } (\ell_{\text{TT}} < 650) + \text{ACT} + \text{BK18}, \quad (4.23)$$

$$\epsilon_3 < -0.053 \quad 68\% \text{ CL, P18 } (\ell_{\text{TT}} < 650) + \text{ACT} + \text{BK18}, \quad (4.24)$$

$$\epsilon_1 < 0.0023 \quad 95\% \text{ CL, P18} + \text{ACT } (\ell_{\text{TT}} > 1800) + \text{BK18}, \quad (4.25)$$

$$\epsilon_2 = 0.0274^{+0.0047}_{-0.0063} \quad 68\% \text{ CL, P18} + \text{ACT } (\ell_{\text{TT}} > 1800) + \text{BK18}, \quad (4.26)$$

$$\epsilon_3 = -0.08^{+0.23}_{-0.19} \quad 68\% \text{ CL, P18} + \text{ACT } (\ell_{\text{TT}} > 1800) + \text{BK18}, \quad (4.27)$$

$$\epsilon_1 < 0.0024 \quad 95\% \text{ CL, P18} + \text{SPT} + \text{BK18}, \quad (4.28)$$

$$\epsilon_2 = 0.0354 \pm 0.0066 \quad 68\% \text{ CL, P18} + \text{SPT} + \text{BK18}, \quad (4.29)$$

$$\epsilon_3 = 0.13^{+0.19}_{-0.12} \quad 68\% \text{ CL, P18} + \text{SPT} + \text{BK18}. \quad (4.30)$$

Also in this case, we find small differences between the second-order and the third-order case and again with ϵ_4 unconstrained, see table 4 and table 5 for the results including the external datasets. We report the full results for the third-order case only for the combined datasets with the addition of external data; see table 5.

The combination P18+ACT is closer to the *Planck* alone results for both the two multipole cuts applied in temperature. While the case with the cut on ACT data, with $\ell_{\text{TT}}^{\text{ACT}} > 1800$, $n_s = 0.9694 \pm 0.0034$ at 68% CL (0.3σ) agrees well with *Planck* results, the case cutting *Planck* temperature data, with $\ell_{\text{TT}}^{\text{P18}} < 650$, gives $n_s = 0.9796 \pm 0.0049$ at 68% CL (2.1σ) when considering primary CMB only; we find 0.6σ and 2.3σ including second-order corrections, respectively. Results for the scalar running for which the combination P18+ACT with $\ell_{\text{TT}}^{\text{ACT}} > 1800$ are looser to the constraints obtained with *Planck* data alone; we find $\alpha_s = 0.0014^{+0.0062}_{-0.0040}$ with the cut on ACT data and $\alpha_s =$

	P18 ($\ell_{\text{TT}} < 650$) + ACT + BK18	P18 + ACT ($\ell_{\text{TT}} > 1800$) + BK18	P18 + SPT + BK18
FIRST ORDER			
$\ln(10^{10} A_s)$	3.041 ± 0.016	3.048 ± 0.015	$3.045^{+0.010}_{-0.015}$
ϵ_1 (at 95% CL)	< 0.0024	< 0.0022	< 0.0022
ϵ_2	0.0183 ± 0.0059	0.0312 ± 0.0044	0.0327 ± 0.0044
$n_{s,0.05}$	0.9794 ± 0.0056	0.9667 ± 0.0040	0.9651 ± 0.0041
$r_{0.05}$ (at 95% CL)	< 0.038	< 0.035	< 0.035
$n_{t,0.05}$	$-0.0023^{+0.0017}_{-0.0010}$	$-0.0021^{+0.0015}_{-0.0009}$	$-0.0021^{+0.0015}_{-0.0009}$
SECOND ORDER			
$\ln(10^{10} A_s)$	3.040 ± 0.016	3.047 ± 0.016	3.046 ± 0.012
ϵ_1 (at 95% CL)	< 0.0024	< 0.0022	< 0.0023
ϵ_2	$0.0166^{+0.0050}_{-0.0063}$	$0.0297^{+0.0055}_{-0.006}$	0.0383 ± 0.0071
ϵ_3 (at 95% CL)	< 0.27	$-0.06^{+0.33}_{-0.38}$	$0.15^{+0.27}_{-0.31}$
$n_{s,0.05}$	0.9796 ± 0.0055	0.9674 ± 0.0040	0.9640 ± 0.0041
$\alpha_{s,0.05}$	$0.0020^{+0.0045}_{-0.0027}$	$0.0010^{+0.0063}_{-0.0045}$	-0.0064 ± 0.0062
$r_{0.05}$ (at 95% CL)	< 0.038	< 0.035	< 0.036
$n_{t,0.05}$	$-0.0023^{+0.0016}_{-0.0010}$	$-0.0021^{+0.0016}_{-0.0010}$	$-0.0023^{+0.0016}_{-0.0010}$
$10^5 \alpha_{t,0.05}$	$-3.6^{+2.7}_{-1.4}$	$-6.1^{+4.4}_{-2.5}$	$-8.4^{+5.9}_{-3.5}$

Table 4. Constraints on the main (inflationary related) parameters and derived ones (at 68% CL if not otherwise stated) considering the combination P18+ACT+BK18 with two different multipole cuts, and P18+SPT-3G+BK18.

$0.0021^{+0.0045}_{-0.0026}$ by cutting *Planck* data, both at 68% CL. The combination P18+SPT agrees with *Planck* findings but with tighter error bars.

In fig. 6, we show the 68% CL and 95% CL of the HFFs obtained for the first-order analysis both for *Planck*, ACT, and SPT alone and their combinations. Our findings are consistent with the global picture that CMB data prefer potentials which are concave, i.e. $V_{\phi\phi} < 0$, in the observable window, with exception of the ACT+BK18 case. In fig. 7, we show the 68% CL and 95% CL of the HFFs obtained for the second-order analysis both for *Planck*, ACT, and SPT alone on the left and their combinations on the right.

Finally, we show the 68% CL and 95% CL marginalised constraints on the scalar inflationary parameters, derived using eqs. (C.20) to (C.22), that are for the second-order HFF expansion the scalar spectral index n_s and its running α_s in fig. 8 while for the third-order expansion include also the running of the running of the scalar spectral index β_s , see fig. 8. Although current constraints are consistent with small values for $1 - n_s$, α_s , and β_s as predicted by single-field slow-roll inflationary models, much larger values are still allowed by current CMB measurements. Here the light shaded region corresponds to $|\alpha_s| > |n_s - 1|^2$ for which we have qualitative violation of the single-field slow-roll predictions and analogously $|\beta_s| > |n_s - 1|^3$, as presented in Ref. [75].

	P18 ($\ell_{\text{TT}} < 650$) + ACT + BK18 + ext	P18 + ACT ($\ell_{\text{TT}} > 1800$) + BK18 + ext	P18 + SPT + BK18 + ext
FIRST ORDER			
$\ln(10^{10} A_s)$	3.048 ± 0.014	3.052 ± 0.013	$3.052^{+0.026}_{-0.020}$
ϵ_1 (at 95% CL)	< 0.0024	< 0.0023	< 0.0022
ϵ_2	0.0183 ± 0.0051	0.0292 ± 0.0037	0.0311 ± 0.0036
$n_{s,0.05}$	0.9794 ± 0.0049	0.9687 ± 0.0035	0.9667 ± 0.0033
$r_{0.05}$ (at 95% CL)	< 0.038	< 0.036	< 0.036
$n_{t,0.05}$	$-0.0023^{+0.0016}_{-0.0010}$	$-0.0021^{+0.0016}_{-0.0009}$	$-0.0022^{+0.0016}_{-0.0009}$
SECOND ORDER			
$\ln(10^{10} A_s)$	3.047 ± 0.014	3.051 ± 0.014	3.048 ± 0.011
ϵ_1 (at 95% CL)	< 0.0023	< 0.0023	< 0.0024
ϵ_2	$0.0166^{+0.0045}_{-0.0057}$	$0.0274^{+0.0047}_{-0.0063}$	0.0354 ± 0.0066
ϵ_3 (at 95% CL)	< 0.26	$-0.08^{+0.32}_{-0.40}$	$0.13^{+0.30}_{-0.34}$
$n_{s,0.05}$	0.9796 ± 0.0049	0.9694 ± 0.0034	0.9661 ± 0.0035
$\alpha_{s,0.05}$	$0.0021^{+0.0045}_{-0.0026}$	$0.0014^{+0.0062}_{-0.0040}$	-0.0055 ± 0.0062
$r_{0.05}$ (at 95% CL)	< 0.037	< 0.035	< 0.037
$n_{t,0.05}$	$-0.0023^{+0.0016}_{-0.0010}$	$-0.0022^{+0.0016}_{-0.0010}$	$-0.0023^{+0.0016}_{-0.0010}$
$10^5 \alpha_{t,0.05}$	$-3.6^{+2.6}_{-1.4}$	$-5.7^{+4.0}_{-2.4}$	$-8.0^{+5.5}_{-3.3}$
THIRD ORDER			
$\ln(10^{10} A_s)$	3.046 ± 0.014	3.052 ± 0.014	3.048 ± 0.011
ϵ_1 (at 95% CL)	< 0.0024	< 0.0022	< 0.0023
ϵ_2	$0.0166^{+0.0047}_{-0.0063}$	$0.0291^{+0.0049}_{-0.0066}$	$0.0363^{+0.0068}_{-0.0085}$
ϵ_3 (at 95% CL)	< 0.34	$0.00^{+0.37}_{-0.35}$	> -0.13
ϵ_4	–	–	–
$n_{s,0.05}$	0.9804 ± 0.0049	0.9695 ± 0.0035	0.9673 ± 0.0038
$\alpha_{s,0.05}$	$0.0019^{+0.0046}_{-0.0039}$	$-0.0002^{+0.0054}_{-0.0047}$	$-0.0056^{+0.0064}_{-0.0051}$
$\beta_{s,0.05}$	$-0.0011^{+0.0018}_{-0.0007}$	$-0.0010^{+0.0020}_{-0.0006}$	$-0.0025^{+0.0043}_{-0.0012}$
$r_{0.05}$ (at 95% CL)	< 0.037	< 0.035	< 0.036
$n_{t,0.05}$	$-0.0023^{+0.0016}_{-0.0010}$	$-0.0022^{+0.0015}_{-0.0010}$	$-0.0023^{+0.0016}_{-0.0010}$
$10^5 \alpha_{t,0.05}$	$-3.6^{+2.7}_{-1.3}$	$-6.2^{+4.5}_{-2.5}$	$-8.9^{+6.4}_{-3.7}$
$10^5 \beta_{t,0.05}$	$0.2^{+1.0}_{-0.6}$	$-0.4^{+1.4}_{-0.7}$	$-2.2^{+2.6}_{-1.1}$

Table 5. Same as table 4 in combination with the external datasets, which are BAO and RSD measurements, SNe, and CMB lensing.

4.3 Future CMB Constraints

In this subsection, we explore the forecasted capabilities of a concept for a future CMB space mission. Assuming that CMB anisotropies follow a Gaussian distribution and are statistically isotropic, we use the following Gaussian likelihood \mathcal{L} [76, 77]

$$-2 \ln \mathcal{L} = \sum_{\ell} (2\ell + 1) f_{\text{sky}} \left(\text{Tr}[\hat{\mathbf{C}}_{\ell} \bar{\mathbf{C}}_{\ell}^{-1}] + \ln |\hat{\mathbf{C}}_{\ell} \bar{\mathbf{C}}_{\ell}^{-1}| - 4 \right), \quad (4.31)$$

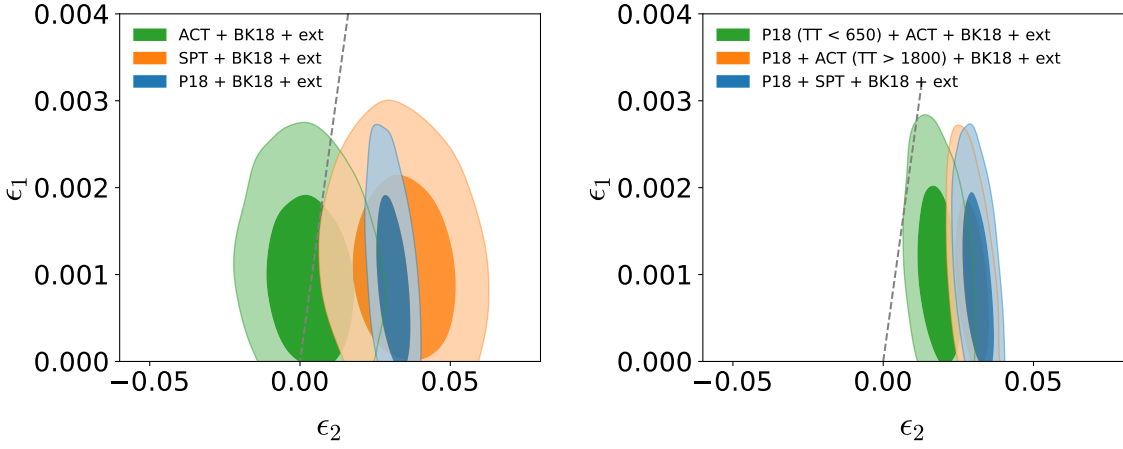


Figure 6. Marginalised joint confidence contours for the first two HFF parameters ϵ_1 and ϵ_2 assuming first-order slow-roll predictions. The grey dashed line divide the parameter space from convex (left side) to concave (right side) single-field slow-roll potentials.

where \bar{C}_ℓ denote the theoretical data covariance matrices

$$\bar{C}_\ell \equiv \begin{bmatrix} \bar{C}_\ell^{TT} + N_\ell^{TT} & \bar{C}_\ell^{TE} & 0 & 0 \\ \bar{C}_\ell^{TE} & \bar{C}_\ell^{EE} + N_\ell^{EE} & 0 & 0 \\ 0 & 0 & \bar{C}_\ell^{BB} + N_\ell^{BB} & 0 \\ 0 & 0 & 0 & \bar{C}_\ell^{\phi\phi} + N_\ell^{\phi\phi} \end{bmatrix}, \quad (4.32)$$

and \hat{C}_ℓ are the fiducial data covariance matrices

$$\hat{C}_\ell \equiv \begin{bmatrix} \hat{C}_\ell^{TT} & \hat{C}_\ell^{TE} & 0 & 0 \\ \hat{C}_\ell^{TE} & \hat{C}_\ell^{EE} & 0 & 0 \\ 0 & 0 & \hat{C}_\ell^{BB} & 0 \\ 0 & 0 & 0 & \hat{C}_\ell^{\phi\phi} \end{bmatrix}. \quad (4.33)$$

Noise power spectra for the temperature and polarisation angular power spectra account for isotropic noise deconvolved with the instrumental Gaussian beam as

$$N_\ell^{XX} = w_{XX}^{-1} e^{\ell(\ell+1) \frac{\theta_{\text{FWHM}}^2}{8 \ln 2}}. \quad (4.34)$$

We assume an effective noise variance $w_{\text{TT}}^{-1/2} = 1.2 \mu\text{K arcmin}$ and $w_{\text{EE}}^{-1/2} = w_{\text{BB}}^{-1/2} = \sqrt{2} w_{\text{TT}}^{-1/2}$ and an effective beam resolution of $\theta_{\text{FWHM}} = 5.5 \text{ arcmin}$ over 70% of the sky considering the multipole range $2 \leq \ell \leq 3000$. These instrumental specifications corresponds to a CMB experiment cosmic-variance limited up to $\ell = 2800$ in temperature, $\ell = 2000$ in E-mode polarisation, and $\ell = 800$ in the gravitational lensing over almost the full sky.

Together with the primary temperature and polarisation anisotropy signal, we also take into account information from CMB weak lensing, considering the power spectrum of the CMB lensing potential $C_\ell^{\phi\phi}$. For the CMB lensing noise power spectrum, we

adopt the minimum-variance quadratic estimator for the lensing reconstruction [78] in the range $30 \leq \ell \leq 3000$, combining the TT, EE, BB, TE, TB, and EB estimators and applying iterative lensing reconstruction according to Refs. [79, 80].

Finally, we consider internal delensing [81–83], with the above specifications, of the B-mode angular power spectrum in order to reduce the non-primordial contribution induced by lensing. We implement the delensing removing the lensing contribution to the B-mode angular power spectra and adding an error contribution to the instrumental noise N_ℓ^{BB} .

We assume a flat Universe with a cosmological constant, two massless neutrino with $N_{\text{eff}} = 2.046$, and a massive one with fixed minimum mass $m_\nu = 0.06$ eV. To generate the fiducial angular power spectra, we have fixed the HFFs to the expected numbers for T-model of α -attractor inflation with $\alpha = 1$ assuming $N_* = 55$ at $k_* = 0.05 \text{ Mpc}^{-1}$. This corresponds to $\epsilon_1 = 0.000235$, $\epsilon_2 = 0.0352$, $\epsilon_3 = 0.0175$, and $\epsilon_4 = 0.0175$. On these simulated measurements, we analyse the PPS equations at second order, with $\epsilon_4 = 0$ and neglecting third-order corrections, and the full third-order expressions. The results are shown in fig. 9. We conclude that for a futuristic CMB

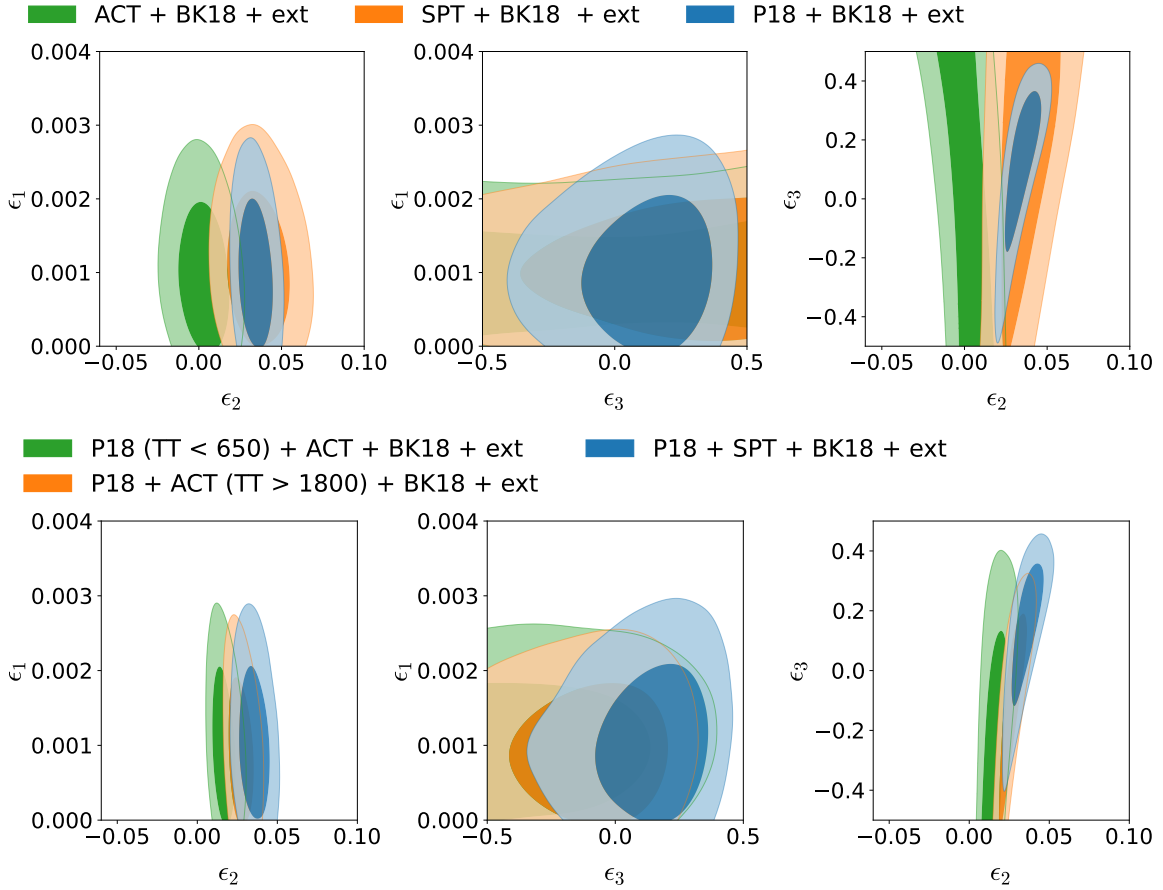


Figure 7. Marginalised joint confidence contours for the first three HFF parameters ϵ_1 , ϵ_2 , and ϵ_3 assuming second-order slow-roll predictions.

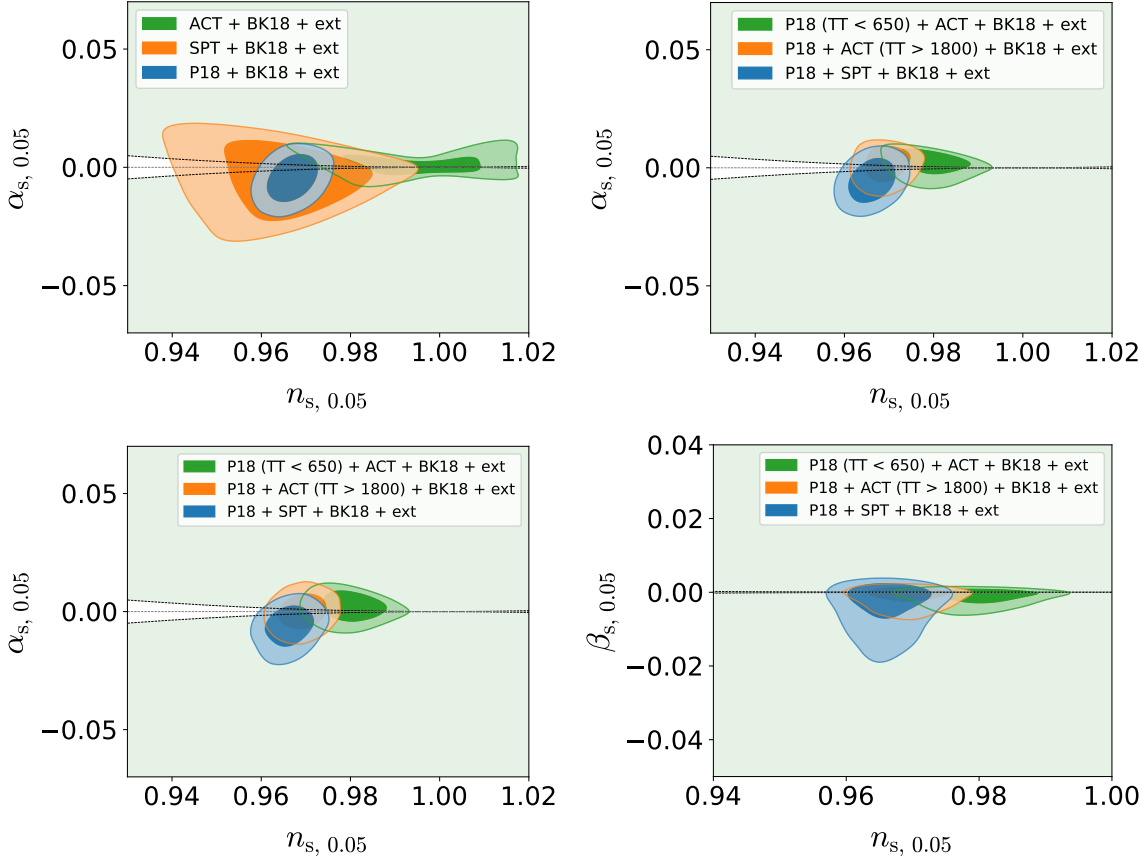


Figure 8. Marginalised joint confidence contours for the scalar spectral index n_s and its running α_s assuming second-order slow-roll predictions (upper panels) and for the scalar spectral index n_s , its running α_s , and the running of the running β_s assuming third-order slow-roll predictions (lower panels).

experiment alone:

- HFFs are well recovered without any bias or significant change in the uncertainties stopping at second order;
- the fourth HFF ϵ_4 remains unconstrained considering CMB experiments only;
- uncertainties on the HFFs are significantly reduced with a high significance statistical detection of ϵ_2 (for this specific fiducial also ϵ_1 is well measured). For these case, we obtain $\epsilon_1 = 0.000239 \pm 0.000016$, $\epsilon_2 = 0.0357 \pm 0.0018$, and $\epsilon_3 = 0.023 \pm 0.066$ at 68% CL consistently with previous forecast studies, see Ref. [84].

5 Conclusions

In this paper, we conducted an extensive analysis of the primordial power spectra (PPS) for both scalar and tensor perturbations, focusing on the higher-order corrections

within the slow-roll inflationary framework. By utilising Green’s function techniques to solve the Mukhanov-Sasaki equation and its tensor counterpart, we were able to extend our analytical calculations up to third-order corrections, thereby refining the perturbative expansion in terms of slow-roll parameters. Third-order corrections for both scalar and tensor PPS have already been calculated in Ref. [21]. Here we have used a different strategy to solve the integrals, and found some, but small, differences in some of the coefficients which multiply the third-order terms. These different coefficients only appear in the constant part of the PPS without the results obtained for the spectral indices and their slopes. We have verified that the differences in PPS are numerically negligible.

Our results demonstrate that higher-order corrections significantly enhance the accuracy of the predicted power spectra, spectral indices, and their derivatives. However going from the second to the third-order expansion, the improvement becomes appreciable at very small scales $k \gtrsim 10 \text{ Mpc}^{-1}$ leaving almost unaffected the CMB

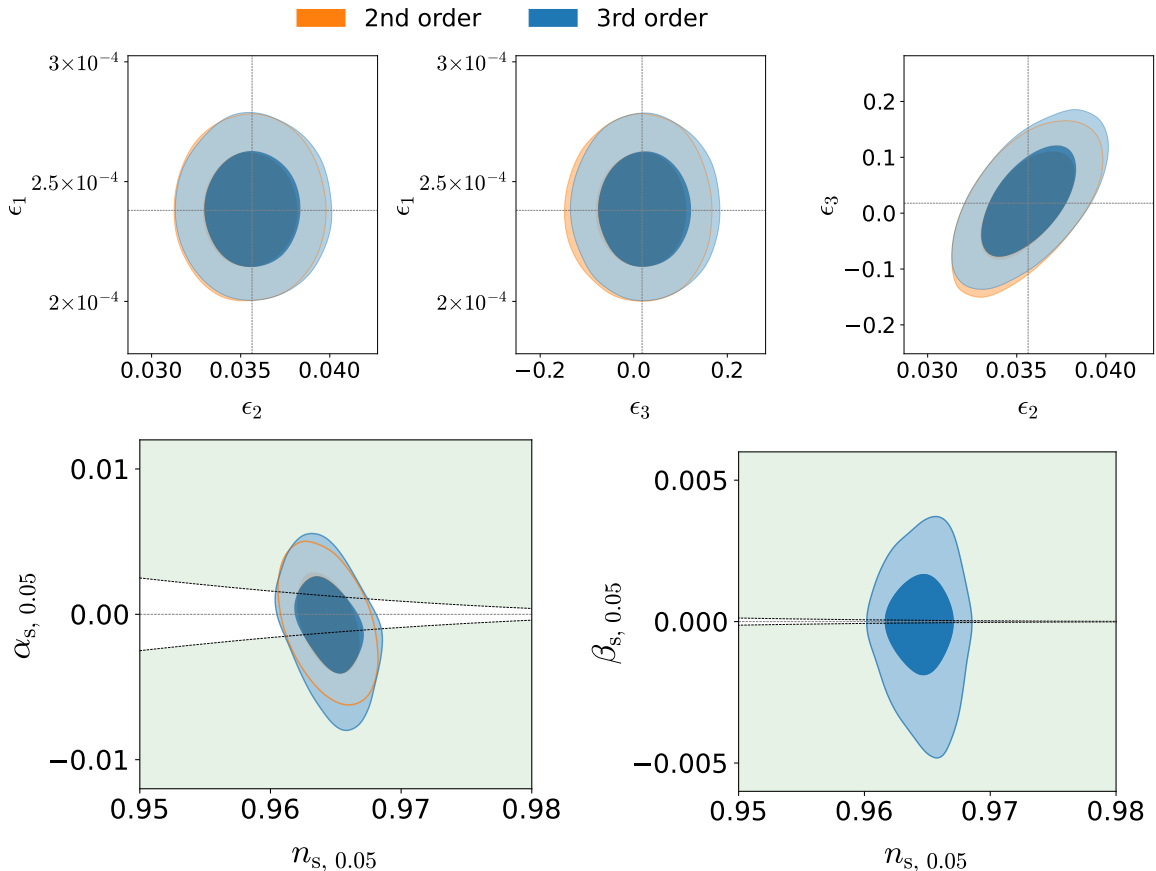


Figure 9. Marginalised joint confidence contours for the first two HFF parameters ϵ_1 , ϵ_2 , and ϵ_3 assuming second- and third-order slow-roll predictions (upper panels). Marginalised joint confidence contours for the scalar spectral index n_s and its running α_s assuming second- and third-order slow-roll predictions (lower left panel) and for the scalar spectral index n_s and its running of the running β_s assuming third-order slow-roll predictions (lower right panel).

angular power spectra, see figs. 1 to 5. Since the accuracy requirement for tensor quantities is less than on the scalars, it is the scalars upon which attention should be focused.

We investigated the constraints on the first four HFFs ϵ_i obtained from CMB anisotropy measurements in combination with late-time cosmological observations such as uncalibrated Type Ia Supernovae from the Pantheon catalogue, baryon acoustic oscillations and redshift space distortions from SDSS/BOSS/eBOSS. Regarding the CMB datasets considered, we study the impact of different combination of temperature and E-mode polarisation data from *Planck*, ACT, and SPT. We always included in our analysis B-mode polarisation measurements from BICEP/Keck. Our analysis yields a stringent upper limit for the first HFF, $\epsilon_1 \lesssim 0.002$ at 95% CL, primarily constrained by BICEP/Keck data. This result underscores the robustness of ϵ_1 across various combinations of observational datasets. By combining data from *Planck* with late-time cosmological observations, we derived $\epsilon_2 \simeq 0.031 \pm 0.004$ at 68% CL when considering only first-order corrections. Including second- and third-order corrections broadens this constraint to $\epsilon_2 \simeq 0.034 \pm 0.007$ at 68% CL. For the third HFF, our findings indicate a value of $\epsilon_3 \simeq 0.1 \pm 0.4$ at 95% CL, which remains consistent across second- and third-order corrections. The fourth HFF ϵ_4 , however, remains unconstrained by current data as shown also in Ref. [28].

We then add small scale CMB measurements from ACT and SPT to the *Planck* data. Our combination of *Planck* data with measurements from ACT (were we removed the temperature data below $\ell = 1800$ as recommended from the ACT collaboration to avoid correlations between the two datasets) and from SPT led to consistent results with slightly more stringent constraints on ϵ_2 and ϵ_3 . ACT data alone results and the combination of ACT with *Planck* temperature data removed above $\ell = 650$, lead to shifts in the mean values of ϵ_2 and ϵ_3 , which suggest a preference for higher values of the scalar spectral index and positive values for the running of the scalar spectral index.

We studied the case of a futuristic CMB experiments with realistic and almost cosmic-variance limited specifications. These results show that second-order equations are accurate enough to describe current and future CMB observations, see fig. 9. ϵ_4 remains unconstrained also for future CMB measurements.

In conclusion, future small-scale CMB measurements from ACT, SPT, and Simons Observatory will be crucial to further test high-order terms in the slow-roll expansion and the validity of single-field slow-roll predictions. In addition, future data over a wider range of scales such as large-scale structure (LSS) measurements from *Euclid* [85], CMB spectral distortions [86], 21 cm experiments [87], and on smaller scales abundance of primordial black holes can offer useful constraints on the primordial curvature power spectrum [88]. These additional cosmological probes will enable us to confirm single-field slow-roll inflation, for instance through a detection of the running of the scalar spectral index [85, 89, 90], or to falsify it.

Acknowledgments

MB and SSS acknowledge financial support from the INFN InDark initiative. MB also acknowledges financial support from the COSMOS network (www.cosmosnet.it) through the ASI (Italian Space Agency) Grants 2016-24-H.0, 2016-24-H.1-2018, 2020-9-HH.0 (participation in LiteBIRD phase A) and by “Bando Giovani anno 2023 per progetti di ricerca finanziati con il contributo 5x1000 anno 2021”. SSS acknowledges that this publication was produced while attending the PhD program in Space Science and Technology at the University of Trento, Cycle XXXVIII, with the support of a scholarship co-financed by the Ministerial Decree no. 351 of 9th April 2022, based on the NRRP - funded by the European Union - NextGenerationEU - Mission 4 ”Education and Research”, Component 2 ”From Research to Business”, Investment 3.3. SSS acknowledges that this publication is based upon work from COST Action CA21136 – “Addressing observational tensions in cosmology with systematics and fundamental physics (CosmoVerse)”, supported by COST (European Cooperation in Science and Technology).

A Useful Integrals

Here some useful integrals used to manipulate the solutions entering in the third-order Green's function solution eq. (2.24). These integrals have been computed by repeatedly applying integration by parts.

$$\int_x^\infty \frac{du}{u^2} e^{2iu} = \frac{e^{2ix}}{x} + 2i \int_x^\infty \frac{du}{u} e^{2iu} \quad (\text{A.1a})$$

$$\int_x^\infty \frac{du}{u^3} e^{2iu} = \left(\frac{1}{2x^2} + \frac{i}{x} \right) e^{2ix} - 2 \int_x^\infty \frac{du}{u} e^{2iu} \quad (\text{A.1b})$$

$$\int_x^\infty \frac{du}{u^4} e^{2iu} = \left(\frac{1}{3x^3} + \frac{i}{3x^2} - \frac{2}{3x} \right) e^{2ix} - \frac{4i}{3} \int_x^\infty \frac{du}{u} e^{2iu} \quad (\text{A.1c})$$

$$\begin{aligned} \int_x^\infty \frac{du}{u^2} e^{-2iu} \int_u^\infty \frac{dt}{t} e^{2it} &= -\frac{1}{x} + \frac{e^{-2ix}}{x} \int_x^\infty \frac{du}{u} e^{2iu} \\ &\quad - 2i \int_x^\infty \frac{du}{u} e^{-2iu} \int_u^\infty \frac{dt}{t} e^{2it} \end{aligned} \quad (\text{A.2a})$$

$$\begin{aligned} \int_x^\infty \frac{du}{u^3} e^{-2iu} \int_u^\infty \frac{dt}{t} e^{2it} &= -\left(\frac{1}{4x^2} - \frac{i}{x} \right) + \left(\frac{1}{2x^2} - \frac{i}{x} \right) e^{-2ix} \int_x^\infty \frac{du}{u} e^{2iu} \\ &\quad - 2 \int_x^\infty \frac{du}{u} e^{-2iu} \int_u^\infty \frac{dt}{t} e^{2it} \end{aligned} \quad (\text{A.2b})$$

$$\begin{aligned} \int_x^\infty \frac{du}{u^4} e^{-2iu} \int_u^\infty \frac{dt}{t} e^{2it} &= -\left(\frac{1}{9x^3} - \frac{i}{6x^2} - \frac{2}{3x} \right) + \left(\frac{1}{3x^3} - \frac{i}{3x^2} - \frac{2}{3x} \right) e^{-2ix} \int_x^\infty \frac{du}{u} e^{2iu} \\ &\quad + \frac{4i}{3} \int_x^\infty \frac{du}{u} e^{-2iu} \int_u^\infty \frac{dt}{t} e^{2it} \end{aligned} \quad (\text{A.2c})$$

$$\int_x^\infty \frac{du}{u^2} e^{2iu} \ln u = \frac{e^{2ix}}{x} + \frac{e^{2ix} \ln x}{x} + 2i \int_x^\infty \frac{du}{u} e^{2iu} + 2i \int_x^\infty \frac{du}{u} e^{2iu} \ln u \quad (\text{A.3a})$$

$$\begin{aligned} \int_x^\infty \frac{du}{u^3} e^{2iu} \ln u &= \left(\frac{1}{4x^2} + \frac{3i}{2x} \right) e^{2ix} + \left(\frac{1}{2x^2} + \frac{i}{x} \right) e^{2ix} \ln x \\ &\quad - 3 \int_x^\infty \frac{du}{u} e^{2iu} - 2 \int_x^\infty \frac{du}{u} e^{2iu} \ln u \end{aligned} \quad (\text{A.3b})$$

$$\begin{aligned} \int_x^\infty \frac{du}{u^4} e^{2iu} \ln u &= \left(\frac{1}{9x^3} + \frac{5i}{18x^2} - \frac{11}{9x} \right) e^{2ix} + \left(\frac{1}{3x^3} + \frac{i}{3x^2} - \frac{2}{3x} \right) e^{2ix} \ln x \\ &\quad - \frac{22i}{9} \int_x^\infty \frac{du}{u} e^{2iu} - \frac{4i}{3} \int_x^\infty \frac{du}{u} e^{2iu} \ln u \end{aligned} \quad (\text{A.3c})$$

$$\begin{aligned} \int_x^\infty \frac{du}{u^2} \int_u^\infty \frac{dt}{t} e^{-2it} \int_t^\infty \frac{ds}{s} e^{2is} &= \frac{1}{x} - \frac{e^{-2ix}}{x} \int_x^\infty \frac{du}{u} e^{2iu} \\ &\quad + \left(\frac{1}{x} + 2i \right) \int_x^\infty \frac{du}{u} e^{-2iu} \int_u^\infty \frac{dt}{t} e^{2it} \end{aligned} \quad (\text{A.4a})$$

$$\begin{aligned} \int_x^\infty \frac{du}{u^4} \int_u^\infty \frac{dt}{t} e^{-2it} \int_t^\infty \frac{ds}{s} e^{2is} &= \left(\frac{1}{27x^3} - \frac{i}{18x^2} - \frac{2}{9x} \right) \\ &\quad - \left(\frac{1}{9x^3} - \frac{i}{9x^2} - \frac{2}{9x} \right) e^{-2ix} \int_x^\infty \frac{du}{u} e^{2iu} \\ &\quad + \left(\frac{1}{3x^3} - \frac{4i}{9} \right) \int_x^\infty \frac{du}{u} e^{-2iu} \int_u^\infty \frac{dt}{t} e^{2it} \end{aligned} \quad (\text{A.4b})$$

$$\begin{aligned}
\int_x^\infty \frac{du}{u^2} e^{2iu} \int_u^\infty \frac{dt}{t} e^{-2it} \int_t^\infty \frac{ds}{s} e^{2is} &= \frac{e^{2ix}}{x} - \left(\frac{1}{x} - 2i \right) \int_x^\infty \frac{du}{u} e^{2iu} \\
&+ \frac{e^{2ix}}{x} \int_x^\infty \frac{du}{u} e^{-2iu} \int_u^\infty \frac{dt}{t} e^{2it} \\
&+ 2i \int_x^\infty \frac{du}{u} e^{2iu} \int_u^\infty \frac{dt}{t} e^{-2it} \int_t^\infty \frac{ds}{s} e^{2is}
\end{aligned} \tag{A.5a}$$

$$\begin{aligned}
\int_x^\infty \frac{du}{u^3} e^{2iu} \int_u^\infty \frac{dt}{t} e^{-2it} \int_t^\infty \frac{ds}{s} e^{2is} &= \left(\frac{1}{8x^2} + \frac{5i}{4x} \right) e^{2ix} - \left(\frac{1}{4x^2} + \frac{i}{x} + \frac{5}{2} \right) \int_x^\infty \frac{du}{u} e^{2iu} \\
&+ \left(\frac{1}{2x^2} + \frac{i}{x} \right) e^{2ix} \int_x^\infty \frac{du}{u} e^{-2iu} \int_u^\infty \frac{dt}{t} e^{2it} \\
&- 2 \int_x^\infty \frac{du}{u} e^{2iu} \int_u^\infty \frac{dt}{t} e^{-2it} \int_t^\infty \frac{ds}{s} e^{2is}
\end{aligned} \tag{A.5b}$$

$$\begin{aligned}
\int_x^\infty \frac{du}{u^4} e^{2iu} \int_u^\infty \frac{dt}{t} e^{-2it} \int_t^\infty \frac{ds}{s} e^{2is} &= \left(\frac{1}{27x^3} + \frac{13i}{108x^2} - \frac{49}{54x} \right) e^{2ix} \\
&- \left(\frac{1}{9x^3} + \frac{i}{6x^2} - \frac{2}{3x} + \frac{49i}{27} \right) \int_x^\infty \frac{du}{u} e^{2iu} \\
&+ \left(\frac{1}{3x^3} + \frac{i}{3x^2} - \frac{2}{3x} \right) e^{2ix} \int_x^\infty \frac{du}{u} e^{-2iu} \int_u^\infty \frac{dt}{t} e^{2it} \\
&- \frac{4i}{3} \int_x^\infty \frac{du}{u} e^{2iu} \int_u^\infty \frac{dt}{t} e^{-2it} \int_t^\infty \frac{ds}{s} e^{2is}
\end{aligned} \tag{A.5c}$$

$$\begin{aligned} \int_x^\infty \frac{du}{u^2} e^{-2iu} \int_u^\infty \frac{dt}{t} e^{2it} \ln t &= -\frac{1}{x} - \frac{\ln x}{x} + \frac{e^{-2ix}}{x} \int_x^\infty \frac{du}{u} e^{2iu} \ln u \\ &\quad - 2i \int_x^\infty \frac{du}{u} e^{-2iu} \int_u^\infty \frac{dt}{t} e^{2it} \ln t \end{aligned} \quad (\text{A.6a})$$

$$\begin{aligned} \int_x^\infty \frac{du}{u^3} e^{-2iu} \int_u^\infty \frac{dt}{t} e^{2it} \ln t &= -\left(\frac{1}{8x^2} - \frac{i}{x}\right) - \left(\frac{1}{4x^2} - \frac{i}{x}\right) \ln x \\ &\quad + \left(\frac{1}{2x^2} - \frac{i}{x}\right) e^{-2ix} \int_x^\infty \frac{du}{u} e^{2iu} \ln u \\ &\quad - 2 \int_x^\infty \frac{du}{u} e^{-2iu} \int_u^\infty \frac{dt}{t} e^{2it} \ln t \end{aligned} \quad (\text{A.6b})$$

$$\begin{aligned} \int_x^\infty \frac{du}{u^4} e^{-2iu} \int_u^\infty \frac{dt}{t} e^{2it} \ln t &= -\left(\frac{1}{27x^3} - \frac{i}{12x^2} - \frac{2}{3x}\right) - \left(\frac{1}{9x^3} - \frac{i}{6x^2} - \frac{2}{3x}\right) \ln x \\ &\quad + \left(\frac{1}{3x^3} - \frac{i}{3x^2} - \frac{2}{3x}\right) e^{-2ix} \int_x^\infty \frac{du}{u} e^{2iu} \ln u \\ &\quad + \frac{4i}{3} \int_x^\infty \frac{du}{u} e^{-2iu} \int_u^\infty \frac{dt}{t} e^{2it} \ln t \end{aligned} \quad (\text{A.6c})$$

$$\int_x^\infty \frac{du}{u^2} \int_u^\infty \frac{dt}{t} e^{2it} = -\frac{e^{2ix}}{x} + \left(\frac{1}{x} - 2i\right) \int_x^\infty \frac{du}{u} e^{2iu} \quad (\text{A.7a})$$

$$\int_x^\infty \frac{du}{u^3} \int_u^\infty \frac{dt}{t} e^{2it} = -\left(\frac{1}{4x^2} + \frac{i}{2x}\right) e^{2ix} + \left(\frac{1}{2x^2} + 1\right) \int_x^\infty \frac{du}{u} e^{2iu} \quad (\text{A.7b})$$

$$\int_x^\infty \frac{du}{u^4} \int_u^\infty \frac{dt}{t} e^{2it} = -\left(\frac{1}{9x^3} + \frac{i}{9x^2} - \frac{2}{9x}\right) e^{2ix} + \left(\frac{1}{3x^3} + \frac{4i}{9}\right) \int_x^\infty \frac{du}{u} e^{2iu} \quad (\text{A.7c})$$

$$\begin{aligned} \int_x^\infty \frac{du}{u^2} \int_u^\infty \frac{dt}{t} e^{2it} \ln t &= -\frac{e^{2ix}}{x} - \frac{e^{2ix} \ln x}{x} \\ &\quad - 2i \int_x^\infty \frac{du}{u} e^{2iu} + \left(\frac{1}{x} - 2i\right) \int_x^\infty \frac{du}{u} e^{2iu} \ln u \end{aligned} \quad (\text{A.8a})$$

$$\begin{aligned} \int_x^\infty \frac{du}{u^4} \int_u^\infty \frac{dt}{t} e^{2it} \ln t &= -\left(\frac{1}{27x^3} + \frac{5i}{54x^2} - \frac{11}{27x}\right) e^{2ix} - \left(\frac{1}{9x^3} + \frac{i}{9x^2} - \frac{2}{9x}\right) e^{2ix} \ln x \\ &\quad + \frac{22i}{27} \int_x^\infty \frac{du}{u} e^{2iu} + \left(\frac{1}{3x^3} + \frac{4i}{9}\right) \int_x^\infty \frac{du}{u} e^{2iu} \ln u \end{aligned} \quad (\text{A.8b})$$

$$\begin{aligned}
\int_x^\infty \frac{du}{u^2} e^{-2iu} \ln u \int_u^\infty \frac{dt}{t} e^{2it} &= -\frac{2}{x} - \frac{\ln x}{x} + \frac{e^{-2ix}}{x} \int_x^\infty \frac{du}{u} e^{2iu} \\
&+ \frac{e^{-2ix} \ln x}{x} \int_x^\infty \frac{du}{u} e^{2iu} - 2i \int_x^\infty \frac{du}{u} e^{-2iu} \int_u^\infty \frac{dt}{t} e^{2it} \\
&- 2i \int_x^\infty \frac{du}{u} e^{-2iu} \ln u \int_u^\infty \frac{dt}{t} e^{2it} \tag{A.9a}
\end{aligned}$$

$$\begin{aligned}
\int_x^\infty \frac{du}{u^3} e^{-2iu} \ln u \int_u^\infty \frac{dt}{t} e^{2it} &= -\left(\frac{1}{4x^2} - \frac{5i}{2x}\right) - \left(\frac{1}{4x^2} - \frac{i}{x}\right) \ln x \\
&+ \left(\frac{1}{4x^2} - \frac{3i}{2x}\right) e^{-2ix} \int_x^\infty \frac{du}{u} e^{2iu} \\
&+ \left(\frac{1}{2x^2} - \frac{i}{x}\right) e^{-2ix} \ln x \int_x^\infty \frac{du}{u} e^{2iu} \\
&- 3 \int_x^\infty \frac{du}{u} e^{-2iu} \int_u^\infty \frac{dt}{t} e^{2it} \\
&- 2 \int_x^\infty \frac{du}{u} e^{-2iu} \ln u \int_u^\infty \frac{dt}{t} e^{2it} \tag{A.9b}
\end{aligned}$$

$$\begin{aligned}
\int_x^\infty \frac{du}{u^4} e^{-2iu} \ln u \int_u^\infty \frac{dt}{t} e^{2it} &= -\left(\frac{2}{27x^3} - \frac{2i}{9x^2} - \frac{17}{9x}\right) - \left(\frac{1}{9x^3} - \frac{i}{6x^2} - \frac{2}{3x}\right) \ln x \\
&+ \left(\frac{1}{9x^3} - \frac{5i}{18x^2} - \frac{11}{9x}\right) e^{-2ix} \int_x^\infty \frac{du}{u} e^{2iu} \\
&+ \left(\frac{1}{3x^3} - \frac{i}{3x^2} - \frac{2}{3x}\right) e^{-2ix} \ln x \int_x^\infty \frac{du}{u} e^{2iu} \\
&+ \frac{22i}{9} \int_x^\infty \frac{du}{u} e^{-2iu} \int_u^\infty \frac{dt}{t} e^{2it} \\
&+ \frac{4i}{3} \int_x^\infty \frac{du}{u} e^{-2iu} \ln u \int_u^\infty \frac{dt}{t} e^{2it} \tag{A.9c}
\end{aligned}$$

$$\begin{aligned}
\int_x^\infty \frac{du}{u^2} \ln u \int_u^\infty \frac{dt}{t} e^{2it} &= -\frac{2e^{2ix}}{x} - \frac{e^{2ix} \ln x}{x} + \left(\frac{1}{x} - 4i\right) \int_x^\infty \frac{du}{u} e^{2iu} \\
&\quad + \frac{\ln x}{x} \int_x^\infty \frac{du}{u} e^{2iu} - 2i \int_x^\infty \frac{du}{u} e^{2iu} \ln u
\end{aligned} \tag{A.10a}$$

$$\begin{aligned}
\int_x^\infty \frac{du}{u^4} \ln u \int_u^\infty \frac{dt}{t} e^{2it} &= -\left(\frac{2}{27x^3} + \frac{7i}{54x^2} - \frac{13}{27x}\right) e^{2ix} - \left(\frac{1}{9x^3} - \frac{i}{9x^2} - \frac{2}{9x}\right) e^{2ix} \ln x \\
&\quad + \left(\frac{1}{9x^3} + \frac{26i}{27}\right) \int_x^\infty \frac{du}{u} e^{2iu} \\
&\quad + \frac{\ln x}{3x^3} \int_x^\infty \frac{du}{u} e^{2iu} \\
&\quad + \frac{4i}{9} \int_x^\infty \frac{du}{u} e^{2iu} \ln u
\end{aligned} \tag{A.10b}$$

$$\begin{aligned}
\int_x^\infty \frac{du}{u^2} e^{2iu} \ln^2 u &= \frac{2e^{2ix}}{x} + \frac{2e^{2ix} \ln x}{x} + \frac{e^{2ix} \ln^2 x}{x} \\
&\quad + 4i \int_x^\infty \frac{du}{u} e^{2iu} + 4i \int_x^\infty \frac{du}{u} e^{2iu} \ln u \\
&\quad + 2i \int_x^\infty \frac{du}{u} e^{2iu} \ln^2 u
\end{aligned} \tag{A.11a}$$

$$\begin{aligned}
\int_x^\infty \frac{du}{u^3} e^{2iu} \ln^2 u &= \left(\frac{1}{4x^2} + \frac{7i}{2x}\right) e^{2ix} + \left(\frac{1}{2x^2} + \frac{3i}{x}\right) e^{2ix} \ln x \\
&\quad + \left(\frac{1}{2x^2} + \frac{i}{x}\right) e^{2ix} \ln^2 x - 7 \int_x^\infty \frac{du}{u} e^{2iu} \\
&\quad - 6 \int_x^\infty \frac{du}{u} e^{2iu} \ln u - 2 \int_x^\infty \frac{du}{u} e^{2iu} \ln^2 u
\end{aligned} \tag{A.11b}$$

$$\begin{aligned}
\int_x^\infty \frac{du}{u^4} e^{2iu} \ln^2 u &= \left(\frac{2}{27x^3} + \frac{19i}{54x^2} - \frac{85}{27x}\right) e^{2ix} + \left(\frac{2}{9x^3} + \frac{5i}{9x^2} - \frac{22}{9x}\right) e^{2ix} \ln x \\
&\quad + \left(\frac{1}{3x^3} + \frac{i}{3x^2} - \frac{2}{3x}\right) e^{2ix} \ln^2 x \\
&\quad - \frac{170i}{27} \int_x^\infty \frac{du}{u} e^{2iu} - \frac{44i}{9} \int_x^\infty \frac{du}{u} e^{2iu} \ln u \\
&\quad - \frac{4i}{3} \int_x^\infty \frac{du}{u} e^{2iu} \ln^2 u
\end{aligned} \tag{A.11c}$$

B Super-Hubble Limits for the Integrals

We report here the calculation of the integrals appearing in eqs. (2.25), (2.27a), (2.27b), (2.30), (2.33) and (2.35) and their asymptotic solutions, calculated in the super-Hubble limit, required to calculate the PPS of scalar and tensor perturbations.

We start recognising that eq. (2.25) corresponds to the exponential integral

$$\text{Ei}(-2ix) = \int_x^\infty \frac{du}{u} e^{2iu}, \quad (\text{B.1})$$

defined for $x > 0$ whose series is

$$\text{Ei}(z) \equiv \gamma + \ln(-z) + \sum_{n=1}^{+\infty} \frac{(z)^n}{n!n}. \quad (\text{B.2})$$

Afterwards, in order to compute the super-Hubble limit for $x \rightarrow 0$, we consider terms up to the linear one, obtaining

$$\lim_{x \rightarrow 0} \int_x^\infty \frac{du}{u} e^{2iu} = \alpha + \frac{i\pi}{2} - 2 - 2ix - \ln x + \mathcal{O}(x^2), \quad (\text{B.3})$$

where $\alpha = 2 - \gamma - \ln 2$. Analogously, using the exponential integral properties, we can obtain

$$\lim_{x \rightarrow 0} \int_x^\infty \frac{du}{u} e^{2iu} \ln u = 2 - i\pi - \frac{\pi^2}{24} + 2ix - 2\alpha + \frac{i\pi\alpha}{2} - 2ix \ln x - \frac{\ln^2 x}{2} + \mathcal{O}(x^2), \quad (\text{B.4})$$

$$\begin{aligned} \lim_{x \rightarrow 0} \int_x^\infty \frac{du}{u} e^{2iu} \ln^2 u = & -\frac{8}{3} + 2i\pi + \frac{\pi^2}{6} + \frac{i\pi^3}{24} - 4ix + 4\alpha - 2i\pi\alpha - \frac{\pi^2\alpha}{12} - 2\alpha^2 \\ & + \frac{i\pi\alpha^2}{2} + \frac{\alpha^3}{3} - \frac{2\zeta(3)}{3} + 4ix \ln x - 2ix \ln^2 x - \frac{\ln^3 x}{3} + \mathcal{O}(x^2), \end{aligned} \quad (\text{B.5})$$

see for details Refs. [91, 92].

The double integral in eq. (2.27a) has a known solution, see Ref. [91]. We take again the leading terms in x , corresponding to

$$\begin{aligned} \lim_{x \rightarrow 0} \int_x^\infty \frac{du}{u} e^{-2iu} \int_u^\infty \frac{dt}{t} e^{2it} = & 2 - i\pi + \frac{\pi^2}{8} - \pi x - 2\alpha + \frac{i\pi\alpha}{2} + 2ix\alpha + \frac{\alpha^2}{2} \\ & + \left(2 - \frac{i\pi}{2} - 2ix - \alpha\right) \ln x + \frac{\ln^2 x}{2} + \mathcal{O}(x^2). \end{aligned} \quad (\text{B.6})$$

For the double integral in eq. (2.32), we expand the integrand in the limit $u \rightarrow 0$ and then integrate the expansion between x and 1 to ensure convergence of the leading terms. This is possible because for large arguments the exponential function is

suppressed by $\ln x/x$. We obtain

$$\begin{aligned}
\lim_{x \rightarrow 0} \int_x^\infty \frac{du}{u} e^{2iu} \ln u \int_u^\infty \frac{dt}{t} e^{-2it} &\simeq \lim_{x \rightarrow 0} \int_x^1 du \left[-2i \ln^2 u + 2i \ln u \right. \\
&\quad \left. - \frac{1}{2} i \ln(16) \ln u - \frac{\ln(2u) \ln u}{u} - \gamma \frac{\ln u}{u} \right. \\
&\quad \left. - \frac{i\pi \ln u}{2u} + \pi \ln u - 2i\gamma \ln u \right] \\
&= -2i - \pi + 2ix + \pi x - 2i\alpha + 2ix\alpha - (2ix + \pi x + 2ix\alpha) \ln x \\
&\quad + \left(1 + \frac{i\pi}{4} + 2ix - \frac{\alpha}{2} \right) \ln^2 x + \frac{\ln^3 x}{x} + \mathcal{O}(x^2).
\end{aligned} \tag{B.7}$$

This allow us to calculate the double integral entering eq. (2.30), whose asymptotic form is

$$\begin{aligned}
\lim_{x \rightarrow 0} \int_x^\infty \frac{du}{u} e^{-2iu} \int_u^\infty \frac{dt}{t} e^{2it} \ln t &= (-4 + 2i) + (1 + i)\pi - \frac{5\pi^2}{12} + \frac{i\pi^3}{48} - 2ix + 2\pi x - \frac{i\pi^2 x}{12} \\
&\quad + (6 + 2i)\alpha - i\pi\alpha + \frac{5\pi^2\alpha}{24} - 4ix\alpha - \pi x\alpha - 3\alpha^2 + \frac{i\pi\alpha^2}{4} \\
&\quad + i\alpha^2 x + \frac{\alpha^3}{2} + \left(-2 + i\pi + \frac{\pi^2}{24} + 4ix + 2\alpha - \frac{i\pi\alpha}{2} - \frac{\alpha^2}{2} \right) \ln x \\
&\quad - ix \ln^2 x + \frac{\ln^3 x}{6} + \mathcal{O}(x^2).
\end{aligned} \tag{B.8}$$

In eq. (2.33), we also have the complex conjugate of eq. (B.7)

$$\begin{aligned}
\lim_{x \rightarrow 0} \int_x^\infty \frac{du}{u} e^{-2iu} \ln u \int_u^\infty \frac{dt}{t} e^{2it} &= 2i - \pi - 2ix + \pi x + 2i\alpha - 2ix\alpha + (2ix - \pi x + 2ix\alpha) \ln x \\
&\quad + \left(1 - \frac{i\pi}{4} - 2ix - \frac{\alpha}{2} \right) \ln^2 x + \frac{\ln^3 x}{x} + \mathcal{O}(x^2).
\end{aligned} \tag{B.9}$$

Finally, for the triple integral entering eq. (2.30), we take the limit for $u \rightarrow 0$ of the integrand, which is eq. (B.6), and then we integrate the leading contributions of order $\mathcal{O}(x^0)$ between x and ∞ . Then we also expand in the super-Hubble limit

$$\begin{aligned}
\lim_{x \rightarrow 0} \int_x^\infty \frac{du}{u} e^{2iu} \int_u^\infty \frac{dt}{t} e^{-2it} \int_t^\infty \frac{ds}{s} e^{2is} &= -\frac{4}{3} + i\pi - \frac{\pi^2}{4} + \frac{5i\pi^3}{48} + 2\alpha - i\pi\alpha + \frac{\pi^2\alpha}{8} - \alpha^2 \\
&\quad + \frac{i\pi\alpha^2}{4} + \frac{\alpha^3}{6} - \frac{\zeta(3)}{3} + \left(-2 + i\pi - \frac{\pi^2}{8} + 2\alpha - \frac{i\pi\alpha}{2} - \frac{\alpha^2}{2} \right) \ln x \\
&\quad + \left(-1 + \frac{i\pi}{4} + \frac{\alpha}{2} \right) \ln^2 x - \frac{\ln^3 x}{6} + \mathcal{O}(x^2),
\end{aligned} \tag{B.10}$$

where ζ is the Riemann zeta function.

All the asymptotic solutions entering the PPS equations agree with the results previously calculated in Ref. [21], except for one term in eq. (B.10). We find $-\zeta(3)/3$ while in Ref. [21] there is a $-7\zeta(3)/3$.

C Parameterisation of the Power Spectra

The power spectra of scalar and tensor perturbations can be estimated through analytical methods. Typically, this involves expanding the power spectra around a specific wavenumber, denoted as k_* , and then determining the coefficients through a slow-roll expansion or another suitable approximation technique. Because the analysis must span multiple orders of magnitude in k , the most effective expansion variable is $\ln k$. In this regard, two expansions have been proposed in the literature [20]. The first one, already presented up to third-order terms in Ref. [21], consists in expanding directly the power spectrum in $\ln k$, leading to

$$\frac{\mathcal{P}_X(k)}{\mathcal{P}_{X0}(k_*)} = a_{X0} + a_{X1} \ln\left(\frac{k}{k_*}\right) + \frac{a_{X2}}{2} \ln^2\left(\frac{k}{k_*}\right) + \frac{a_{X3}}{3!} \ln^3\left(\frac{k}{k_*}\right), \quad (\text{C.1})$$

where $X = [\zeta, t]$ and

$$\mathcal{P}_{\zeta 0}(k_*) = \frac{H_*^2}{8\pi^2 M_{\text{Pl}}^2 \epsilon_{1*}}, \quad \mathcal{P}_{t0}(k_*) = \frac{2H_*^2}{\pi^2 M_{\text{Pl}}^2}. \quad (\text{C.2})$$

Therefore, the coefficients $a_{\zeta i}$ and a_{ti} at third order are respectively

$$\begin{aligned} a_{\zeta 0} = & 1 - 2(1 - \alpha)\epsilon_{1*} + \left(-3 - 2\alpha + 2\alpha^2 + \frac{\pi^2}{2}\right) \epsilon_{1*}^2 + \alpha\epsilon_{2*} \\ & + \left(-6 + \alpha + \alpha^2 + \frac{7\pi^2}{12}\right) \epsilon_{1*}\epsilon_{2*} + \frac{1}{8}(-8 + 4\alpha^2 + \pi^2) \epsilon_{2*}^2 \\ & + \frac{1}{24}(-12\alpha^2 + \pi^2) \epsilon_{2*}\epsilon_{3*} - \frac{1}{24}(-16 + 24\alpha - 4\alpha^3 - 3\alpha\pi^2 + 2\zeta(3)) (8\epsilon_{1*}^3 + \epsilon_{2*}^3) \\ & + \frac{1}{12}(-72\alpha + 36\alpha^2 + 13\pi^2 + 8\alpha\pi^2 - 12\zeta(3)) \epsilon_{1*}^2 \epsilon_{2*} \\ & - \frac{1}{24}(16 + 24\alpha - 12\alpha^2 - 8\alpha^3 - 15\pi^2 - 6\alpha\pi^2 + 28\zeta(3)) \epsilon_{1*}\epsilon_{2*}^2 \\ & + \frac{1}{24}(16 + 4\alpha^3 - \alpha\pi^2 - 8\zeta(3)) (\epsilon_{2*}\epsilon_{3*}^2 + \epsilon_{2*}\epsilon_{3*}\epsilon_{4*}) \\ & + \frac{1}{24}(48\alpha - 12\alpha^3 - 5\alpha\pi^2) \epsilon_{2*}^2 \epsilon_{3*} \\ & + \frac{1}{12}(-8 + 72\alpha - 12\alpha^2 - 8\alpha^3 + \pi^2 - 6\alpha\pi^2 - 8\zeta(3)) \epsilon_{1*}\epsilon_{2*}\epsilon_{3*}, \end{aligned} \quad (\text{C.3})$$

$$\begin{aligned}
a_{\zeta 1} = & -2\epsilon_{1*} + 2(-2\alpha + 1)\epsilon_{1*}^2 - \epsilon_{2*} - (2\alpha + 1)\epsilon_{1*}\epsilon_{2*} - \alpha\epsilon_{2*}^2 + \alpha\epsilon_{2*}\epsilon_{3*} \\
& - \frac{1}{8}(-8 + 4\alpha^2 + \pi^2)(8\epsilon_{1*}^3 + \epsilon_{2*}^3) - 6\left(-1 + \alpha + \frac{\pi^2}{9}\right)\epsilon_{1*}^2\epsilon_{2*} \\
& - \frac{1}{4}(-4 + 4\alpha + 4\alpha^2 + \pi^2)\epsilon_{1*}\epsilon_{2*}^2 + \left(-6 + 2\alpha + 2\alpha^2 + \frac{\pi^2}{2}\right)\epsilon_{1*}\epsilon_{2*}\epsilon_{3*} \\
& + \frac{1}{24}(-12\alpha^2 + \pi^2)(\epsilon_{2*}\epsilon_{3*}^2 + \epsilon_{2*}\epsilon_{3*}\epsilon_{4*}) + \frac{1}{24}(-48 + 36\alpha^2 + 5\pi^2)\epsilon_{2*}^2\epsilon_{3*}, \quad (\text{C.4})
\end{aligned}$$

$$\begin{aligned}
a_{\zeta 2} = & 4\epsilon_{1*}^2 + 2\epsilon_{1*}\epsilon_{2*} + 6\epsilon_{1*}^2\epsilon_{2*} + \epsilon_{2*}^2 - \epsilon_{2*}\epsilon_{3*} + (1 + 2\alpha)(\epsilon_{1*}\epsilon_{2*}^2 - 2\epsilon_{1*}\epsilon_{2*}\epsilon_{3*}) \\
& + \alpha(8\epsilon_{1*}^3 + \epsilon_{2*}^3 - 3\epsilon_{2*}^2\epsilon_{3*} + \epsilon_{2*}\epsilon_{3*}^2 + \epsilon_{2*}\epsilon_{3*}\epsilon_{4*}), \quad (\text{C.5})
\end{aligned}$$

$$a_{\zeta 3} = -8\epsilon_{1*}^3 - 2\epsilon_{1*}\epsilon_{2*}^2 - \epsilon_{2*}^3 + 4\epsilon_{1*}\epsilon_{2*}\epsilon_{3*} + 3\epsilon_{2*}^2\epsilon_{3*} - \epsilon_{2*}\epsilon_{3*}^2 - \epsilon_{2*}\epsilon_{3*}\epsilon_{4*}, \quad (\text{C.6})$$

$$\begin{aligned}
a_{t0} = & 1 + 2(-1 + \alpha)\epsilon_{1*} + \left(-3 - 2\alpha + 2\alpha^2 + \frac{\pi^2}{2}\right)\epsilon_{1*}^2 \\
& + \left(-2 + 2\alpha - \alpha^2 + \frac{\pi^2}{12}\right)\epsilon_{1*}\epsilon_{2*} - \frac{1}{3}(-16 + 24\alpha - 4\alpha^3 - 3\alpha\pi^2 + 2\zeta(3))\epsilon_{1*}^3 \\
& + \frac{1}{12}(-96 + 72\alpha + 36\alpha^2 - 24\alpha^3 + 13\pi^2 - 10\alpha\pi^2)\epsilon_{1*}^2\epsilon_{2*} \\
& - \frac{1}{12}(8 - 24\alpha + 12\alpha^2 - 4\alpha^3 - \pi^2 + \alpha\pi^2 + 8\zeta(3))(\epsilon_{1*}\epsilon_{2*}^2 + \epsilon_{1*}\epsilon_{2*}\epsilon_{3*}), \quad (\text{C.7})
\end{aligned}$$

$$\begin{aligned}
a_{t1} = & -2\epsilon_{1*} + 2(-2\alpha + 1)\epsilon_{1*}^2 + (-2 + 2\alpha)\epsilon_{1*}\epsilon_{2*} - (-8 + 4\alpha^2 + \pi^2)\epsilon_{1*}^3 \\
& + 6\left(-1 - \alpha + \alpha^2 + \frac{5\pi^2}{36}\right)\epsilon_{1*}^2\epsilon_{2*} \\
& + \left(-2 + 2\alpha - \alpha^2 + \frac{\pi^2}{12}\right)(\epsilon_{1*}\epsilon_{2*}^2 + \epsilon_{1*}\epsilon_{2*}\epsilon_{3*}), \quad (\text{C.8})
\end{aligned}$$

$$a_{t2} = 4\epsilon_{1*}^2 + 8\alpha\epsilon_{1*}^3 - 2\epsilon_{1*}\epsilon_{2*} + 2(3 - 6\alpha)\epsilon_{1*}^2\epsilon_{2*} - 2(1 - \alpha)(\epsilon_{1*}\epsilon_{2*}^2 + \epsilon_{1*}\epsilon_{2*}\epsilon_{3*}), \quad (\text{C.9})$$

$$a_{t3} = -8\epsilon_{1*}^3 + 12\epsilon_{1*}^2\epsilon_{2*} - 2\epsilon_{1*}\epsilon_{2*}^2 - 2\epsilon_{1*}\epsilon_{2*}\epsilon_{3*}. \quad (\text{C.10})$$

Some numerical coefficient of the $\zeta(3)$ entering the third-order terms in eqs. (C.3) and (C.7) differ from the ones reported in Ref. [21]; this is due to the differences in the asymptotic solution of eq. (B.10).

Alternatively, the second kind of expansion consists of expanding the logarithm of the power spectrum in $\ln k$ as

$$\ln \left[\frac{\mathcal{P}_X(k)}{\mathcal{P}_{X0}(k_*)} \right] = b_{X0} + b_{X1} \ln \left(\frac{k}{k_*} \right) + \frac{b_{X2}}{2} \ln^2 \left(\frac{k}{k_*} \right) + \frac{b_{X3}}{3!} \ln^3 \left(\frac{k}{k_*} \right). \quad (\text{C.11})$$

Here we present the coefficients b_{ζ_i} and b_{t_i} up to third-order corrections, they are respectively

$$\begin{aligned}
b_{\zeta_0} = & -2(1-\alpha)\epsilon_{1*} + \left(-5 + 2\alpha + \frac{\pi^2}{2}\right)\epsilon_{1*}^2 + \alpha\epsilon_{2*} + \left(-6 + 3\alpha - \alpha^2 + \frac{7\pi^2}{12}\right)\epsilon_{1*}\epsilon_{2*} \\
& + \frac{1}{24}(-12\alpha^2 + \pi^2)\epsilon_{2*}\epsilon_{3*} - \frac{1}{24}(80 - 48\alpha - 24\pi^2 + 16\zeta(3))\epsilon_{1*}^3 + \left(-1 + \frac{\pi^2}{8}\right)\epsilon_{2*}^2 \\
& - \frac{1}{12}(-8 + \zeta(3))\epsilon_{2*}^3 + \left(-12 + 15\alpha - 3\alpha^2 + \frac{27\pi^2}{12} - \alpha\pi^2 - \zeta(3)\right)\epsilon_{1*}^2\epsilon_{2*} \\
& - \frac{1}{24}(64 - 168\alpha + 36\alpha^2 - 8\alpha^3 - 21\pi^2 + 14\alpha\pi^2 + 28\zeta(3))\epsilon_{1*}\epsilon_{2*}^2 \\
& + \frac{1}{24}(16 + 4\alpha^3 - \alpha\pi^2 - 8\zeta(3))(\epsilon_{2*}\epsilon_{3*}^2 + \epsilon_{2*}\epsilon_{3*}\epsilon_{4*}) + \left(2\alpha - \frac{\alpha\pi^2}{4}\right)\epsilon_{2*}^2\epsilon_{3*} \\
& + \frac{1}{12}(-8 + 72\alpha - 24\alpha^2 + 4\alpha^3 + 2\pi^2 - 7\alpha\pi^2 - 8\zeta(3))\epsilon_{1*}\epsilon_{2*}\epsilon_{3*}, \tag{C.12}
\end{aligned}$$

$$\begin{aligned}
b_{\zeta_1} = & -2\epsilon_{1*} - 2\epsilon_{1*}^2 - 2\epsilon_{1*}^3 - \epsilon_{2*} - (3 - 2\alpha)\epsilon_{1*}\epsilon_{2*} + \alpha\epsilon_{2*}\epsilon_{3*} - \frac{2}{3}\left(\frac{45}{2} - 9\alpha - \frac{3\pi^2}{2}\right)\epsilon_{1*}^2\epsilon_{2*} \\
& - \left(7 - 3\alpha + \alpha^2 - \frac{7\pi^2}{12}\right)\epsilon_{1*}\epsilon_{2*}^2 + \left(-6 + 4\alpha - \alpha^2 + \frac{7\pi^2}{12}\right)\epsilon_{1*}\epsilon_{2*}\epsilon_{3*} \\
& + \frac{1}{24}(-12\alpha^2 + \pi^2)(\epsilon_{2*}\epsilon_{3*}^2 + \epsilon_{2*}\epsilon_{3*}\epsilon_{4*}) + \left(-2 + \frac{\pi^2}{4}\right)\epsilon_{2*}^2\epsilon_{3*}, \tag{C.13}
\end{aligned}$$

$$\begin{aligned}
b_{\zeta_2} = & -2\epsilon_{1*}\epsilon_{2*} - 6\epsilon_{1*}^2\epsilon_{2*} - (3 - 2\alpha)\epsilon_{1*}\epsilon_{2*}^2 - \epsilon_{2*}\epsilon_{3*} \\
& - 2(2 - \alpha)\epsilon_{1*}\epsilon_{2*}\epsilon_{3*} + \alpha\epsilon_{2*}\epsilon_{3*}^2 + \alpha\epsilon_{2*}\epsilon_{3*}\epsilon_{4*}, \tag{C.14}
\end{aligned}$$

$$b_{\zeta_3} = -2\epsilon_{1*}\epsilon_{2*}^2 - 2\epsilon_{1*}\epsilon_{2*}\epsilon_{3*} - \epsilon_{2*}\epsilon_{3*}^2 - \epsilon_{2*}\epsilon_{3*}\epsilon_{4*}, \tag{C.15}$$

$$\begin{aligned}
b_{t_0} = & -2(1-\alpha)\epsilon_{1*} + \frac{1}{2}(-10 + 4\alpha + \pi^2)\epsilon_{1*}^2 + \left(-2 + 2\alpha - \alpha^2 + \frac{\pi^2}{12}\right)\epsilon_{1*}\epsilon_{2*} \\
& - \frac{1}{3}(10 - 6\alpha - 3\pi^2 + 2\zeta(3))\epsilon_{1*}^3 + \left(-12 + 14\alpha - 3\alpha^2 + \frac{15\pi^2}{12} - \alpha\pi^2\right)\epsilon_{1*}^2\epsilon_{2*} \\
& - \frac{1}{12}(8 - 24\alpha + 12\alpha^2 - 4\alpha^3 - \pi^2 + \alpha\pi^2 + 8\zeta(3))(\epsilon_{1*}\epsilon_{2*}^2 + \epsilon_{1*}\epsilon_{2*}\epsilon_{3*}), \tag{C.16}
\end{aligned}$$

$$\begin{aligned}
b_{t_1} = & -2\epsilon_{1*} - 2\epsilon_{1*}^2 + 2(-1 + \alpha)\epsilon_{1*}\epsilon_{2*} - 2\epsilon_{1*}^3 + (-14 + 6\alpha + \pi^2)\epsilon_{1*}^2\epsilon_{2*} \\
& + \left(-2 + 2\alpha - \alpha^2 + \frac{\pi^2}{12}\right)(\epsilon_{1*}\epsilon_{2*}^2 + \epsilon_{1*}\epsilon_{2*}\epsilon_{3*}), \tag{C.17}
\end{aligned}$$

$$b_{t_2} = -2\epsilon_{1*}\epsilon_{2*} - 6\epsilon_{1*}^2\epsilon_{2*} - 2(1-\alpha)\epsilon_{1*}\epsilon_{2*}^2 - 2(1-\alpha)\epsilon_{1*}\epsilon_{2*}\epsilon_{3*}, \tag{C.18}$$

$$b_{t3} = -2\epsilon_{1*}\epsilon_{2*}^2 - 2\epsilon_{1*}\epsilon_{2*}\epsilon_{3*}. \quad (\text{C.19})$$

Using the latter parameterisation, it is possible to write directly both the scalar and tensor spectral indices, runnings, and runnings of the running with respect to the coefficients b_{X_i} as follows

$$n_s = 1 + b_{\zeta 1} + b_{\zeta 2} \ln\left(\frac{k}{k_*}\right) + \frac{b_{\zeta 3}}{2} \ln^2\left(\frac{k}{k_*}\right), \quad (\text{C.20})$$

$$\alpha_s = b_{\zeta 2} + b_{\zeta 3} \ln\left(\frac{k}{k_*}\right), \quad (\text{C.21})$$

$$\beta_s = b_{\zeta 3}, \quad (\text{C.22})$$

$$n_t = b_{t1} + b_{t2} \ln\left(\frac{k}{k_*}\right) + \frac{b_{t3}}{2} \ln^2\left(\frac{k}{k_*}\right), \quad (\text{C.23})$$

$$\alpha_t = b_{t2} + b_{t3} \ln\left(\frac{k}{k_*}\right), \quad (\text{C.24})$$

$$\beta_t = b_{t3}. \quad (\text{C.25})$$

D Impact of the Prior Range

In this section, we investigate the sensitivity of the cosmological constraints on the HFF parameters to the choice of prior width, as previously done in Ref. [68] for third-order results, but using a different combination of datasets and different priors. To assess the effect of the prior width on the results, we repeated our analysis by varying the sampled range of the HFF parameters as $\epsilon_{i \geq 2} \in [-1, 1]$. By expanding and contracting the prior ranges, we aim to quantify how these choices affect the posterior distributions, especially with respect to the validity of the analytical equations. This analysis allows us to test the robustness of our results and ensure that the numbers presented in section 4 are weakly dependent on the range of priors. In particular, the prior effects arise from the correlation between ϵ_3 , which is not well constrained by current cosmological data, and ϵ_2 ; as shown in Ref. [68].

When the full *Planck* data are included (meaning the combinations P18+BK18, P18+ACT+BK18 with ACT temperature data truncated, and P18+SPT+BK18), no significant effect on the mean and width of the one-dimensional posterior distributions is observed, as shown in fig. 10. However, in cases where *Planck* data are excluded or the temperature data are truncated when combined with ACT data, ϵ_2 and ϵ_3 are less constrained, leading to a small impact on the uncertainties on ϵ_2 and α_s , with a shift of less than 0.5σ in the mean value of α_s for the combination P18+ACT+BK18 with the *Planck* temperature data truncated. This is shown in fig. 11. For the cases including SPT data, where the posterior distributions of the HFF parameters are centred around zero, these effects are smaller compared to the analysis performed with the full ACT dataset.

We conclude that while the narrower prior ranges may appear safer in terms of perturbative expressions and to minimise the spread of the tails of the posterior

distributions of the poorly constrained parameters, there is no strong indication against using $\epsilon_{i \geq 2} \in [-1, 1]$ which should ensure the validity of the perturbative regime under which we derived the equations.

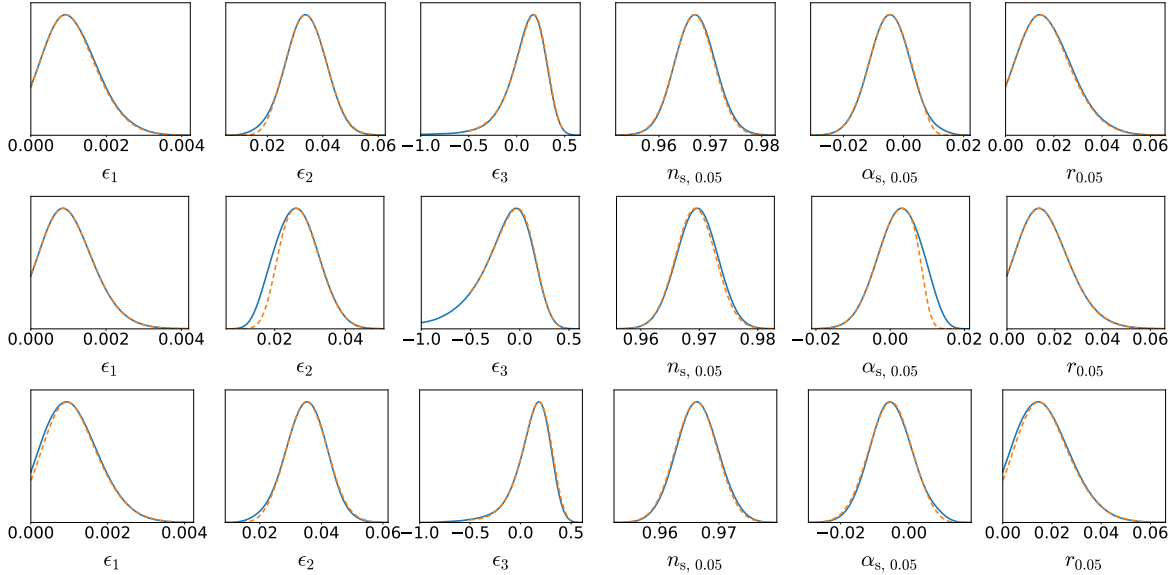


Figure 10. One-dimensional marginalised posterior distributions for the first three HFF parameters ϵ_1 , ϵ_2 , and ϵ_3 and for the scalar spectral index n_s , its running α_s assuming, and the tensor-to-scalar ratio r derived using second-order slow-roll equations. Solid blue lines correspond to larger prior range $\epsilon_{2,3} \in [-1, 1]$ while dashed orange lines correspond to tighter priors used in the main text, that are $\epsilon_{2,3} \in [-0.5, 0.5]$. Different rows correspond to different datasets: P18+BK18 (upper row), P18+ACT+BK18 with ACT data truncated (central row), and P18+SPT+BK18 (lower row), all in combination with the external datasets.

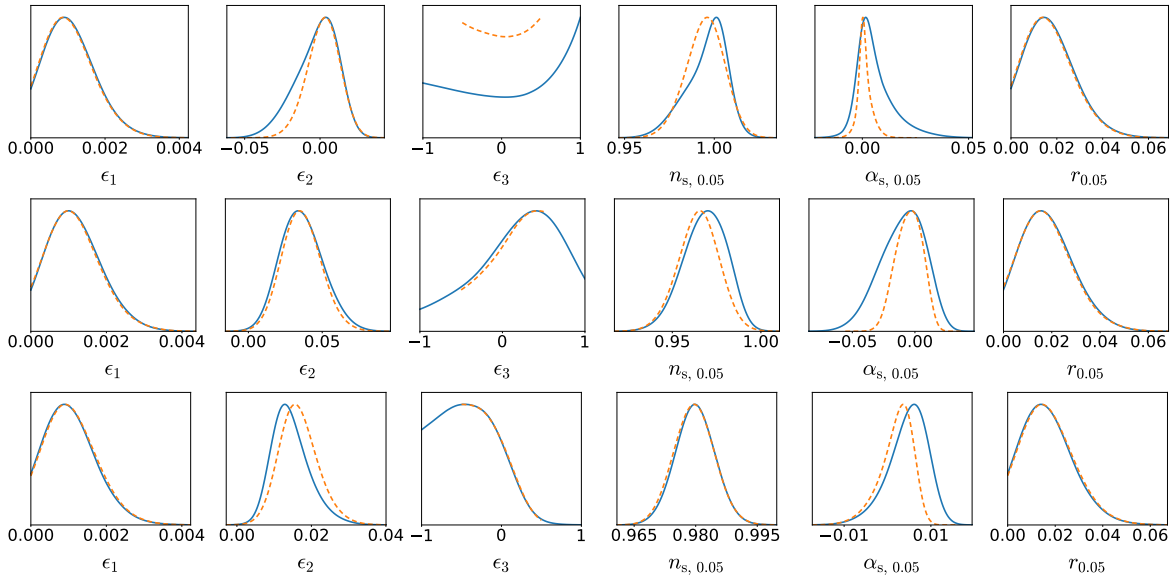


Figure 11. Same as fig. 10 for ACT+BK18 (upper row), and SPT+BK18 (central row), and for the combination P18+ACT+BK18 with *Planck* data truncated, all in combination with the external datasets.

References

- [1] A.A. Starobinsky, *A new type of isotropic cosmological models without singularity*, *Physics Letters B* **91** (1980) 99.
- [2] A.H. Guth, *Inflationary universe: A possible solution to the horizon and flatness problems*, *Phys. Rev. D* **23** (1981) 347.
- [3] A.D. Linde, *A new inflationary universe scenario: A possible solution of the horizon, flatness, homogeneity, isotropy and primordial monopole problems*, *Physics Letters B* **108** (1982) 389.
- [4] A. Albrecht and P.J. Steinhardt, *Cosmology for Grand Unified Theories with Radiatively Induced Symmetry Breaking*, *Phys. Rev. Lett.* **48** (1982) 1220.
- [5] S.W. Hawking, I.G. Moss and J.M. Stewart, *Bubble collisions in the very early universe*, *Phys. Rev. D* **26** (1982) 2681.
- [6] A.D. Linde, *Chaotic inflation*, *Physics Letters B* **129** (1983) 177.
- [7] V.F. Mukhanov, *Gravitational instability of the universe filled with a scalar field*, *Soviet Journal of Experimental and Theoretical Physics Letters* **41** (1985) 493.
- [8] M. Sasaki, *Large Scale Quantum Fluctuations in the Inflationary Universe*, *Progress of Theoretical Physics* **76** (1986) 1036.
- [9] Planck Collaboration, P.A.R. Ade, N. Aghanim, C. Armitage-Caplan, M. Arnaud, M. Ashdown et al., *Planck 2013 results. XXII. Constraints on inflation*, *A&A* **571** (2014) A22 [[1303.5082](#)].
- [10] Planck Collaboration, P.A.R. Ade, N. Aghanim, M. Arnaud, F. Arroja, M. Ashdown

- et al., *Planck 2015 results. XX. Constraints on inflation*, *A&A* **594** (2016) A20 [[1502.02114](#)].
- [11] Planck Collaboration, Y. Akrami, F. Arroja, M. Ashdown, J. Aumont, C. Baccigalupi et al., *Planck 2018 results. X. Constraints on inflation*, *A&A* **641** (2020) A10 [[1807.06211](#)].
- [12] E.D. Stewart and J.O. Gong, *The density perturbation power spectrum to second-order corrections in the slow-roll expansion*, *Physics Letters B* **510** (2001) 1 [[astro-ph/0101225](#)].
- [13] A.A. Starobinskiĭ, *Spectrum of relict gravitational radiation and the early state of the universe*, *Soviet Journal of Experimental and Theoretical Physics Letters* **30** (1979) 682.
- [14] V.F. Mukhanov, *Quantum theory of gauge-invariant cosmological perturbations*, *Soviet Journal of Experimental and Theoretical Physics* **67** (1988) 1297.
- [15] E.D. Stewart and D.H. Lyth, *A more accurate analytic calculation of the spectrum of cosmological perturbations produced during inflation*, *Physics Letters B* **302** (1993) 171 [[gr-qc/9302019](#)].
- [16] A.R. Liddle, P. Parsons and J.D. Barrow, *Formalizing the slow-roll approximation in inflation*, *Phys. Rev. D* **50** (1994) 7222 [[astro-ph/9408015](#)].
- [17] T.T. Nakamura and E.D. Stewart, *The spectrum of cosmological perturbations produced by a multi-component inflaton to second order in the slow-roll approximation*, *Physics Letters B* **381** (1996) 413 [[astro-ph/9604103](#)].
- [18] M.B. Hoffman and M.S. Turner, *Kinematic constraints to the key inflationary observables*, *Phys. Rev. D* **64** (2001) 023506 [[astro-ph/0006321](#)].
- [19] D.J. Schwarz, C.A. Terrero-Escalante and A.A. García, *Higher order corrections to primordial spectra from cosmological inflation*, *Physics Letters B* **517** (2001) 243 [[astro-ph/0106020](#)].
- [20] S.M. Leach, A.R. Liddle, J. Martin and D.J. Schwarz, *Cosmological parameter estimation and the inflationary cosmology*, *Phys. Rev. D* **66** (2002) 023515 [[astro-ph/0202094](#)].
- [21] P. Auclair and C. Ringeval, *Slow-roll inflation at N3LO*, *Phys. Rev. D* **106** (2022) 063512 [[2205.12608](#)].
- [22] E. Bianchi and M. Gamonal, *Primordial power spectrum at N3LO in effective theories of inflation*, *arXiv e-prints* (2024) arXiv:2405.03157 [[2405.03157](#)].
- [23] S. Habib, K. Heitmann, G. Jungman and C. Molina-París, *The Inflationary Perturbation Spectrum*, *Phys. Rev. Lett.* **89** (2002) 281301 [[astro-ph/0208443](#)].
- [24] J. Martin and D.J. Schwarz, *WKB approximation for inflationary cosmological perturbations*, *Phys. Rev. D* **67** (2003) 083512 [[astro-ph/0210090](#)].
- [25] R. Casadio, F. Finelli, M. Luzzi and G. Venturi, *Improved WKB analysis of slow-roll inflation*, *Phys. Rev. D* **72** (2005) 103516 [[gr-qc/0510103](#)].
- [26] R. Casadio, F. Finelli, A. Kamenshchik, M. Luzzi and G. Venturi, *The method of*

- comparison equations for cosmological perturbations, *J. Cosmology Astropart. Phys.* **2006** (2006) 011 [[gr-qc/0603026](#)].
- [27] J. Martin, C. Ringeval and V. Vennin, *Encyclopædia Inflationaris, Physics of the Dark Universe* **5** (2014) 75 [[1303.3787](#)].
- [28] J. Martin, C. Ringeval and V. Vennin, *Cosmic Inflation at the Crossroads*, *arXiv e-prints* (2024) [arXiv:2404.10647](#) [[2404.10647](#)].
- [29] M. Ballardini, *Chasing cosmic inflation: constraints for inflationary models and reheating insights*, [2408.03321](#).
- [30] P. Ade, J. Aguirre, Z. Ahmed, S. Aiola, A. Ali, D. Alonso et al., *The Simons Observatory: science goals and forecasts*, *J. Cosmology Astropart. Phys.* **2019** (2019) [056](#) [[1808.07445](#)].
- [31] K. Abazajian, G. Addison, P. Adshead, Z. Ahmed, S.W. Allen, D. Alonso et al., *CMB-S4 Science Case, Reference Design, and Project Plan*, *arXiv e-prints* (2019) [arXiv:1907.04473](#) [[1907.04473](#)].
- [32] K. Abazajian, G.E. Addison, P. Adshead, Z. Ahmed, D. Akerib, A. Ali et al., *CMB-S4: Forecasting Constraints on Primordial Gravitational Waves*, *ApJ* **926** (2022) [54](#) [[2008.12619](#)].
- [33] LiteBIRD Collaboration, E. Allys, K. Arnold, J. Aumont, R. Aurlien, S. Azzoni et al., *Probing cosmic inflation with the LiteBIRD cosmic microwave background polarization survey*, *Progress of Theoretical and Experimental Physics* **2023** (2023) [042F01](#) [[2202.02773](#)].
- [34] D. Paoletti, F. Finelli, J. Valiviita and M. Hazumi, *Planck and BICEP/Keck Array 2018 constraints on primordial gravitational waves and perspectives for future B -mode polarization measurements*, *Phys. Rev. D* **106** (2022) [083528](#) [[2208.10482](#)].
- [35] R. Laureijs, J. Amiaux, S. Arduini, J.L. Auguères, J. Brinchmann, R. Cole et al., *Euclid Definition Study Report*, *arXiv e-prints* (2011) [arXiv:1110.3193](#) [[1110.3193](#)].
- [36] L. Amendola, S. Appleby, A. Avgoustidis, D. Bacon, T. Baker, M. Baldi et al., *Cosmology and fundamental physics with the Euclid satellite*, *Living Reviews in Relativity* **21** (2018) [2](#) [[1606.00180](#)].
- [37] Euclid Collaboration, A. Blanchard, S. Camera, C. Carbone, V.F. Cardone, S. Casas et al., *Euclid preparation. VII. Forecast validation for Euclid cosmological probes*, *A&A* **642** (2020) [A191](#) [[1910.09273](#)].
- [38] Euclid Collaboration, S. Ilić, N. Aghanim, C. Baccigalupi, J.R. Bermejo-Climent, G. Fabbian et al., *Euclid preparation. XV. Forecasting cosmological constraints for the Euclid and CMB joint analysis*, *A&A* **657** (2022) [A91](#) [[2106.08346](#)].
- [39] Planck Collaboration, N. Aghanim, Y. Akrami, F. Arroja, M. Ashdown, J. Aumont et al., *Planck 2018 results. I. Overview and the cosmological legacy of Planck*, *A&A* **641** (2020) [A1](#) [[1807.06205](#)].
- [40] S. Aiola, E. Calabrese, L. Maurin, S. Naess, B.L. Schmitt, M.H. Abitbol et al., *The Atacama Cosmology Telescope: DR4 maps and cosmological parameters*, *J. Cosmology Astropart. Phys.* **2020** (2020) [047](#) [[2007.07288](#)].

- [41] L. Balkenhol, D. Dutcher, A. Spurio Mancini, A. Doussot, K. Benabed, S. Galli et al., *Measurement of the CMB temperature power spectrum and constraints on cosmology from the SPT-3G 2018 TT, TE, and EE dataset*, *Phys. Rev. D* **108** (2023) 023510 [[2212.05642](#)].
- [42] P.A.R. Ade, Z. Ahmed, M. Amiri, D. Barkats, R.B. Thakur, C.A. Bischoff et al., *Improved Constraints on Primordial Gravitational Waves using Planck, WMAP, and BICEP/Keck Observations through the 2018 Observing Season*, *Phys. Rev. Lett.* **127** (2021) 151301 [[2110.00483](#)].
- [43] V.F. Mukhanov and G.V. Chibisov, *Quantum fluctuations and a nonsingular universe*, *Soviet Journal of Experimental and Theoretical Physics Letters* **33** (1981) 532.
- [44] A. Kosowsky and M.S. Turner, *CMB anisotropy and the running of the scalar spectral index*, *Phys. Rev. D* **52** (1995) R1739 [[astro-ph/9504071](#)].
- [45] R. Kallosh, A. Linde and D. Roest, *Universal Attractor for Inflation at Strong Coupling*, *Phys. Rev. Lett.* **112** (2014) 011303 [[1310.3950](#)].
- [46] S. Ferrara, R. Kallosh, A. Linde and M. Porrati, *Minimal supergravity models of inflation*, *Phys. Rev. D* **88** (2013) 085038 [[1307.7696](#)].
- [47] R. Kallosh, A. Linde and D. Roest, *Superconformal inflationary α -attractors*, *Journal of High Energy Physics* **2013** (2013) 198 [[1311.0472](#)].
- [48] R. Kallosh, A. Linde and D. Roest, *Large field inflation and double α -attractors*, *Journal of High Energy Physics* **2014** (2014) 52 [[1405.3646](#)].
- [49] R. Kallosh, A. Linde and D. Roest, *The double attractor behavior of induced inflation*, *Journal of High Energy Physics* **2014** (2014) 62 [[1407.4471](#)].
- [50] M. Galante, R. Kallosh, A. Linde and D. Roest, *Unity of Cosmological Inflation Attractors*, *Phys. Rev. Lett.* **114** (2015) 141302.
- [51] S. Kachru, R. Kallosh, A. Linde and S.P. Trivedi, *de Sitter vacua in string theory*, *Phys. Rev. D* **68** (2003) 046005 [[hep-th/0301240](#)].
- [52] R. Kallosh and T. Wrase, *dS Supergravity from 10d*, *Fortschritte der Physik* **67** (2019) 1800071 [[1808.09427](#)].
- [53] J. Blåbäck, U. Danielsson and G. Dibitetto, *A new light on the darkest corner of the landscape*, *arXiv e-prints* (2018) arXiv:1810.11365 [[1810.11365](#)].
- [54] V. Vennin, *Horizon-flow off-track for inflation*, *Phys. Rev. D* **89** (2014) 083526 [[1401.2926](#)].
- [55] S. Habib, A. Heinen, K. Heitmann and G. Jungman, *Inflationary perturbations and precision cosmology*, *Phys. Rev. D* **71** (2005) 043518 [[astro-ph/0501130](#)].
- [56] A. Lewis, *Efficient sampling of fast and slow cosmological parameters*, *Phys. Rev. D* **87** (2013) 103529 [[1304.4473](#)].
- [57] A. Lewis, A. Challinor and A. Lasenby, *Efficient Computation of Cosmic Microwave Background Anisotropies in Closed Friedmann-Robertson-Walker Models*, *ApJ* **538** (2000) 473 [[astro-ph/9911177](#)].

- [58] C. Howlett, A. Lewis, A. Hall and A. Challinor, *CMB power spectrum parameter degeneracies in the era of precision cosmology*, *J. Cosmology Astropart. Phys.* **2012** (2012) 027 [[1201.3654](#)].
- [59] A. Lewis, *GetDist: a Python package for analysing Monte Carlo samples*, *arXiv e-prints* (2019) [arXiv:1910.13970](#) [[1910.13970](#)].
- [60] P. Auclair, B. Blachier and C. Ringeval, *Clocking the End of Cosmic Inflation*, *arXiv e-prints* (2024) [arXiv:2406.14152](#) [[2406.14152](#)].
- [61] Planck Collaboration, N. Aghanim, Y. Akrami, M. Ashdown, J. Aumont, C. Baccigalupi et al., *Planck 2018 results. V. CMB power spectra and likelihoods*, *A&A* **641** (2020) A5 [[1907.12875](#)].
- [62] S.K. Choi, M. Hasselfield, S.-P.P. Ho, B. Koopman, M. Lungu, M.H. Abitbol et al., *The Atacama Cosmology Telescope: a measurement of the Cosmic Microwave Background power spectra at 98 and 150 GHz*, *J. Cosmology Astropart. Phys.* **2020** (2020) 045 [[2007.07289](#)].
- [63] S. Alam, M. Aubert, S. Avila, C. Balland, J.E. Bautista, M.A. Bershadsky et al., *Completed SDSS-IV extended Baryon Oscillation Spectroscopic Survey: Cosmological implications from two decades of spectroscopic surveys at the Apache Point Observatory*, *Phys. Rev. D* **103** (2021) 083533 [[2007.08991](#)].
- [64] D.M. Scolnic, D.O. Jones, A. Rest, Y.C. Pan, R. Chornock, R.J. Foley et al., *The Complete Light-curve Sample of Spectroscopically Confirmed SNe Ia from Pan-STARRS1 and Cosmological Constraints from the Combined Pantheon Sample*, *ApJ* **859** (2018) 101 [[1710.00845](#)].
- [65] Planck Collaboration, N. Aghanim, Y. Akrami, M. Ashdown, J. Aumont, C. Baccigalupi et al., *Planck 2018 results. VIII. Gravitational lensing*, *A&A* **641** (2020) A8 [[1807.06210](#)].
- [66] J. Martin and C. Ringeval, *First CMB constraints on the inflationary reheating temperature*, *Phys. Rev. D* **82** (2010) 023511 [[1004.5525](#)].
- [67] C. Ringeval, *Fast Bayesian inference for slow-roll inflation*, *MNRAS* **439** (2014) 3253 [[1312.2347](#)].
- [68] J. Martin, C. Ringeval and V. Vennin, *Vanilla Inflation Predicts Negative Running*, *arXiv e-prints* (2024) [arXiv:2404.15089](#) [[2404.15089](#)].
- [69] L.T. Hergt, W.J. Handley, M.P. Hobson and A.N. Lasenby, *Bayesian evidence for the tensor-to-scalar ratio r and neutrino masses m_ν : Effects of uniform vs logarithmic priors*, *Phys. Rev. D* **103** (2021) 123511 [[2102.11511](#)].
- [70] G. Galloni, S. Henrot-Versillé and M. Tristram, *Robust constraints on tensor perturbations from cosmological data: a comparative analysis from Bayesian and frequentist perspectives*, *arXiv e-prints* (2024) [arXiv:2405.04455](#) [[2405.04455](#)].
- [71] Planck Collaboration, N. Aghanim, Y. Akrami, M. Ashdown, J. Aumont, C. Baccigalupi et al., *Planck 2018 results. VI. Cosmological parameters*, *A&A* **641** (2020) A6 [[1807.06209](#)].
- [72] J.-Q. Jiang and Y.-S. Piao, *Toward early dark energy and $n_s=1$ with Planck, ACT, and SPT observations*, *Phys. Rev. D* **105** (2022) 103514 [[2202.13379](#)].

- [73] E. Di Valentino, W. Giarè, A. Melchiorri and J. Silk, *Quantifying the global 'CMB tension' between the Atacama Cosmology Telescope and the Planck satellite in extended models of cosmology*, *MNRAS* **520** (2023) 210 [[2209.14054](#)].
- [74] W. Giarè, F. Renzi, O. Mena, E. Di Valentino and A. Melchiorri, *Is the Harrison-Zel'dovich spectrum coming back? ACT preference for $n_s = 1$ and its discordance with Planck*, *MNRAS* **521** (2023) 2911 [[2210.09018](#)].
- [75] J.P.P. Vieira, C.T. Byrnes and A. Lewis, *Can power spectrum observations rule out slow-roll inflation?*, *J. Cosmology Astropart. Phys.* **2018** (2018) 019 [[1710.08408](#)].
- [76] L. Knox, *Determination of inflationary observables by cosmic microwave background anisotropy experiments*, *Phys. Rev. D* **52** (1995) 4307 [[astro-ph/9504054](#)].
- [77] S. Hamimeche and A. Lewis, *Likelihood analysis of CMB temperature and polarization power spectra*, *Phys. Rev. D* **77** (2008) 103013 [[0801.0554](#)].
- [78] W. Hu and T. Okamoto, *Mass Reconstruction with Cosmic Microwave Background Polarization*, *ApJ* **574** (2002) 566 [[astro-ph/0111606](#)].
- [79] C.M. Hirata and U. Seljak, *Reconstruction of lensing from the cosmic microwave background polarization*, *Phys. Rev. D* **68** (2003) 083002 [[astro-ph/0306354](#)].
- [80] K.M. Smith, D. Hanson, M. LoVerde, C.M. Hirata and O. Zahn, *Delensing CMB polarization with external datasets*, *J. Cosmology Astropart. Phys.* **2012** (2012) 014 [[1010.0048](#)].
- [81] L. Knox and Y.-S. Song, *Limit on the Detectability of the Energy Scale of Inflation*, *Phys. Rev. Lett.* **89** (2002) 011303 [[astro-ph/0202286](#)].
- [82] M. Kesden, A. Cooray and M. Kamionkowski, *Separation of Gravitational-Wave and Cosmic-Shear Contributions to Cosmic Microwave Background Polarization*, *Phys. Rev. Lett.* **89** (2002) 011304 [[astro-ph/0202434](#)].
- [83] U. Seljak and C.M. Hirata, *Gravitational lensing as a contaminant of the gravity wave signal in the CMB*, *Phys. Rev. D* **69** (2004) 043005 [[astro-ph/0310163](#)].
- [84] F. Finelli, M. Bucher, A. Achúcarro, M. Ballardini, N. Bartolo, D. Baumann et al., *Exploring cosmic origins with CORE: Inflation*, *J. Cosmology Astropart. Phys.* **2018** (2018) 016 [[1612.08270](#)].
- [85] M. Ballardini, F. Finelli, C. Fedeli and L. Moscardini, *Probing primordial features with future galaxy surveys*, *J. Cosmology Astropart. Phys.* **2016** (2016) 041 [[1606.03747](#)].
- [86] G. Cabass, E. Di Valentino, A. Melchiorri, E. Pajer and J. Silk, *Constraints on the running of the running of the scalar tilt from CMB anisotropies and spectral distortions*, *Phys. Rev. D* **94** (2016) 023523 [[1605.00209](#)].
- [87] J.B. Muñoz, E.D. Kovetz, A. Raccanelli, M. Kamionkowski and J. Silk, *Towards a measurement of the spectral runnings*, *J. Cosmology Astropart. Phys.* **2017** (2017) 032 [[1611.05883](#)].
- [88] G. Sato-Polito, E.D. Kovetz and M. Kamionkowski, *Constraints on the primordial curvature power spectrum from primordial black holes*, *Phys. Rev. D* **100** (2019) 063521 [[1904.10971](#)].

- [89] B. Bahr-Kalus, D. Parkinson and R. Easther, *Constraining cosmic inflation with observations: Prospects for 2030*, *MNRAS* **520** (2023) 2405 [[2212.04115](#)].
- [90] R. Easther, B. Bahr-Kalus and D. Parkinson, *Running primordial perturbations: Inflationary dynamics and observational constraints*, *Phys. Rev. D* **106** (2022) L061301 [[2112.10922](#)].
- [91] M. Geller and E.W. Ng, *A Table of Integrals of the Exponential Integral*, *National Institute of Standards and Technology Journal of Research* **73B** (1969) 191.
- [92] M. Abramowitz and I.A. Stegun, *Handbook of Mathematical Functions* (1972).